Development of white light source based on laser diode and suitable phosphor

Ada Czesnakowska

THÈSE

En vue de l'obtention du

DOCTORAT DE L'UNIVERSITÉ DE TOULOUSE

Délivré par l'Université Toulouse 3 - Paul Sabatier

Présentée et soutenue par

Ada CZESNAKOWSKA

Le 3 octobre 2018

Développement d'une source de lumière blanche grâce au couplage d'une diode laser et d'un luminophore adaptés.

Ecole doctorale : **GEET - Génie Electrique Electronique et Télécommunications : du système au nanosystème**

Spécialité : **Génie Electrique**

Unité de recherche :
LAPLACE - Laboratoire PLAsma et Conversion d'Énergie - CNRS-UPS-INPT

Thèse dirigée par
Georges ZISSIS et Gérald LEDRU

Jury

M. Carsten DAM-HANSEN, Rapporteur
M. Luc CHASSAGNE, Rapporteur
M. Benoit GLORIEUX, Examinateur
M. Stelios COURIS, Examinateur
Mme Christelle AUPETIT, Examinateur
M. Georges ZISSIS, Directeur de thèse
M. Gerald LEDRU, Co-directeur de thèse

À mon père…

Remerciement

Les travaux présentés dans ce mémoire ont été réalisés au sein de l'équipe : « Lumière et Matière » du Laboratoire Plasma et Conversion d'Energie (LAPLACE) de l'Université Toulouse III Paul Sabatier, sous la direction des **Georges Zissis** et **Gerald Ledru.**

Tout d'abord, je remercie la direction du laboratoire représentée actuellement par **Thierry Lebey** pour m'avoir accueilli pendant ces trois années.

Ensuite, je souhaite exprimer toute ma gratitude aux membres du jury qui ont accepté d'évaluer mon manuscrit et de participer à ma soutenance. Merci à **Luc Chassagne** et **Carsten Dam-Hansen** d'avoir accepté de lire et juger mon manuscrit de thèse. Merci à **Christelle Aupetit** et **Stelios Couris** pour avoir accepté d'assister à ma soutenance.

Je souhaite remercier particulièrement **Georges Zissis** pour m'avoir donné l'opportunité de réaliser cette thèse, et m'avoir encadré tout au long de ces trois années.

Je remercie profondément **Gerald Ledru**. Son aide, ses compétences et sa disponibilité tout au long de ces trois années m'ont été nécessaires pour affronter les difficultés.

Mes remerciements vont aussi à **Pascal Dupuis** pour son aide précieuse, malgré tous problèmes techniques que nous avons eu pendant le long de ce projet.

Je tiens à remercier **Benoit Glorieux**, chargé de recherche au laboratoire ICMCB à Bordeaux pour toutes les connaissances chimiques qu'il m'a apporté afin de réaliser mes échantillons et de m'avoir fait confiance pour utiliser leur salle de manip au labo ICMCB.

Un grand merci à **David Buso**, **Marc Ternisien**, **Cedric Renaud**, **Laurent Canal**, membres de l'équipe LM pour leur accueil et leur sympathie.

Je voudrais remercier le personnel technique du LAPLACE : **Cedric Trupin, Benoit Lantin**, **Stephane Martin**, **Jacques Salon**, **Nordine Ouahhabi** et **Philippe De Vivo** pour leur aide tout au long de ce projet.

Merci à **Marjorie Morvan**, **Estelle Guerry** et tous les autres doctorants avec qui j'ai partagé le bureau, pour la possibilité de râler ensemble.

Je remercie évidemment ma famille : Babcia Halina et Dziadek Marian et surtout ma **mère** et mon grand petit **frère** qui ont pris le temps de m'écouter tout le long de ces années, qui ont cru en moi et qui étaient toujours présents malgré la distance. Dziekuje.

Enfin, je veux remercier **M.K.K.** pour son énorme patience, et encore patience, et sa petite voix à chaque croisement des carrefours de la vie. Merci pour ton soutien inconditionnel.

“Eat the elephant, one bite at a time…!”

C. Abrams (1914-1974)

Résumé

Ces dernières années les semi-conducteurs à base de InGaN sont devenus attractifs pour des applications d'éclairage. Les sources blanches à base de LED sont de plus en plus utilisées en raison de leur petite taille, leur longue durée de vie et leur faible consommation d'énergie. La lumière blanche peut être générée à partir de LED principalement de trois manières : en mélangeant la lumière issue de LED rouge, verte et bleue, en couplant une LED UV avec un luminophore ou en couplant une LED bleue avec un luminophore jaune. Cette dernière méthode est la plus pratique et efficace, c'est la plus utilisée dans les LED blanches.

Malheureusement les LED utilisées dans ces dispositifs subissent une perte de rendement quantique externe quand leur courant d'alimentation augmente. Ceci se traduit par un décalage du maximum d'émission ainsi qu'un élargissement spectral. Ces variations d'émission impactent la conversion de lumière bleue en lumière blanche, ce qui diminue l'efficacité du procédé.

Une méthode alternative pour obtenir de la lumière blanche en travaillant à forte puissance serait l'utilisation de diodes laser (DL) à la place des LED. Contrairement aux LED, elles sont moins affectées par les pertes d'efficacité. La puissance lumineuse et le rendement quantique externe des diodes laser augmentent linéairement avec le courant d'alimentation, ce qui maintient la stabilité de la lumière blanche produite.

Dans cette étude, une source de lumière blanche basée sur l'utilisation d'une diode laser bleue a été mise au point. Tout d'abord, une diode bleue a été couplée avec différents types de luminophores jaunes. Par la suite, pour éliminer les inconvénients de ce système d'éclairage, les différents processus de vieillissement ont été étudiés. Le problème commun des sources de la lumière basée sur les semi-conducteurs, est leur chauffage quand le courant augmente. Pour éviter la dégradation de la diode causée par la chaleur et assurer une longue durée de vie, le module de refroidissement est nécessaire. L'autre aspect de la diminution de l'efficacité peut se produire en raison du vieillissement du luminophore. Différents types d'irradiations ont été effectués pour trouver celui qui a le plus d'influence sur la dégradation du luminophore.

Comme alternative pour la diode bleue, une diode proche-UV (405 nm) peut être utilisée quand elle est couplée à un mélange de luminophores bleus et jaunes. Des études supplémentaires des effets de saturation sur le luminophore ont également été réalisées

Abstract

In past few years InGaN-based semiconductors have attracted much more attention for application in solid-state lighting sources. Recently, their usage is constantly increasing on worldwide market. High-brightness white LEDs have been used due to their size, long life and energy saving. Moreover, with the LED it is possible to generate a white light in three major ways: mixing blue, red and green diode, coupling a UV diode with RGB phosphor or blue LED with yellow phosphor.

However, LEDs used in light sources suffer from a loss in external quantum efficiency as an operating current increases. This loss may lead to a shift in peak emission wavelength and broadening of emission spectrum. Laser diodes, in contrary to LEDs, do not suffer this loss. The output power increases linearly with injection current. Moreover, they can reach higher luminosity, for the same power, than LEDs. Additionally, laser-based devices can be operated in reflection mode, allowing for the phosphor to be placed on a reflection substrate that may also act as a heat sink to effectively dissipate heat away from the phosphor.

The source based on laser diode was introduced. Firstly, the blue diode with different types of yellow phosphors were coupled. Subsequently, to eliminate the maximum of disadvantages of this light system, different aging processes were studied. Common problem of SSL based on semiconductors is their heating, when the current increases. To avoid the diode degradation caused by heat and to assure long-life, the cooling module is required. The other aspect of efficiency decrease may occur due to phosphor aging. Different types of irradiations were performed to find the one, which has the most influence on degradation of phosphor plate.

As an alternative for blue diode, the n-UV diode can be used. The system with a laser diode 405 nm and mixed of phosphor was investigated. Additional studies of saturation effects on phosphor were also performed.

Table of contents

Remerciement **5**

Résumé **9**

Abstract **11**

List of Figures **17**

List of Tables **21**

General Introduction **23**

Light and Light Sources **27**

1. Brief History of the Light **28**

2. Human Eye **28**

3. Colors **31**

4. Spectroscopy **32**

4.1 Spontaneous Emission 32

4.2 Stimulated Emission 33

4.3 Absorption 33

5. Photometric and Radiometric Parameters of Light Sources **33**

5.1 Radiometric quantities 34

5.2 Photometric quantities 36

5.3 Color Rendering Index 37

5.4 Correlated Color Temperature 38

6. Sources of Light **39**

6.1 Sun 39

6.2 Incandescent lamps 39

6.2.1 Traditional incandescent bulb 39

6.2.2 Halogen lamp 41

6.3 Low pressure and high pressure sodium lamps 41

6.3.1 Low pressure sodium lamp 41

6.3.2 High pressure sodium lamp 42

6.4 Fluorescent lamp 43

6.5 Solid-State Lighting 45

6.5.1 Light Emitting Diodes 46

6.5.2 Organic Light Emitting Diodes 48

6.5.3 Laser Diode 50

7. Conclusions **51**

White Light Based on Blue Laser Diode 55

1. Phosphor conversion 56
1.1 Quantum model of atom 56
1.2 Atomic orbitals 57
1.3 Configurational coordinate model 57
1.4 Material preparation 58
1.5 YAG:Ce^{3+} in silicon 59
1.6 GYAG:Ce^{3+} with Nitride in silicon 62
1.7 Phosphor on glass 64

2. White light 67
2.1 Transmission 67
2.1.1 Results – YAG phosphor 70
2.1.2 Results – GYAG with Nitride phosphor 73
2.1.3 Results – phosphor on glass 75
2.2 Reflection 78
2.2.1 Results 78

3. Optical power dependencies 79
3.1 Thickness and concentration 80
3.2 Number of particles 81
3.2.1 Calculation of particles number 81
3.2.2 Dependency on CCT and CIE coordinates 83

4. Conclusions 85

Mechanisms of Aging 89

1. Aging of semiconductors 90
1.1 FEM Analysis 90
1.1.1. Steady State 92
1.1.2 Transient State 94
1.2 Influence of temperature variation on white light 95
1.3 Aging of laser diode 98

2. Aging of materials 100
2.1 Aging by laser irradiation 100
2.1.1. YAG:Ce^{3+} aging process 101
2.1.2. GYAG:Ce^{3+} with Nitride aging process 102
2.1.3. FTIR analysis after irradiation 102
2.1.4. Silicon aging process 104
2.1.5. Glass aging process 105
2.2. Aging by artificial sun 106
2.3. Aging by blue LEDs 109
2.4. Temperature distribution on different phosphor plates 111

3. Conclusions 115

White Light Based on n-UV Laser Diode 119

1 Near-UV laser diode 120

2 Blue phosphors 121

3 BAM: Eu^{2+} 124

3.1 Aging of BAM: Eu^{2+} 125

3.2 Optical power dependencies 126

3.2.1 Number of particles 126

4 White light 127

4.1 BAM: Eu^{2+} and YAG:Ce^{3+} 128

4.2 BAM: Eu^{2+} and GYAG:Ce^{3+} with Nitride 129

4.3 Phosphor mix 131

4.4 Filter application 133

4.5 Number of particles 140

5 Saturation effects on phosphor materials 142

6 Conclusions 146

Conclusions and Perspectives 149

References 153

Publications and communications 161

List of Figures

Fig. I-1. Electromagnetic radiations. 28
Fig. I-2. Human eye. [7] 29
Fig. I-3. The scotopic and the photonic vision curves of relative spectral luminous efficiency. [8] 30
Fig. I-4. Influence of monochromatic light of different wavelengths on the melatonin suppression for 72 healthy human subjects. [8] 29
Fig. I-5. CIE 1931 Chromaticity Diagram. 31
Fig. I-6. Distribution of radiant flux. 34
Fig. I-7. Illumination a) normal collimated, b) oblique collimated, c) diffuse. 34
Fig. I-8. Plane angle. 35
Fig. I-9. Solid angle. 35
Fig. I-10. CIE 1931 luminosity. [16] 36
Fig. I-11. Incandescent bulb.[19] 40
Fig. I-12. Example of spectrum and chromaticity coordinates of incandescent lamp (ref. Mazda 10001651). 40
Fig. I-13. Halogen Lamp. 41
Fig. I-14. Low Pressure Sodium Lamp. [20] 42
Fig. I-15. High Pressure Sodium Lamp. [21] 42
Fig. I-16. Example of spectrum and chromaticity coordinates of high pressure sodium lamp (ref. SON-150W-Osram). 43
Fig. I-17. Fluorescent tube (a) [22] and compact fluorescent lamp (b). 44
Fig. I-18. Example of spectrum and chromaticity coordinates of fluorescence tube (ref. Eroski 18 W) 44
Fig. I-19. Structure of LED. [24] 46
Fig. I-20. Blue LED coated with yellow phosphor. 47
Fig. I-21. Structure of oLED. [33] 48
Fig. I-22. Multilayer oLED approach. [35] 49
Fig. I-23. Example of spectrum and chromaticity coordinates of OLED (Ref. OLED OSRAM ORBEOS). 49
Fig. I-24. Schema of a laser diode. [36] 50
Fig. I-25. Headlights based on laser (a) and comparison of distance seen with a laser diode and LED (b). [36] 51
Fig. II-1. Model of Bohr. 56
Fig. II-2. Sublevels. [3] 57
Fig. II-3. Schematic illustration of a configurational coordinate model. [1] 58
Fig. II-4. Sol-gel method of obtaining phosphor samples. 59
Fig. II-5. YAG:Ce^{3+} 60
Fig. III-1. Schema of the chip of the laser diode used for thermal simulation. 91
Fig. III-2. Schema of a laser diode used for thermal simulation. 91
Fig. III-3. Distribution of the temperature in steady state without temperature control.92

Fig. III-4. Distribution of the temperature for 25°C (a) and 55°C (b). 93
Fig. III-5. Characteristics of temperature with diode in the temperature regulating mode. 94
Fig. III-6. Characteristic of temperature in time evolution in active layer without cooling module. 94
Fig. III-7. Spectrum of blue laser diode for different temperature. 96
Fig. III-8. Electrical characteristics for different temperatures. 95
Fig. III-9. Spectrum of converted light by YAG (a) and GYAG (b) for different temperature. 96
Fig. III-10. Level of the emission by different excitation wavelength for YAG (a), GYAG (b), nitride (c). 97
Fig. III-11. CIE chromaticity coordinates for YAG (a) and GYAG (b). 98
Fig. III-12. Optical power evolution for different current after stressing (a) and evolution of threshold current (b). 98
Fig. III-13. Decrease of optical power for current 1.6A. 99
Fig. III-14. Decrease of optical power under stressing for Light Emitting Diode. 100
Fig. III-15. Schema of experimental setup for aging process. 101
Fig. III-16. Effect of laser irradiation on YAG. 101
Fig. III-17. Effect of laser irradiation on mix of GYAG and Nitride. 102
Fig. III-18. Example of full spectrum from infrared analysis. 103
Fig. III-19. Infrared spectrum between 2900-2800 cm^{-1}. 103
Fig. III-20. Degradation of bond CH2=CH2 (A) and recombining to create CH3 particles (B) 104
Fig. III-21. Darkening of silicon after heating to 200°C. 105
Fig. III-22. Spectrum before and after irradiation for 120h. 105
Fig. III-23. Chromaticity coordinates before and after irradiation. 106
Fig. III-24. Experimental setup for aging the sample by artificial sun (xenon lamp). 107
Fig. III-25. Spectrum of "artificial sun". 107
Fig. III-26. Emission after aging by YAG and silicon. 108
Fig. III-27. Phosphor and silicon not aged. 108
Fig. III-28. Image of diodes mounted in the box for aging process. 109
Fig. III-29. Evolution of maximum peak of emission of phosphor sand silicon. 110
Fig. III-30. Spectrum of box with LEDs. 110
Fig. III-31. Variation of temperature and voltage for constant current. 111
Fig. III-32. Experimental setup. Phosphor in silicon placed in front of laser diode in Peltier module. 111
Fig. III-33. Distribution of the temperature on silicon in time evolution. 112
Fig. III-34. Temperature evolution in a function of time on silicon plate. 113
Fig. III-35. Experimental setup. Phosphor in glass placed in front of laser in Peltier module. 113
Fig. III-36. Distribution of the temperature on phosphor in glass. 114
Fig. III-37. Temperature evolution in a function of time on phosphor in glass. 115
Fig. IV-1. Characteristics of optical power and threshold current for a violet laser diode. 120
Fig. IV-2. Spectrum of laser diode 405 nm for different temperatures. 121

Fig. IV-3. Propositions of blue phosphors: BAM, RCA, Pba..... 121
Fig. IV-4. Excitation by different wavelength for BAM, RCA and Pba..... 122
Fig. IV-5. CIE chromaticity coordinates of light emitted by diode nUV and blue phosphor. 123
Fig. IV-6. Excitation spectrum by violet laser diode of different material..... 123
Fig. IV-7. Excitation spectrum of BAM Philips and BAM Sigma Aldrich by violet laser diode. 125
Fig. IV-8. Aging process of BAM. 126
Fig. IV-9. Number of particles in dependency on optical power..... 127
Fig. IV-10. Experimental setup. Spectro-radiometer as an output of an integrating sphere..... 128
Fig. IV-11. Spectrum of converted light by laser diode 405nm and two phosphor's samples: BAM and YAG. 128
Fig. IV-12. CIE Chromaticity for BAM and YAG excited by 405 nm laser diode. 129
Fig. IV-13. Spectrum of converted light by a laser diode 405nm and two phosphor samples: BAM and GYAG..... 130
Fig. IV-14. CIE Chromaticity for BAM and GYAG with Nitride excited by 405 nm laser diode. 130
Fig. IV-15. Silicon resin of 1 mm and 2 mm and difference of the light intensity passing through. 131
Fig. IV-16. CIE chromaticity coordinates of mixes of the phosphor..... 132
Fig. IV-17. Spectra of the light of different mixes..... 131
Fig. IV-18. Schema of experimental setup for measurements with the filter. 133
Fig. IV-19. Mixture of phosphors - spectra without the filter. 134
Fig. IV-20. Characteristics of transmission of filter 425 nm long pass and 475 long pass from Edmund Optics..... 133
Fig. IV-21. Mixture of phosphors – spectra with the filter. 135
Fig. IV-22. Chromaticity coordinates after adding a filter 475 nm. 137
Fig. IV-23. Mixture of phosphors – with filter of 475 nm 137
Fig. IV-24. With and without filter - two phosphor in different silicon plate. 138
Fig. IV-25. With and without filter - BAM 20% and GYAG with Nitride 5%..... 139
Fig. IV-26. Dependency of the optical power on number of particles for two separated plates of phosphor. 140
Fig. IV-27. Dependency of optical power on number of particles for mixture of two phosphors. 141
Fig. IV-28. Output characteristics of a laser diode. 142
Fig. IV-29. Experimental setup for measuring the beam size. 143
Fig. IV-30. Relation between size of beam and the position of LD. 143
Fig. IV-31. Relation between position of beam scanner and intensity. 144
Fig. IV-32. Spectra for different currents for the biggest size beam normalized to peak of emission. 145
Fig. IV-33. Spectra for different currents for the smallest size of beam normalized to peak of emission. 145

List of Tables

Table I-1. Values of Color Rendering Index required for different application.[16]..... 37
Table I-2. CCT for different sources [18]. 38
Table I-3. Light output: comparison between LED vs. Incandescent and Fluorescent. [27] 46
Table II-1. Color Rendering Index for different concentration of YAG phosphor in silicon. 71
Table II-2. CCT of YAG in different concentrations and thicknesses. 71
Table II-3. CCT of GYAG in different concentrations and thicknesses. 74
Table II-4. Color Rendering Index for different phosphors in glass 76
Table II-5. CCT of phosphor in glass 76
Table II-6. CIE chromaticity coordinates of YAG. 83
Table II-7. CIE chromaticity coordinates of GYAG. 84
Table III-1. Material parameters at 25°C. 91
Table III-2. Color Rendering Index for different temperature. 97
Table III-3. Correlated Color Temperature for different temperature. 97
Table III-4. CCT and CRI before and after irradiation. 106
Table IV-1. CRI of mixed phosphor. 132
Table IV-2. Areas under the violet peak and converted light peak. 135
Table IV-3. Parameters of the light without the filter. 136
Table IV-4. Parameters of the light with the filter. 136
Table IV-5. Parameters of the light without filter. 139
Table IV-6. Parameters of the light with filter. 139
Table IV-7. Parameters of the light. 140
Table IV-8. CIE and CCT for different current in condition of small spot size. 146

General Introduction

Solid State Lighting has attracted much interest since the first development of Light Emitting Diode (LED) using blue emitting InGaN diode by Nakamura in 1995 [1]. They possess some advantages with respect to incandescence and fluorescent lamps like: high lifetime, luminescence and compactness. [2][3] Moreover, the very important aspect of replacing traditional light source by SSL is usage of electricity. Nowadays, the 20% [4] of electricity is used for lighting. Due to the low energy consumption of SSL sources, these statistics have a chance to change.

Generally coupling a blue diode with yellow phosphor can generate white light. We can also obtain white light by mixing blue and yellow phosphor, and excites it by violet diode. [5]

Unfortunately, LEDs used in these devices suffer a loss in external quantum efficiency, as an operating current increases, known as a droop. This may lead to shift in a peak emission wavelength and broadening of the emission spectrum caused by an increase in the temperature. Variation of spectrum of LEDs and phosphor change the ratio of the light emitted by each component, resulting in shift in the color coordinates of the emitting light and decrease the overall device efficiency. [6][7]

As an alternative to obtain a white light can be a blue laser diode. In contrast to LEDs, they do not exhibit efficiency loss. The output power and external quantum efficiency of a laser diode increases and maintain color stability of laser emission. Additionally, laser-based devices can be operated in a reflection mode, allowing for the phosphor to be placed on a reflection substrate that may also act as a heat sink to effectively dissipate heat away from the phosphor.

In spite of all these advantages, there is still a lot of work to make, to improve the source of light based on blue laser diode. In this thesis we focused on different problems, which need to be improve.

This thesis was done in LAPLACE laboratory, with material support from ICMCB laboratory in Pessac.

This manuscript was divided into 4 parts. In the first part, the development of the light was described. The advantages and disadvantages of different light sources were described, as well, their principles of work. The description and understanding of previous lights sources let us improve the drawbacks. Moreover, it may also lead to find a proper alternative. The goal of this chapter was also to explain the necessity of developing SSL source based on a laser diode.

In Chapter II the method of obtaining white light based on blue laser diode was presented. In these studies, the different types of phosphors were used, to investigate the light parameters like Color Rendering Index, Correlated Color Temperature and CIE chromaticity coordinates. The goal was to look for the optimum CRI and the CIE

chromaticity coordinates close to (0.33; 0.33), which corresponds to daylight parameters. Different doping, host material and resin were introduced, to have wide comparison between the results. Another study described in this part shows the dependency between particles number of phosphor incorporated into silicon resin and optical power and Correlated Color Temperature.

To have a long lasting and reliable source of light, its weak point should be eliminated. In Chapter III we studied different mechanisms of aging, which may occur in a source based on a laser diode and lead to its accelerated functioning failure. We started by focusing on the semiconductor and we performed the thermal analysis. We verify the importance of the proper heat sink, also we study the evolution of the temperature in time for different temperature conditions. We show the influence of the temperature variation on the parameters of the light.

After studies on the laser itself, we passed to the phosphor material. We put it under intensive laser irradiation, to accelerate the aging. The Fourier Transform Infrared (FTIR) analysis on effect of this irradiation was performed to deeply investigate the changes.

Another type of aging performed on the phosphor plates was leaving them for 500 hours under the artificial sun, and also under blue LEDs, to see the influence of the UV and blue light. The aged samples were compared with the one, that were not influenced by a light treatment.

We distinguish the process of phosphor aging and silicon/glass aging.

The distribution and the value of the temperature on the phosphors also may lead to its aging. We investigate the effects of temperature distribution on the two different type of a resin: silicon and glass.

White light based on n-UV laser diode was studied in Chapter IV. In this investigation we used blue and yellow phosphor – in two separate plates, but also as a mix. We also verify the resistance of the blue phosphor on a laser irradiation. The difference between a number of particles depending on optical power for separated and mixed phosphor was explained.

We finished this part by performing a studies about saturation effect on phosphor materials.

The final conclusion summarizes the work achieve during the PhD, highlights the most notable discoveries, and identifies follow-up work and research topics that could be worth pursuing.

Chapter I

Light and Light Sources

Table of contents

Light and Light Sources **27**

1. Brief History of the Light **28**

2. Human Eye **28**

3. Colors **31**

4. Spectroscopy **32**

4.1 Spontaneous Emission 32

4.2 Stimulated Emission 33

4.3 Absorption 33

5. Photometric and Radiometric Parameters of Light Sources **33**

5.1 Radiometric quantities 34

5.2 Photometric quantities 36

5.3 Color Rendering Index 37

5.4 Correlated Color Temperature 38

6. Sources of Light **39**

6.1 Sun 39

6.2 Incandescent lamps 39

6.2.1 Traditional incandescent bulb 39

6.2.2 Halogen lamp 41

6.3 Low pressure and high pressure sodium lamps 41

6.3.1 Low pressure sodium lamp 41

6.3.2 High pressure sodium lamp 42

6.4 Fluorescent lamp 43

6.5 Solid-State Lighting 45

6.5.1 Light Emitting Diodes 46

6.5.2 Organic Light Emitting Diodes 48

6.5.3 Laser Diode 50

7. Conclusions **51**

1. Brief History of the Light

The history of research on light has started already in 5th century [8]. After astronomy, optics is the second oldest science. Everything started in Ancient Greece, where the three great philosophers: Aristotle, Socrates and Plato established the basics of astronomy, biology, mathematics and politics. Than Euclid summarized the fundamental knowledge of optics, such as diffusion, reflection and vision. These concepts on light established in the age of Ancient Greece rendered a large effect up until the appearance of Newton in the late 17th century. [9]

Isaac Newton is credited with three major discoveries: universal gravitation, infinitesimal calculus and spectral decomposition of light. In his paper, in 1672, he announced that *light is a mixture of various colors having different refractivity*, rather than *the pure white sunlight* proposed by Aristotle, which he proved by demonstrating his famous prism experiment. Later, at the beginning of 18th century, he authored a book *Opticks*, where he reveals his light particle theory. [10]

The great breakthrough came in 1905, made by German theoretical physicist – Albert Einstein. He published three papers about photoelectric effect theory, where light is made up of particles called photons, the theory of Brownian motion and the theory of special relativity. In 1921 his work on theoretically revealing the photoelectric effect based on the light quantum hypothesis won him the Nobel Prize in physics. [11]

Today, we define the light as electromagnetic radiation, which refers to the waves of electromagnetic field, propagating through space-time, carrying electromagnetic radiant energy. Under this definition we can find not only visible light, but also radio waves, microwaves, infrared, ultraviolet, x-rays and gamma rays.

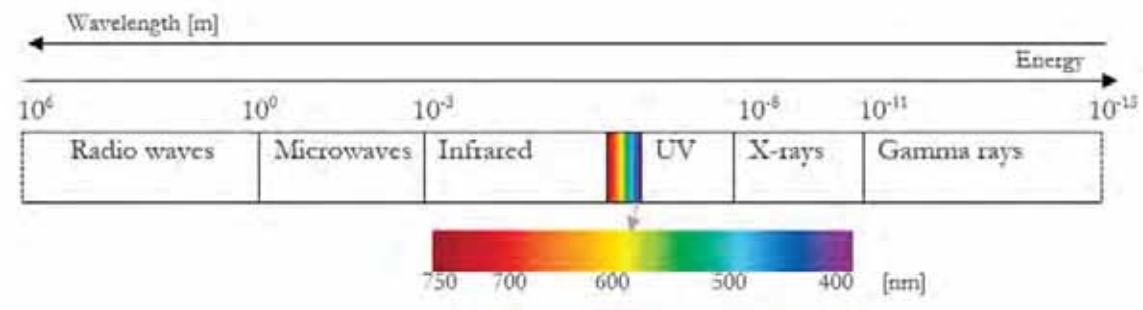

Fig. I-1. Electromagnetic radiations.

2. Human Eye

The recipient of the light is the human eye. If we want to create or optimize an artificial source of light, we should understand human eye. The assessment of light sources with respect to light quality or efficiency is strongly related to the characteristics of human eye.

The human eye is very complex sense organ. The light enters through the pupil – circular hole in the iris -, passes through the lens and is projected on the retina at the back of the eye (Fig. I-1). The iris is a colored ring of muscle fibers, that in response to different lighting conditions, can expand or contract over a range from 1 to 8 mm pupil diameter. Muscles moving the eyeball, allows us focus the image at yellowish central point of retina (macula lutea). The light that passes through the pupil is focused by the lens, which can change the focal length. [12]

The retina contains three types of photoreceptors: rods, cones and retinal ganglion cells. Here, we will focus on the traditional: rods and cones. Rods are more sensitive to light than cones – they are able to detect already two or three photons. Moreover, they are responsible for sensitive motion detection and the peripheral vision. Cones are colors provider and the

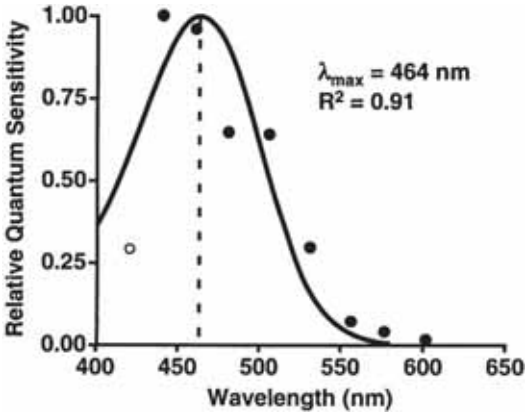

Fig. I-2. Influence of monochromatic light of different wavelengths on the melatonin suppression for 72 healthy human subjects. [8]

highest acuteness of vision. [13]

The sensitivity as a function of wavelength of light is different for rods and cones. The rods are responsible for dark adapted or scotopic vision and are more sensitive to blue-green light with the highest sensitivity for a wavelength of around 500 nm (Fig.2). For the

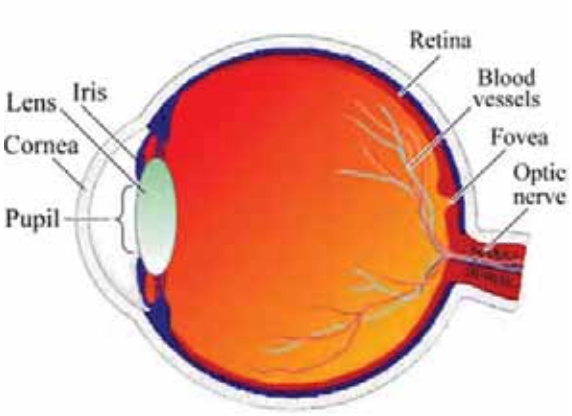

Fig. I-3. Human eye. [7]

cones, this peak is equal to 555 nm.[12]

The photonic responsive curve is the basis for the assessment of the quality of light output and the luminous flux, which is important for the comparison of different light sources or their development. Recent publications [14] have shown that there is third type

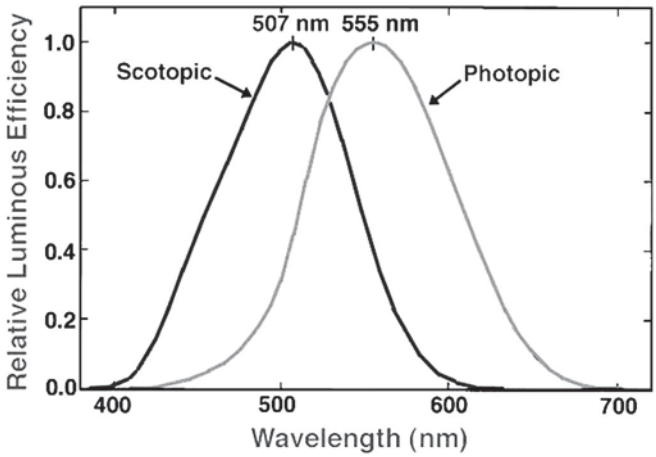

Fig. I-4. The scotopic and the photonic vision curves of relative spectral luminous efficiency. [8]

of photoreceptor. This type of photoreceptor is responsible for synchronizing daily and seasonal rhythm with environmental time using the light arriving at the eye. The sensitivity curve of this type of retinal cells can be measured by the effect in the human body – measuring the concentration of the hormones: cortisol or melatonin before and after exposing the human eye for 90 minutes to a monochromatic light stimulus. As it is known, the level of cortisol in the morning increase, preparing the body for activity. It remains at sufficient level during the day, falling to minimum at night. The level of melatonin drops in the morning. Normally it rises again when it becomes dark, permitting healthy sleep (*sleep hormone*).

Fig. I-4 shows the influence of monochromatic light of different wavelengths on the melatonin suppression. The sensitivity curve has a maximum at 464 nm (blue light). It means that all the devices used before sleeping, where the amount of blue light is high (i.e. LEDs, computer's screen, mobile phones) will lead us to sleepless nights. But it also gives another information: this parameter is extremely important for application, where human beings are exposed to artificial light for longer times.

The artificial light sources might influence on our circadian system in positive or negative way. One example is the illumination in aircrafts. The source of light should safeguard the pilots from getting tired, and reduce the jetlag, especially during overseas connections. The well-adjusted light source would have also great influence on astronauts and their health, while their stay in space-stations. It could create the absent day-night cycle. Also shift workers can be assisted by artificial light sources adjusting their circadian rhythm

to their work rhythm. Furthermore, the streetlights, if optimized, might prevent accidents caused by fatigue.

3. Colors

Light of each wavelength will results in a unique ratio of blue, green and red cone responses. The cones provide us with color vision that distinguished between many colors. Our eye reduces the light signal to the three values, which represents the intensity of each cone types. The overlap between the sensitivity ranges makes not all the combination of stimulations possible. For example, it is impossible to stimulate only green cones – the other cones will be stimulated to some degree at the same time.[12] [15]

Two different light spectra, which have the same effect on the three color receptors in human eyes will be perceived as a same color. This phenomenon is called metamerism [16]. For example, white light emitted by fluorescent lamp, which typically has a spectrum consisting of few narrow bands. The other type of white lite: daylight, has a continuous spectrum. Production of white light by three LEDs: blue, green and red, containing three peaks as a spectrum, can be another example. The human eye cannot distinguish the difference from the spectrums, just by looking at a source of light. On the other hand, the reflected light spectrum from objects might be different, from different white light sources.

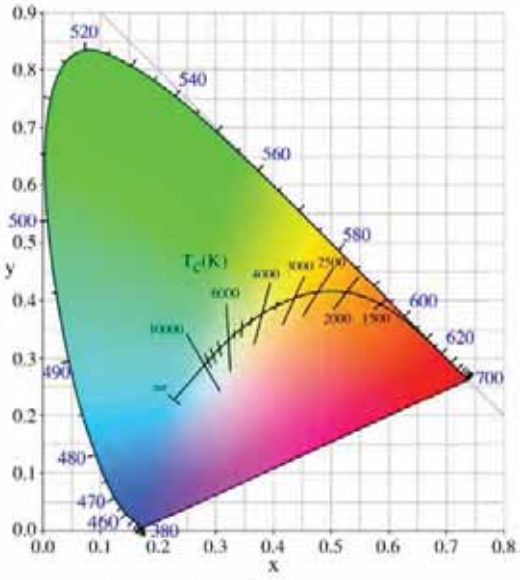

Fig. I-5. CIE 1931 Chromaticity Diagram with black body.

Every stimulation of the eye can be mapped in three-dimensional space, because the light

signal is reduced to the three values. Furthermore, this 3-d color space can be reduced to two dimensional space (see Fig. I-5), by considering colors of the same intensity. In CIE (fr. Commission Internationale de l'Eclairage) chromaticity diagram the parameters x and y specify the chromaticity, Y parameter measure the brightness. [13] The value x corresponds

to the to the simulation of red cones, y value – to the green cones. The simulation of blue cones corresponds to subtraction the sum (x+y) from 1. Overlap between the sensitivity ranges makes x or y equal to 1 impossible. The spectral colors are distributed around the edge of color space and represents all colors perceivable by the human eyes. For example, if we take the red light of 700 nm, which is represented by the value x=0.75, the red cones are simulated the most. In this case also the green cones are simulated (y=0.25). Only the blue cones are not affected. Wavelength smaller than 550 nm stimulates blue cones. Furthermore, if we reach wavelength of 400nm, the green cones are not anymore stimulated, the red ones, only a little bit. The blue cones are the most simulated for 400 nm. The connecting line between 380 and 700 nm is the purple line which cannot be represented by monochromatic light. [12]

4. Spectroscopy

When an atom is excited, it can emit photons, it means the light in the precise parts of spectrum. These spectral rays are characteristics of atoms. The spectrometry distinguishes in its analysis the spectrums of emission and spectrums of absorption. In laboratorial conditions, during the experiment, spectrometry allows us, for example, determined that sodium, in certain conditions of excitation, emits characteristic rays called D-rays, which are situated at 589 nm. Absorption spectrum is also interesting to study. It is rich in information about masses of gases or liquids passing through the light. Light analysis coming from sun, shows presence of black rays or absence of some rays, which are due to absorption by atoms of hydrogen, helium, sodium etc. Other absorptions are due to passing the light by different layers of atmosphere [18].

4.1 Spontaneous Emission

Considering two energy levels, 1 and 2, of some given material, their energies are E_1 and E_2, where $E_1<E_2$. The energies can be any two out of infinity levels of energy. Assuming that an atom is initially on 2 level, and $E_2>E_1$, the atom will tend to decay to level 1. The corresponding energy difference from level 1 and 2 must therefore be released by the atom. When this energy is delivered in the form of electromagnetic wave, the process will be called spontaneous emission. Spontaneous emission is therefore characterized by the emission of photon energy, when the atom decays from level 2 to level 1. The radiative emission is just one of the two possible ways for the atom to decay. The decay can also occur in non-radiative way. In this case the energy difference is delivered in some other form, like kinetic energy of the surrounding molecules. [19]

4.2 Stimulated Emission

Supposing that atom is initially found in level 2 and that an electromagnetic wave of given frequency is incident on the material. Since this wave has the same frequency as atomic frequency, there is a probability that the wave will force the atom to undergo from level 2 to 1. The energy difference, in this case, is delivered in form of electromagnetic wave that adds to the incident one. This phenomenon is called stimulated emission. However, the fundamental distinction between spontaneous and stimulated emission is that, in case of spontaneous emission the atom emits an electromagnetic wave that has no definite phase relation with that emitted by another atom. Moreover, the wave can be emitted in any direction. In case of simulated emission, since the process is forced by electromagnetic wave, the emission of any atom adds in phase to that of the incoming wave. Also, the direction of the emitted wave is determined. [19]

4.3 Absorption

The atom initially laying in level 1, assuming it is a ground level, it will remain there, unless some external stimulus is applied to it. If electromagnetic wave is incident on the material, there is a finite probability that the atom will be raised to level 2. The energy difference E_2-E_1 required by the atom to undergo the transition is obtained from the energy of the incident wave. This is the definition of absorption process.

5. Photometric and Radiometric Parameters of Light Sources

The human eye is not equally sensitive to all wavelengths of visible light. Role of photometry is weighting the measured power at each wavelength with a factor that represent how sensitive the eye is at this wavelength. The aim of radiometry is to measure the energetic radiation of the source. This radiation can have an influence on the receptor, like for example: heating, phosphorescence, luminescence or photochemical effect [18]. Radiometric and photometric characteristics presented below are important only in case of production visible light for humans.

5.1 Radiometric quantities

In terminology for illumination, we can distinguish some spatial quantities like flux, irradiance, intensity and radiance.

Fig. I-6. Distribution of radiant flux.

Radiant flux defines the electromagnetic radiation or energy, emitted or received by the source. This value is the energy depending on time units, which means it can be defined as a power, in units of Watts [W]. The symbol denoted is Φ_e, where "e" stands for "energetic", to avoid confusion with photometric quantities [18].

Irradiance (radiant flux density), E, is the flux per unit area striking a surface. The flux per unit area leaving the surface is called exitance, M. However, in both cases the geometry is the same. Furthermore, when exitance is used, it is usually the flux, that leaves a nonphysical surface such as an exit port of integrating sphere or the real image in an imaging system, which is identical to the irradiance onto the surface.

The irradiance says nothing about the directionally of the flux. Below, if these three examples have the same flux per unit area striking the surface, then they all have the same irradiance. That is the reason why specifications of illuminations systems often qualify the

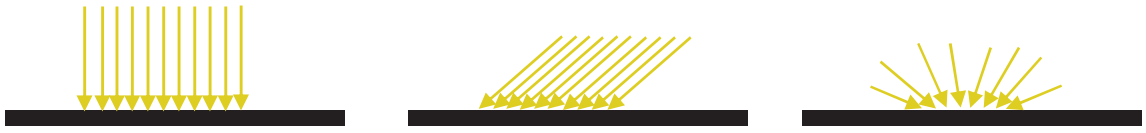

Fig. I-7. Illumination a) normal collimated, b) oblique collimated, c) diffuse.

irradiance with an added description of the desired directional properties. [20]

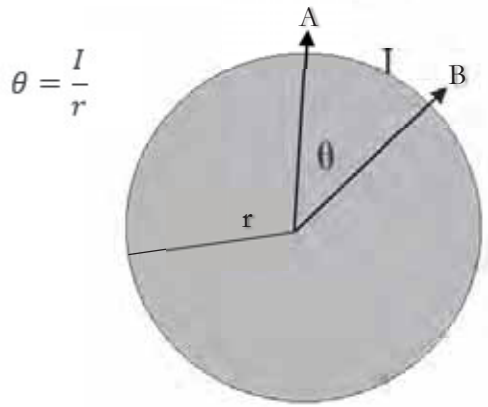

Fig. I-9. Plane angle.

Intensity, I, is the flux per unit solid angle. A solid angle is a 3D angular volume that is defined analogously to the definition of a plane angle in two dimensions. A plane angle, θ, is defined by the arc length of a circle subtended by the lines and by the radius of that circle.

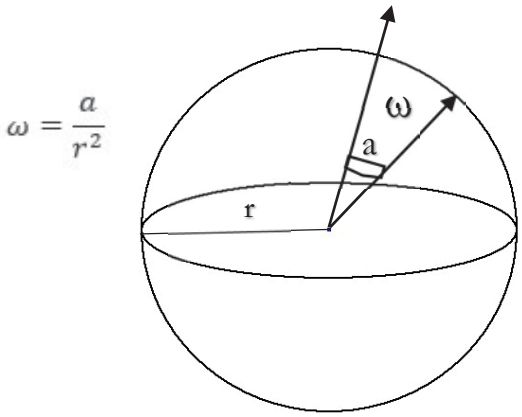

Fig. I-8. Solid angle.

The dimensionless unit of a plane angle is the radian, with 2π radians in a full circle. A solid angle, ω, is defined by a surface area, a, of a sphere subtended by the lines and by the radius of that sphere. The dimensionless unit of a solid angle is steradian, with 4π steradians in a full sphere. [20]

The term *intensity* can be used in many disciplines, some even closely related to optics. It should be the context, which determines the meaning of the world in the particular situation.

Radiance, L, describes the intensity of optical radiation emitted or reflected from certain location on an emitting or reflecting surface in particular direction [21]. Since the eye is an optical system, radiance and luminance are good indicators how bright an object will appear.

5.2 Photometric quantities

Photometry measures the response of the human eye to the light. This response has been standardized by CIE (Commission Internationale de l'Éclairage) 1924 luminous efficiency function and may be used to convert radiant energy into luminous (visible) energy. [20]

The luminous flux (power) in a light source is defined by the photopic luminous function. The following equation calculates the total luminous flux in a source of light:

$$\boldsymbol{\Phi_V = 683.002\ \frac{lm}{W} \cdot \int_0^\infty \bar{y}(\lambda)\Phi_e(\lambda)d\lambda} \qquad \textbf{1)}$$

where Φ_v is a luminous flux, Φ_e is a radiant flux, y(λ) is a dimensionless luminosity function and λ is a wavelength. Factor 683.002 comes from the fundamental definition of the luminous intensity, the candela.

Knowing the luminous flux, we are able to define illuminance, which is the total luminous flux incident on a surface, per unit area. The unit of illuminance is either lux or lumens per square meter.

Luminous efficacy, in lumen per watt, is a measure of the ability of a light source to produce a visual response from its power. In the photopic regions, luminous efficacy peaks

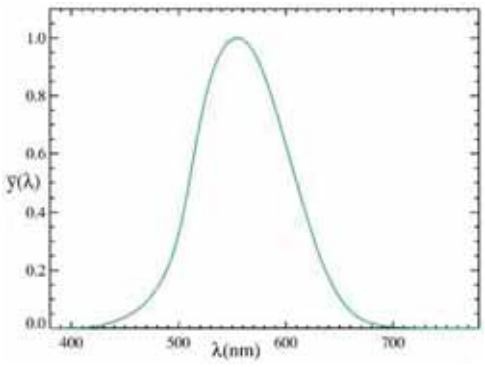

Fig. I-10. CIE 1924 luminosity. [16]

at 683 lumens per watt at 555 nm. The definition is in terms of candela. [20]

Luminescence is emission of light by a substance not resulting from heat but a form of cold-body radiation. It may be caused by chemical reactions, electrical energy, subatomic motions or stress on crystal. We can distinguish some types of luminescence [22]:

- chemiluminescence – the emission of light as a result of chemical reaction,
- crystalloluminescence – produced during crystallization,
- electroluminescence – a result of an electric current passed through a substance,
- mechanoluminescence - a result of a mechanical action on a solid,
- photoluminescence – a result of absorption of photons,

- radiolumiescence – a result of bombardment by ionizing radiation,
- thermoluminescence – the re-emission of absorbed energy when a substance is heated.

5.3 Color Rendering Index

The quality of a light source is defined as dependence on what is illuminated or what are we looking at. The spectral power distribution of light from an illuminated surface is a product of the spectral reflectance of the surface and the spectral power distribution of the light, falling on the surface. The ratio of the light quality is basically comparison the color impression of defined color sample under illumination by the light source under consideration and some sort of standard light source. This result in Color Rendering Index (CRI).

In general CRI measures the ability of the light source to accurately render colors as compared to standards. The CRI (R_a value) is a scale from 0 to 100, which rates a light source by comparing the color appearance of eight color viewed under a standard illuminant. These colors are defined by International Commission on Illumination (CIE). They also precise the definition of different CRI levels. In general, the higher CRI, the better color rendering – value of 100 means source identical to standard illuminant (for example incandescence lamp). A CRI more than 90 gives very good rendering index, between 80 and 90 (found in some fluorescent lamp, metal halide lamp and diode with phosphor light sources) is good, and between 60 and 80 we can talk about just sufficient CRI value. Low CRI, under 60, is found in discharge lamps like sodium or mercury lamps.

CRI is coupled to particular reference source should have the same correlated color temperature (CCT). Two standard light source for different correlated color temperature can show different color rendering index. It means two light sources with the same CRI, but different CCT may show differences in the color rendering index as well. Moreover, even two light sources with the same CRI and the same CCT can show differences in color appearance. This is caused by the definition of general color rendering index, which is the average of eight special color rendering indices. One light source can render color 1 most, the other color 2. However, for high CRI, above 90, none of eight special indices is shifted considerably more than others. [12]

Different light applications require different CRI value. Table below presents the desire approximates values of R_a for different illuminations.

Table I-1. Values of Color Rendering Index required for different application.**[23]**

Application	R_a
Indoor retail	90+
Indoor office/home	80
Indoor work area	60
Outdoor pedestrian area	60+
Outdoor general illumination	40-

Recent studies show [24], that calculations of CRI based on only 8 colors are not sufficient for new sources of light (like LEDs or OLEDs). If a light source has a discontinued spectrum, which maximum values are lower than references values, CRI can be bad, but color perception may be good. In contrary, in some situations, CRI could be good, but rendering of some colors not.

5.4 Correlated Color Temperature

Simple way to characterize the color of a light source is the correlated color temperature (CCT) measured in Kelvins [K]. While in reality the color of the light is determined by the spectral power distribution, the color can be still summarized on a linear scale the CCT. However, light sources with the same CCT may vary widely in the quality (CRI). Also continuity of spectrum stays independent from CCT. In general, correlated color temperature is useful to classify light sources for different field application. A low CCT implies warmer light (closer to the red) while higher value – colder light (more blue). Daylight has a value if temperature around 6500K Near dawn this value is rather low. Nevertheless, CCT does not imply that the light source is at that temperature. The correlated color temperature is obtained by comparing the light source to a black body radiator (Planckian radiator) of a given temperature and characterizing the light source by the temperature of black body radiator which has the same chromaticity to it on CIE chromaticity diagram. CCT refers to the temperature to which one would have to heat a Planckian radiator to produce the light of the same visual color. The preferred colors are between 2500 and 7500 K. Warm light is defined between 2500 and 3300 K, neutral white between 3300 K and 5000 K and daylight between 5000 and 7500 K. [12]

The examples of CCT provide the table 2.

Table I-2. CCT for different sources **[25]**.

Source	Temperature [K]
Low pressure sodium lamp	1700
Candle flame, sunrise/sunset	1850
Standard incandescent lamp	2400
Warm LED lamp	3000
Horizon daylight	5000
Daylight	6500
LCD screen	6500-9500
Clear blue sky	15000-27000

6. Sources of Light

The first commercial technology for lighting was popularized in the 19th century. The source of light based on natural gas served thousands of streets, offices and homes. The competition with Edison's incandescent lamp even led to improvement of gaslight by use of mantles soaked with the rare-earth compound thorium oxide, which converted the gas flames heat energy and UV radiation into visible radiation. However, after a time, incandescence lamp demonstrated in 1879, replaced completely the gaslight. Fluorescent tubes and compact fluorescent lamps became widely available after 1950. Along with high intensity discharge lamps, they offer a long-life and lower power consumption. As before incandescence sources of light had replaced gaslight, at the end of 20th it was century fluorescent tamp that became the mainstream technology in lighting. Unfortunately, fluorescence lamp suffers from a luminous power limit. In contrast, solid state lightning sources is not limited by fundamental factors but rather by the imagination and creativity of engineers and scientists [26]. To understand more the evolution of the lighting sources, their possibilities and principle of working, the main lamp sources are described below.

6.1 Sun

The human's eyes are adapted to the sunlight, inside of the atmosphere, at the sea level. Generating the light with similar spectral power distribution as sun would be perceived as desired one. However, even a spectral power distribution not quite similar to the sun one, may produce good light with respect to the color rendering.

The sun is a hot body. Its surface temperature is around 5778 K. The temperature of outer atmosphere of the sun is about 10^6 K. On the other hand, the center of big sunspot the temperature can reach lower value as 4300 K. The spectrum of the sun can be compare with radiation coming from black body, calculated with the Plank radiation formula. The black body of about 5800 K matches the solar spectrum best, however, this temperature strongly depends on the position of the observer on the earth surface, height above the sea, the position of the sun and the season. [12]

6.2 Incandescent lamps

6.2.1 Traditional incandescent bulb

The incandescence lamp was the second form of electric lamp developed for commercial use, just after carbon arc lamp. It was Thomas Edison, American researcher and businessman and Joseph Swan, British chemist, electrical engineer and inventor, who contrived the incandescence filament lamp in 1879 [27]. This source was also the first success in producing light without combustion, odor or smoke.

Incandescence bulb works by sending an electric current through a filament material and the resistance creates heat. Atoms in the material absorb energy. Electrons around the atoms are excited and temporarily reach an orbital which is further from the nucleus. When the electron orbit collapses to a lower orbital, it ejects the extra energy in the form of a photon.

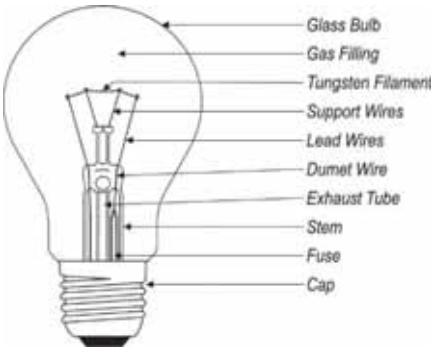

Fig. I-11. Incandescent bulb.[19]

Incandescence is a thermal radiation. Heat is constantly emitted from the objects in the invisible, infrared form. When heat gets intense enough, it reaches the visible wavelengths. It starts from red and goes up through the spectrum. Unfortunately, the most heat energy of incandescent bulb is emitted in infrared spectrum, which makes this source of light highly inefficient. [28]On the Fig. I-11 elements of incandescence bulb are presented. The bulb body is made of soda-lime silicate glass. The filament material is invariably tungsten. This material has the high melting point and low vapor pressure. In spite of its high melting point, the peak of its emitted light lies in infrared region. Support wires are supporting the filament wires. The lead wires are made of nickel. Cap is usually made of aluminum or brass.

To decrease the heat conduction loss from the filament into the surrounding gas, the

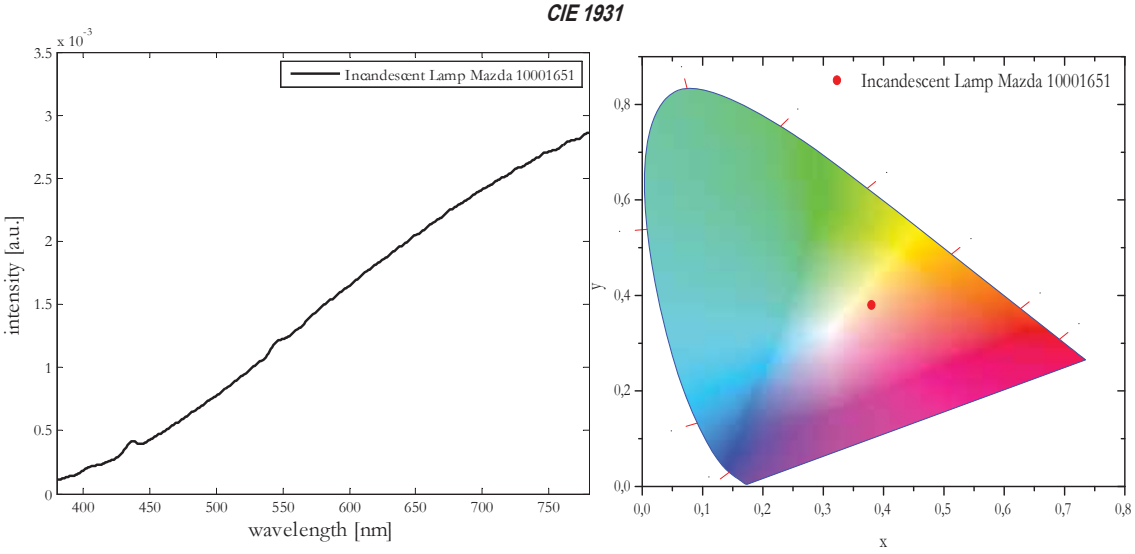

Fig. I-12. Example of spectrum and chromaticity coordinates of incandescent lamp (ref. Mazda 10001651).

filament was twisted and turned into shape of helix.

The advantages of incandescent light bulb are definitely their low cost, possibility of dimming, by voltage adjustment, very high CRI (100 – see Fig. I-12) and instant ON/OFF switching. Moreover, it is possible to obtain CCT in all variations, but the most commons are between 2700-5000. Unlikely, they suffer from short lifetime (1000 hours) and luminous

efficacy. The great disadvantage is also the heating effect, which lead to high running cost. [28]

6.2.2 Halogen lamp

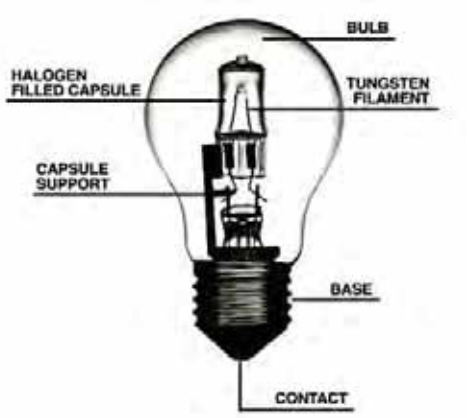

Fig. I-13. Halogen Lamp.

The halogen bulb is known as quartz halogen and tungsten halogen lamp. It is advanced form of traditional incandescence lamp. The halogen bulb has a tungsten filament similar to the standard bulb, nevertheless is much smaller for the same power and much stronger due to high pressure containing [29]. Its principle of operating bases on the evaporation of tungsten and its reaction with the halogen (iodine or bromine), which leads to forming a tungsten halide. Near the filament, which is hot, the tungsten halide dissociates, liberating tungsten again, which redeposits on the filament, replenishing the tungsten loss. Thus, the lost tungsten is recovered to the filament by virtue of halogen reaction cycle. This process prevents from weakening and malfunction of the filament.

Halogen bulb can be operated at a higher temperature, resulting in a little higher luminous efficacy than the traditional incandescent lamp and the same lifetime as a traditional bulb [27]. Also, the glass constituting the bulb body must be made of superior quality, like: alkali-free hard glass or fused silica.

The advantage of halogen bulb is definitely its possible small and compact size. The downside is, similar to traditional incandescence bulb, high surface temperature and still low luminous efficacy. Also, its high Color Rendering Index has to be mentioned (100) as an advantage. Color Temperature obtained with these lamps is around 2800 – 3400 K.

6.3 Low pressure and high pressure sodium lamps

In sodium vapor lamp electric discharge takes place in sodium vapor, which may be filled either at low or high pressure. These lamps are mainly used for street lighting.

6.3.1 Low pressure sodium lamp

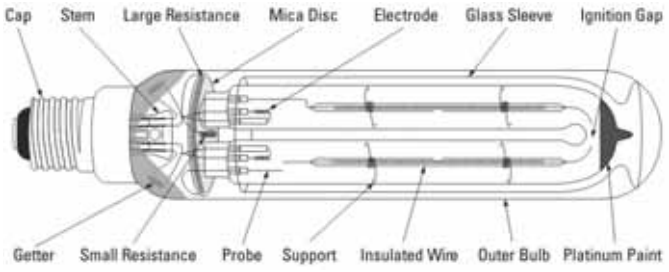

Fig. I-14. Low Pressure Sodium Lamp. [20]

To obtain an optimal efficacy the sodium vapor is kept at low pressure, which calls for a discharge tube of large dimensions having a relatively low operating temperature. This permits the usage of ordinary type of glass. Nevertheless, in term of chemically corrosive sodium vapor, a protective layer of borate glass is blown onto inner surface of the glass tube. The U-shape of tube is used to reduce the length of discharge tube. Tube is dosed with metallic sodium and usually some neon-bases rare gases, to facilitates starting. To ensure high efficiency of the lamp, the thermal insulation is required, which is provided by mounting it inside a secondary outer bulb. Current is supplied by electrodes at their end.

Definitely, the advantage of LP sodium lamp is their high efficiency. Also, they are very powerful and do not suffer lumen output drop with the age. However, these lamps have very low Color Rendering Index – around 45 and gives orange light: Correlated Color Temperature is around 1800 K. Sodium, as a gas, is very hazardous material, which can combust when is exposed to the air. [30]

6.3.2 High pressure sodium lamp

The high pressure sodium lamp has a narrow arc tube supported by a frame in a bulb. The arc tube has a high pressure inside. It usually contains sodium, mercury and xenon.

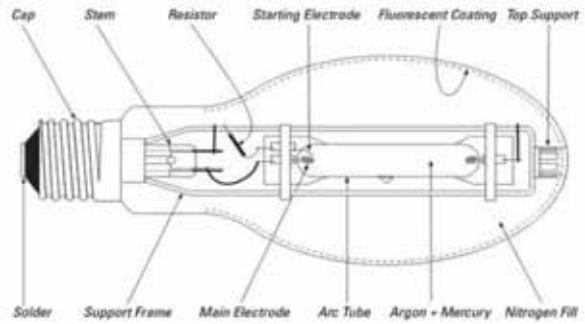

Fig. I-15. High Pressure Sodium Lamp. [21]

The arc tube is made of aluminum oxide ceramic which prevents the corrosive effect of alkalis. Inside of bulb there is an ignitor which sends a pulse of high voltage. This pulse starts an arc through the xenon gas. Subsequently, the arc heats the mercury, vapors and heats the lamp, which lead to heating the sodium. The sodium vapor strikes an arc over

240°C. The blue color of mercury and xenon, mixed with red color of sodium helps to create more white light. [31]

HP sodium lamp compering to LP has few advantages. It offers smaller size, can be used in many fixture types. Also, the lifetime of bulb itself is longer. On the other hand, it still suffers from low CRI (40) and offers the same color of light.

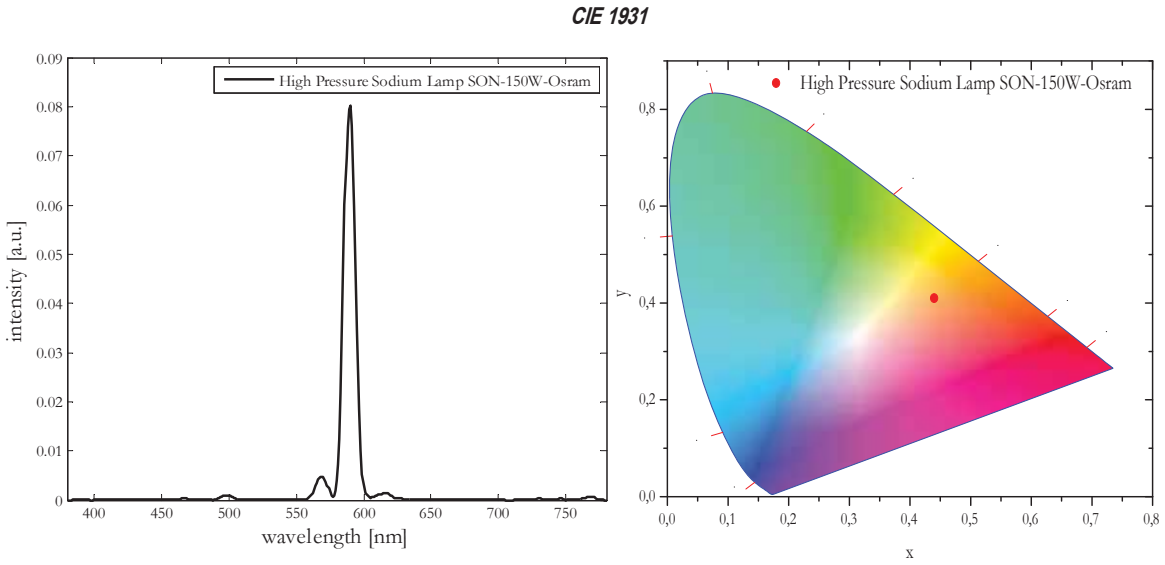

Fig. I-16. Example of spectrum and chromaticity coordinates of high pressure sodium lamp (ref. SON-150W-Osram).

6.4 Fluorescent lamp

The fluorescent lamp is a low-pressure mercury discharge lamp. The two resonance lines of mercury in the UV part of the electromagnetic spectrum are converted into visible light with the help of fluorescent material. The materials used in these lamps have two properties: phosphorescence – light emission some time after irradiation and fluorescence – light emission as long as material is irradiated. [12] This material is coated on the inside of the discharge tube and should have an absorption maximum at 185 and 253 nm. The emission band of fluorescence powder should be a wide one in the visible part of the electromagnetic spectrum.

The spectral power distribution can be adjusted to the specific demand by the proper choice of fluorescence powder. This allows to provide the desired Color Rendering Index, Color Temperature or spectral power distribution.

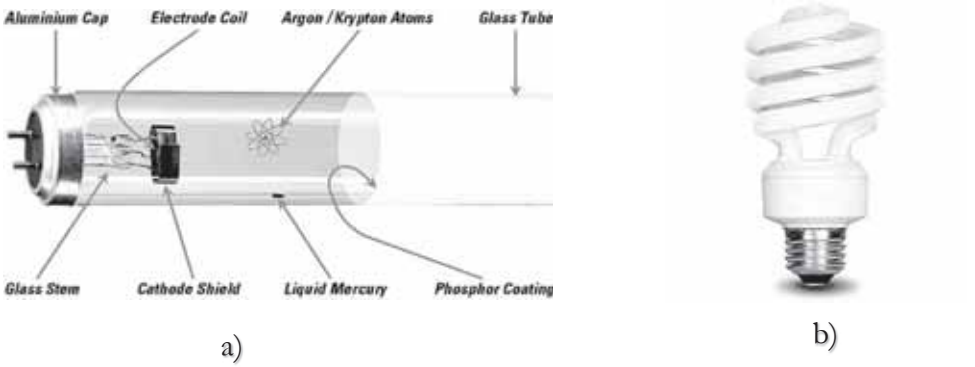

Fig. I-18. Fluorescent tube (a) [22] and compact fluorescent lamp (b).

Fluorescent lamps are typically long, thin cylinders. At each end of cylinder, an electrode

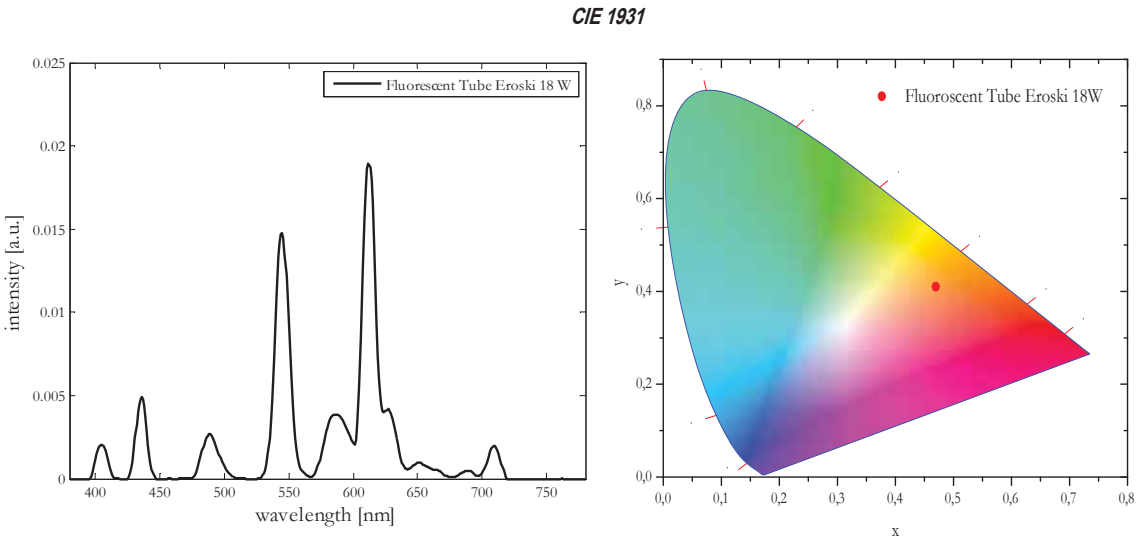

Fig. I-17. Example of spectrum and chromaticity coordinates of fluorescence tube (ref. Eroski 18 W).

mount is sealed. Its cap contains pin connectors for fixing the tube in the fixture on the wall. The electrode mount carries a cathode is made of coiled tungsten wire. The length and the diameter of tube are carefully chosen. The length is determined by operating voltage. For the efficient UV production, an electric field of 1V/cm is required. The width decides about the losses. Too narrow tube can cause rise of losses due to electron bombardment. In contrary, too wide tubes can suffer from losses in UV transportation. The standard lengths are from 15 to 25 cm and typical diameters are usually 1.5, 2.5 and 3.8 cm. It is also possible to find compact fluorescent lamp which are made by folding the discharge tube. [27]The main principle of tube operation, as all discharge lamps, is based on inelastic scattering of electrons. An incident electron collides with an atom in the gas used as an UV emitter. This causes an electron in the atom to temporarily jump to the higher energy level to absorb some of kinetic energy delivered by the colliding electron. The higher energy level is unstable and the atom will emit an ultraviolet photon as the atom's electron reverts to the lower, more stable energy level. The photons released from the chosen gas mixture tend to

have a wavelength in the UV part of spectrum. This part is invisible to a human eye, so it needs to be converted to visible part of light. This is done by fluorescent conversion, which occurs in phosphor coating on the inner part of tube. UV photons are absorbed by electrons in the phosphor's atoms. The phosphor emits the light visible to the human eye. The energy between absorbed UV and emitted light goes to heat up the phosphor coating.

Fluorescent lamps are negative resistance devices, so as more current flows through them, the electrical resistance of the fluorescent lamp drops, allowing even more current to flow. The direct connection to constant voltage mains power line of these lamps would cause rapid self-destruct due to the unlimited current flow. As a prevention, the fluorescent lamps must use a device caused "ballast", to regulate the current flow through the tube (usually reactance – inductor or capacitor). The fluorescent lamps convert more of input power to visible light than incandescent lamps. They also reach good Color Rendering Index Value (over 80, depending on the quantity of powders used in the lamp) and can produce any shade of white (warm/cold). Their low cost is also big advantage. Unfortunately, they contain toxic mercury vapor. The common problem is also the flickering of the light on 50 Hz ferromagnetic ballasts. This issue can be resolved by electronic ballast, which increase the frequency and efficiency, nevertheless it also decrease the cost of lamp. However, the fluorescent lamps have replaced many applications of incandescent lamps with its superior life and energy efficiency. [12] [32]

6.5 Solid-State Lighting

The costs of producing electricity are extremely high. Moreover, not only price in euros in high – there is also environmental cost of smog and carbon dioxide pollution associated with electricity production.

About 20% of electricity is used for lighting. The most widely used sources of artificial illumination are incandescent and fluorescent lamps, but Solid-State Lighting (SSL) devices promise to replace conventional light sources with impression economic (estimated cut by 50% of energy use for lighting) and environmental (reduce of emission of greenhouse gases, acid-rain causing SO_2 and mercury pollution) savings. Table 1 presents the energy consumption comparison between conventional sources and SSL source example (Light Emitting Diode source). [26][4]

Table I-3. Light output: comparison between LED vs. Incandescent and Fluorescent. **[33]**

Light Output	Light Emitting Diodes	Incandescent Bulb	Fluorescent Compact Lamp
Lumens	**Watts**	**Watts**	**Watts**
450	4-5	40	9-13
1100	9-13	75	18-25
2600	25-28	150	30-55

Benefits of some savings are not the only ones. SSL devices are vibration and shock resistant and also exceptionally long-lived. They allow for a wide variety of lighting, including artificial lighting similar to daylight. SSL sources, with appropriate circuitry, have color and intensity easily controlled. Moreover, since the SSL devices can be coupled to the light pipes, light may be flexibly and easily distributed. Also, from the point of design they offer a lot of possibilities: they can be placed on the floors, walls or furniture. [4]

SSL sources can be made from organic or inorganic semiconductors. SSL devices that use inorganic semiconductors are Light Emitting Diodes (LEDs) and Laser Diodes (LD). A light emitting device built with organic semiconductor is an OLED. Below, the detailed description of SSL devices is presented.

6.5.1 Light Emitting Diodes

The history of LEDs reaches 20s' and their invention was based on the another discovery – the phenomenon of luminescence. The essential elements of LEDs are electron-carrying n-layer and a hole-carrying p-layer, placed on substrate. First LEDs were based on gallium nitride (GaN) and a substrate of sapphire. Later, the GaN doping was replaced by InGaN by Nakamura. [1][34] Recently, OSRAM demonstrated InGaN LEDs grown on silicon substrate. [35] Regardless the material type, the principle of working does not change. When a forward voltage is applied to the structure (negative to the n-layer, and positive to the p-layer), electrons are injected from the n-layer and holes from the p-layer. Electrons and holes can radioactively recombine, emitting a photon. The wavelength and color of the photon is determined by the different of the energy levels of the electrons and

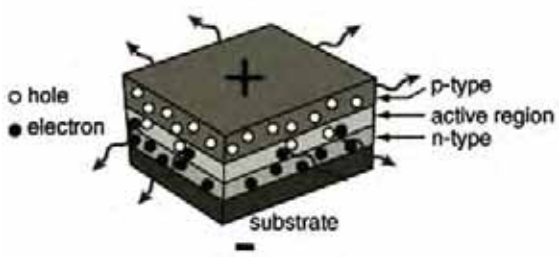

Fig. I-19. Structure of LED. [24]

holes. [4]

Generally, three different approaches of white light generation can be distinguished. The first one base on mixing blue, red and green LED, second let us obtain white light by

coupling ultraviolet LED to stimulate RGB phosphor and the third one gives us a white light from excitation the yellow phosphor by blue LED.

RGB-LEDs has an obvious advantage. The desire color point can be simply achieved by adjusting of RGB ratio illumination. Additionally, one lamp can provide a range of color temperatures. Unfortunately, since a RGB system requires 3 diodes, their individual degradation process may influence on the color stability or variation of driven current. Moreover, the RGB LEDs require different driving currents for different color LEDs, complicating their production and increasing the cost. [4][23]

Coupling n-UV LED with RGB phosphor or blue LED with yellow phosphor base on the same rule. In the n-UV-LED-based white light, a 405 nm diode excites RGB phosphor, to emits in RGB regions. The n-UV light is partly absorbed by blue phosphor. The rest is mixed with emission in blue, red and green, which appear as a white light. In blue LED with yellow phosphor, the diode excites the yellow, and mixing with non-converted blue light from diode also appears as white. [36]

Fig. I-20. Blue LED coated with yellow phosphor.

Today, the blue LEDs with yellow phosphor are well commercialized. However, n-UV diodes has a big potential due to their higher optical stability. Typical LEDs are usually based on 450-470 blue chip covered with yellowish phosphor coating, normally made from YAG: Ce (Fig. I-20). Nevertheless, they suffer from some weaknesses. The Color Rendering Index is not so high (65) and the stability of the color is quite low. The instability in color comes from "efficiency droop" – loss in external quantum efficiency, as operating current increases. As LEDs efficiency decreases, with higher operating currents, the result is an increase of the temperature of a device, since the efficiency is lost as a heat. The increased temperature of the device will also affect phosphor, causing a decrease in an efficiency and a possible shift in the peak emission wavelength of the phosphor. These changes in the LED

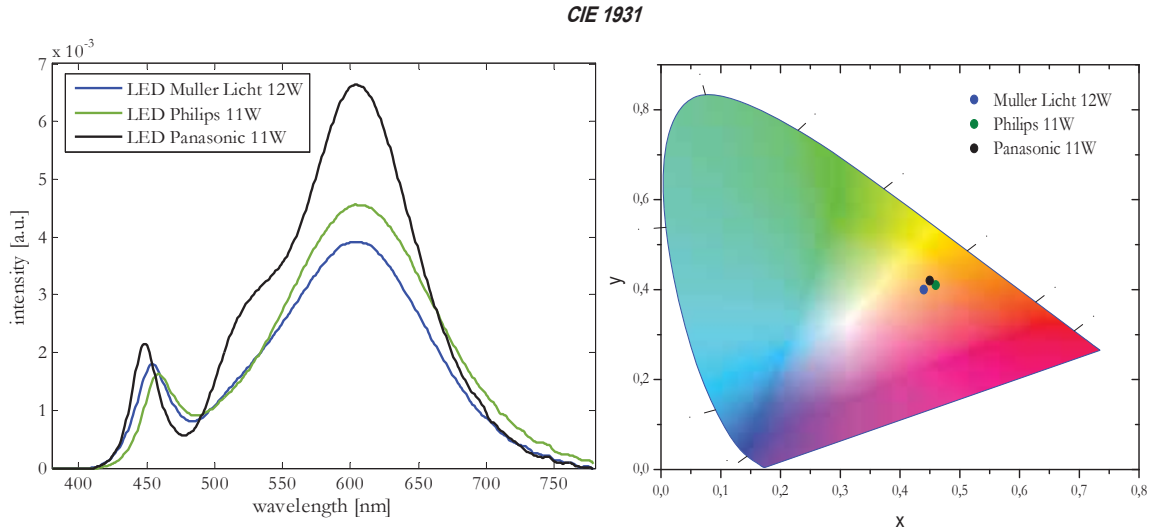

Fig. I-21. Example of spectrum and chromaticity coordinates of LEDs (Ref. Muller Licht 12W, Philips 11W, Panasonic 11W).

spectrum and phosphor will change the ratio of the light emitted by each component, resulting in a shift in color point of the white light, and decrease overall efficiency of the device. [37]

6.5.2 Organic Light Emitting Diodes

In the past years the organic light emitting devices have involved into a truly powerful display technology. They have ease of production, fast response time, wide viewing angle, low operating voltage and a promising application in area flexible, full color flat panel electronic displays. OLEDs displays are light and can be built on flexible substrates such as plastics and paper-thin-substrate. OLEDs are much more rugged and ideal for portable applications, comparing to LEDs. They are also self-emitting, and require neither backlight, nor chemical shutters that must open and close, making them thinner and compact. [38]

OLEDs are thin multilayer devices in which active charge transport and light emitting materials are between two thin film electrodes, of which at least one must be transparent to light. As an anode the transparent indium tin oxide is usually used, and for cathode it is generally a low work function metal such as Ca, Mg, Al or their alloys Mg:Ag, Li:Al. An organic layer with good electron transport and hole blocking properties is typically used between the cathode and the emissive layer. [39]

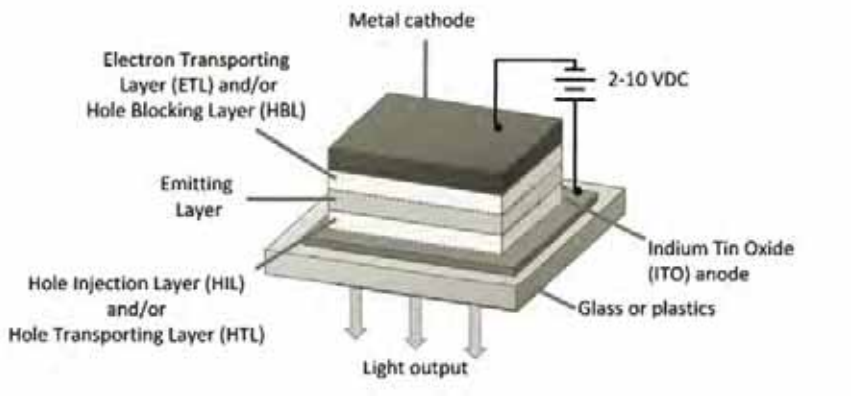

Fig. I-21. Structure of OLED. [33]

Obtaining a white light from OLEDs can base on mixing of colors. One of the approaches is having multilayer structure where simultaneous emission of light from two or more separate emitting layers with different emission colors results in white light. This method deals with many reactions between organic interface, which leads to interface barriers, which may result in inhibition of carrier injection and joule heating. [40]

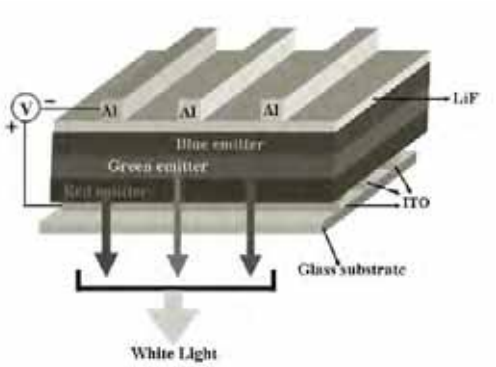

Fig. I-22. Multilayer oLED approach. [35]

Another approach for white light emission is a multiple quantum well structure, which includes two or more emissive layers separated by blocking layers. Unfortunately, this approach is difficult to achieve because it requires the optimization of thickness of various light emitting and blocking layers. [38]

Similar to LED, there is also possibility to get white light in down conversion by phosphor. This approach could be a solution for difficulties of different ageing process in different layers. In this technology blue OLED is coupled with phosphor, which contains inorganic light scattering particles. Unfortunately, the luminous efficiency is still relatively low, comparing to LEDs down converted by phosphor. [38]

OLEDs are promising technology, however, great efforts are necessary to improve the luminous efficiency and to decrease high operating voltage. Differential emitters having

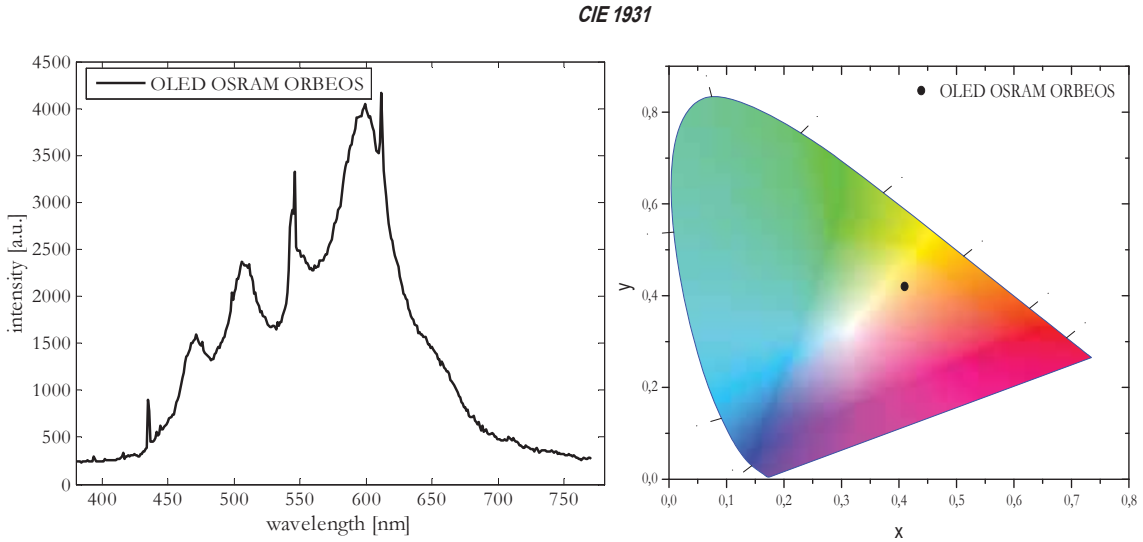

Fig. I-23. Example of spectrum and chromaticity coordinates of OLED (Ref. OLED OSRAM ORBEOS).

different aging time also caused this solution as a white light source less attractive.

6.5.3 Laser Diode

Due to LEDs' efficiency droop and OLEDs' aging and luminous efficiency issues, the laser diode is offered as an alternative of white light generation base [4]. Lasers are operating under stimulated emission and reach higher efficiency at higher input power densities comparing to LEDs. Blue LD as an excitation source has even more advantages. They have higher brightness at the same power level, they do not suffer the efficiency droop and also they can generate polarized light and have better monochromatic spectrum (narrow). Studies show [41] that luminous efficacy decreases with the increasing of excitation spectrum width.

The principle of working of a laser diode bases on application of DC voltage across the laser diode, which makes the free electrons move across the junction region from the n-type material to the p-type material. In this process, some electrons will directly interact with the valence electrons and excites them to the higher energy level whereas some other electrons will recombine with the holes in the p-type semiconductor and releases energy in the form

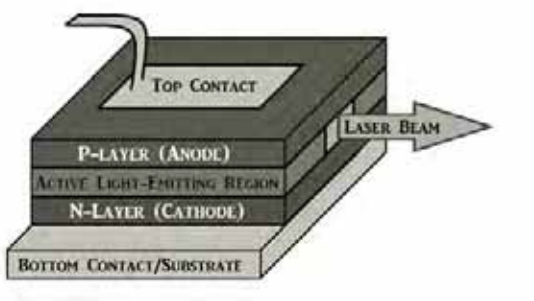

Fig. I-24. Schema of a laser diode. [36]

of light.

The lasers, similar to LEDs, can work based on different compounds. We can find diodes operating with manganese-selenide, zinc-selenide, manganese-sulfide etc. However, these materials still serve some stability problem, degrading rapidly, making commercial applications impossible. Other type of diodes based on InGaN/GaN compounds suffer from bigger amounts of defects, nevertheless, they are much more stable than the first group mentioned. [1]

One of the most promising solution of obtaining white light with a laser diode is coupling it with a suitable phosphor, as in case of LEDs. Either the yellow phosphor is excited by blue laser diode, or n-UV laser diode excites blue and yellow phosphor. This solution has been already commercially used in headlights of BMW.

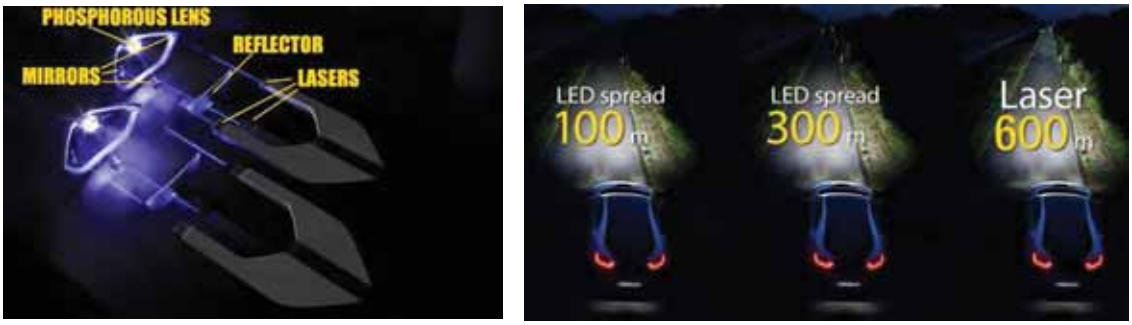

a) b)

Fig. I-25. Headlights based on laser (a) and comparison of distance seen with a laser diode and LED (b). [36]

As a subject of this thesis the development of a light source based on a laser diode was chosen. This device not only gives high luminance at relatively low operation power but also is small and compact. Additionally, having a high luminance allow us to operate in a distance or reflection mode with remote phosphor. This solution eliminates the thermal effects caused by increased temperature of the device, while supplied with a high injected current. Moreover, the elimination of thermal effects let us keep the stability of correlated color temperature and chromaticity coordinates. The laser coupled with different types of phosphor gives possibility of having a result different in color temperature (warm/cold light) and also rendering index, depending on material chosen.

7. Conclusions

In this chapter all the parameters characterizing the light were described. It was mentioned that the optimization of an artificial source of light should base on understanding of human eye, because its quality or efficiency is strongly related to the characteristic of an eye.

The light is described by some photometric and radiometric parameters. Radiometric quantities are flux, irradiance, radiant and luminous intensity and radiance. To photometric quantities belong: luminous flux, illuminance, luminous efficacy and luminescence.

Another parameter which describes quality of light is Color Rendering Index. The CRI measures the ability of the light source to accurately display colors as a compered to standards, in a scale from 0 to 100. Generally, CRI higher than 60 is required for indoor applications, and lower than 40 is tolerable only for outdoor general illumination.

Correlated Color Temperature is independent from Color Rendering Index and is useful to classify light sources for different applications. Low CCT implies warmer light (closer to red), higher values of CCT defines colder light. The warm light is defined between 2500 and 3300 and the cold one, below 5000. Between 3300 and 5000 we can talk about natural white light.

Subsequently, all basic sources of light were described briefly in this chapter. At the beginning the sun was mentioned as a natural source of light, and also as an example of a desired light source to create.

The traditional incandescent lamp was a first source of light without combustion or smoke needed. It was widely used all over the world. Unfortunately, due to its high emission in infrared spectrum, the lamp is inefficient. However, the accuracy of displaying the colors is equal to 100. To improve the incandescent lamps, the advanced form was offered: halogen lamp. Despite it can operate at higher temperature, which results in higher luminous efficiency, the value of this efficiency is still too poor. Nevertheless, their small size can be defiantly an advantage.

Sodium lamps are the sources of the light characterized with low CRI and low Color Temperature. These lamps are used mainly for street lighting application. On the other hand, the efficiency of these lamps is very high, however, sodium, their basic component, can be easily combusted, when exposed to the air.

Fluorescent lamps are low-pressure mercury discharge lamps, and it is them that replaced most of incandescent sources of light. First of all, they reach good CRI value, which is over 80 and can produce any shade of a white light. They superior life and energy efficiency was another reason of replacement of traditional bulb. However, they suffer some flickering of light on 50 Hz magnetic ballast and also contain toxic mercury vapor.

As an alternative, the Solid-State Lighting is offered. It can decrease not only the economic costs, but also the environmental. SSL sources are made from organic (OLEDs) or inorganic semiconductors (LEDs, laser diodes).

The most commercialized SSL source is Light Emitting Diode. Successfully, they started to replace the fluorescent lamps. The white light from LED can be obtained in three different ways: by mixing three diodes: red, blue and green, by coupling n-UV diode with RGB phosphor or by coupling blue diode with yellow phosphor. Today, the last method is the most popular. High luminous efficiency, low cost, compact size defiantly characterizes this method of getting artificial light. However, LEDs suffer from some loss in efficiency, when injected current increases. Due to this loss, some undesirable changings in color of light and chromaticity coordinates can happened.

Another source of SSL, more commercialized in different types of displays is OLED. They have high luminance, they need low operating voltage and also they can be built on flexible substrates. The promising technology, nevertheless, their luminous efficiency and too high operating voltage need to be improve. Moreover, due to different emitters in multilayers solutions and their different aging processes, they seem to be less attractive as long durable white light sources.

Finally, due to efficiency droop in LEDs, and OLEDs' aging and luminous efficiency issues, the laser diode is offered as a source of white light. This solution can be already found in BMW's headlights. Laser diode, in solution with down converted phosphor, can propose higher luminosity and intensity, at the same power level, the current and voltage increase linearly, without efficiency droop, and also the light generated by a laser have better

monochromatic spectrum. White light source based on laser diode assure more stability in Color Temperature and chromaticity coordinates.

Based on all this advantages of a laser diode, it has been decided to develop the source of white light coupled with suitable phosphors as a subject of this thesis.

Chapter II

White Light Based on Blue Laser Diode

Table of contents

White Light Based on Blue Laser Diode 55

1. Phosphor conversion 56
1.1 Quantum model of atom 56
1.2 Atomic orbitals 57
1.3 Configurational coordinate model 57
1.4 Material preparation 58
1.5 YAG:Ce^{3+} in silicon 59
1.6 GYAG:Ce^{3+} with Nitride in silicon 62
1.7 Phosphor on glass 64

2. White light 67
2.1 Transmission 67
2.1.1 Results – YAG phosphor 70
2.1.2 Results – GYAG with Nitride phosphor 73
2.1.3 Results – phosphor on glass 75
2.2 Reflection 78
2.2.1 Results 78

3. Optical power dependencies 79
3.1 Thickness and concentration 80
3.2 Number of particles 81
3.2.1 Calculation of particles number 81
3.2.2 Dependency on CCT and CIE coordinates 83

4. Conclusions 85

1. Phosphor conversion

A great contribution has been made to the development of phosphor for phosphor-converted white light sources, such as micro- and nano-solid material synthesis, functionalization and characterization and the emergence of novel luminescent materials. However, there are still a lot of challenges: improvement of luminous efficiency, stability or optimization of light parameters. To be able to improve these parameters, the very basics of conversion should be understood first.

1.1 Quantum model of atom

The theory of atom was developed in 1913 by Danish physicist Niels Bohr. [42] He explained that electrons can be found in specific places, and suggested that electrons orbit the nucleus of atoms in circles, with quantized orbital angular momentums at quantized orbital distances, known as shells. Each shell has a n value, where $n=1$ is the closest shell to the nucleus of the atom. Each shell is associated with a quantized energy and can only contain a finite number of electrons. It takes less energy for an electron to remain in the closest shell to the nucleus. No matter how little energy electrons have, they cannot move closer to the nucleus than the lowest possible shell.

It takes energy for an electron to move outwards, and it releases energy when it moves inwards. Energy is given and taken in the form of photons. This can result in atomic emission, fluorescence, and charge-exchange. Bohr also explains that electrons do not move gradually from one shell to the next. They seem to disappear from one, and appear in another. Absorption spectra occurs when atoms absorb photons and their electrons gain

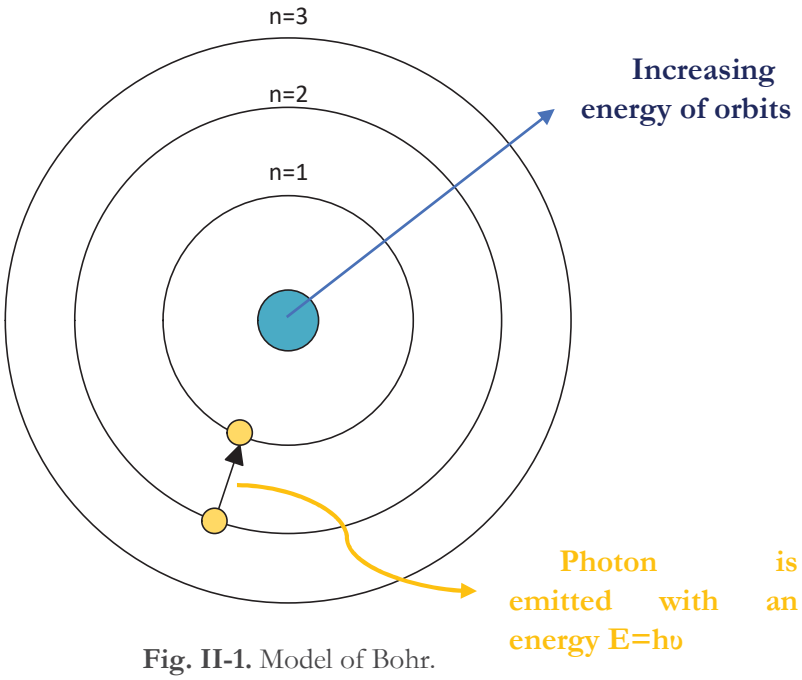

Fig. II-1. Model of Bohr.

enough energy to move into an orbit further from the nucleus. Following the Planck relation, his energy corresponds to a specific frequency of light, and therefore a specific wavelength is missing from the spectrum.

Emission spectrum occurs when electrons drop to a lower energy level and emit photons, again this light has an energy determined by the Planck relation, and the photons always have a specific wavelength. [43]

1.2 Atomic orbitals

An orbital is a quantum mechanical refinement of Bohr's orbit. In contrast to his concept of orbit with a fixed radius, orbitals are mathematically derived regions of space with different probabilities of having an electron. [44]

The quantum mechanical model describes: principal energy level (n), energy sublevel, orbitals in each sublevel and spins.

Principal energy levels indicate the relative size and energy of atomic orbitals. As *n* increases, the orbitals become larger, electron spends more time farther away from nucleus and atom's energy level increases. Principal energy levels are broken down into sublevels. Sublevels define the orbital shape (s, p, d, f)

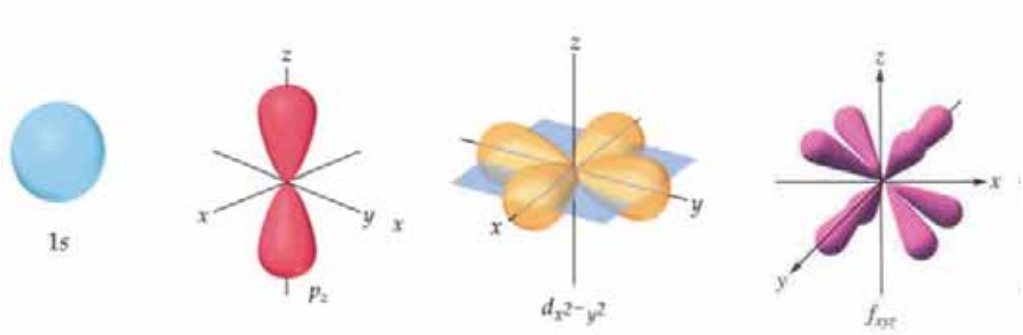

Fig. II-2. Sublevels.
[3]

Each sublevel has a different number of orbitals (s: 1 orbital, p: 2 orbitals, d: 5 orbitals, f: 7 orbitals). Additionally, electrons act like they are spinning on an axis – generates a magnetic field (no two electrons in the same orbital can have the same spin)

1.3 Configurational coordinate model

Fundamental aspect of phosphor-converted white light semiconductors is luminescence. Luminescence arises when atoms of a solid become energized in some way, without heating the bulk material. These atoms then release the excess energy in the form of ultraviolet, visible or infrared radiation. Since the phosphors are excited by the radiative

emission, the luminescence of the phosphor is expressed as photoluminescence. Photoluminescence usually involves the following processes: excitation of the activator to higher energy state, relaxation of the activator ion to the lowest energy level of the excited state and emission of lower-energy photon as the activator ion returns from its excited state to the ground state. To describe the photoluminescence mechanism of the activator, the configurational diagram is usually used (Fig. II-3). The total energy is plotted in the function of distance between metal cations and anions in the lattice. The horizontal dashed lines in ground state and excited state denote the vibration state. The r_0 and r_1 represent the equilibrium distances of the ground state activator and the excited state activator. The excitation (EX) and emission (EM) process are illustrated by vertical arrows. The energy difference between EX and EM is known as a Stokes shift (energy emitted is lower than the

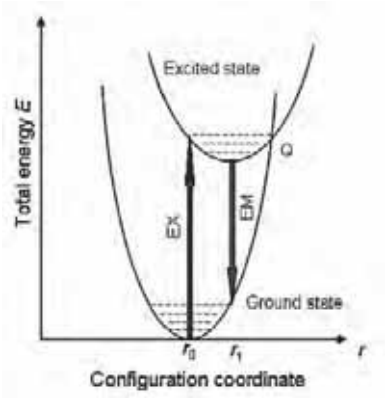

Fig. II-3. Schematic illustration of a configurational coordinate model. [1]

excitation energy).

The excited activator reaches the Q point and then return to ground state without radiation, when the temperature exceeds some certain value. This phenomenon is called thermal-quenching. [45]

Another important phenomenon which occurs in the phosphor converted method of obtaining white light is an energy transfer. The donor (which gives out protons, electrons of energy etc.) is the ion or group which absorbs energy in the form of light or excitation. Then the donor transfers an energy to another ion or group called acceptors, which could emit light and terminate the whole process.[45][46][47]

In the past few years, there has been much attention given to phosphors based on Eu^{3+} and Ce^{3+} activator ions for solid state lighting application. Ce^{3+} doped compound usually shows an emission in the near UV [48], but in a presence of high crystal fields such as in garnet, the visible emission is observed. [49]

1.4 Material preparation

The phosphors in two types of materials were used in this studies: two incorporated into silicon and three coated on the glass. Phosphors in silicon resin were prepared in

ICMCB laboratory in Bordeaux by ourselves. Phosphor in the glass was ordered directly from the distributor.

The technic used to produce the phosphor in silicon resin was sol-gel method. The phosphor arrived as a powder from Intematix company. A two-part high optical transparency silicon Dow Corning® EI-1184, in the form of gel, was used as a matrix. Silicon was filled with different powders (1.) to obtain two different kinds of materials: yttrium aluminum garnet doped with Ce^{3+} (NYAG4354 Intematix) powder (YAG) and mixture of green phosphor doped with Ce^{3+} (GYAG3856-01-13 Intematix) and red nitride phosphor doped with Eu^{2+} in ratio: GYAG/Nitride=4.5/1. Phosphors were incorporated at different weight (2.), to obtain different concentrations, in silicon plate of 15mm diameter. The weight of silicon to prepare 5 samples was 3.8g. After mixing (3.) silicon with powder, to remove air bubbles, the mixture was placed in the vacuum pressure chamber until no bubble emerged (4.). Subsequently it was put into special form to obtained wanted thickness and diameter. Then the form with composite samples was cooked at 120ºC for 20

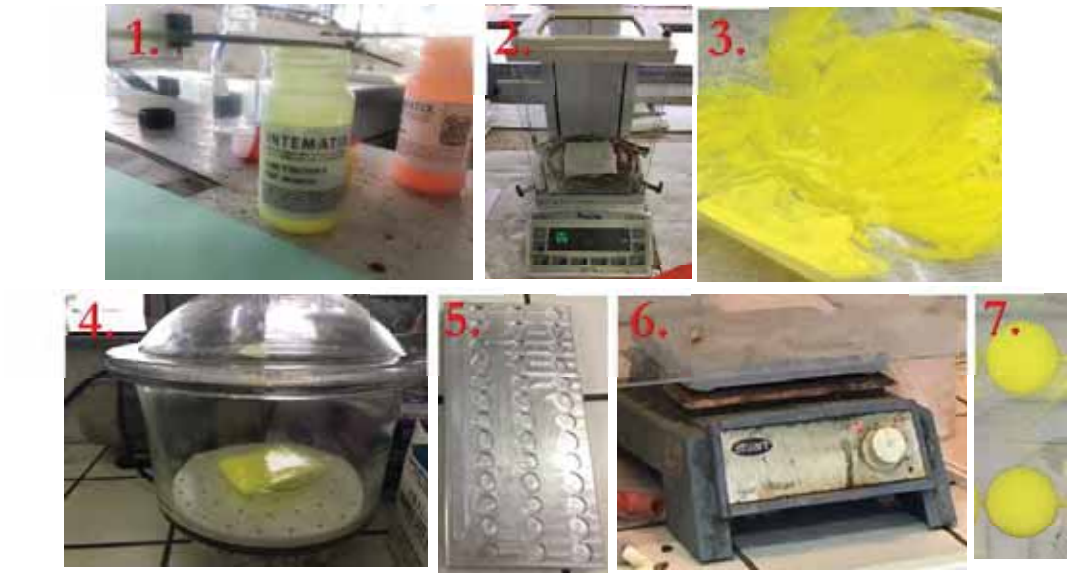

Fig. II-4. Sol-gel method of obtaining phosphor samples.

minutes on the heating plate (6.).

1.5 YAG:Ce^{3+} in silicon

YAG has been extensively used as a host for lasers and phosphors [50]. Since Ce^{3+} is a dopant that has a lower 5d state from which it can emit from the near ultraviolet to the visible, it produces new application over a wide spectral range. Moreover, studies show [49] that phosphors doped with cerium have an emission ranging from yellow to red. These properties are due to possibility of changing the amount of Y or Gd. This is similar to

studies, that increasing the ionic size on the dodecahedral site leads to a red shift in the emission. Increasing the amount of Ce dopant shift emission to slightly longer wavelengths. [51][52]

Fig. II-5. YAG:Ce^{3+}

To see the possibility of absorbance of YAG:Ce^{3+} used in this study, the analysis in spectrofluorometer in ICMCB laboratory was performed.

The spectrofluorometer Fluorolog is equipped in xenon lamp which allows to operate in full range of spectrum. The wavelengths from the lamp were send with step of 1nm from 200 to 525nm, to pass by material. The light is absorbed by phosphor and causes some emission. However, the energy from not all the wavelength is able to excite particles, to cause a yellow emission. On Fig. II-4, the

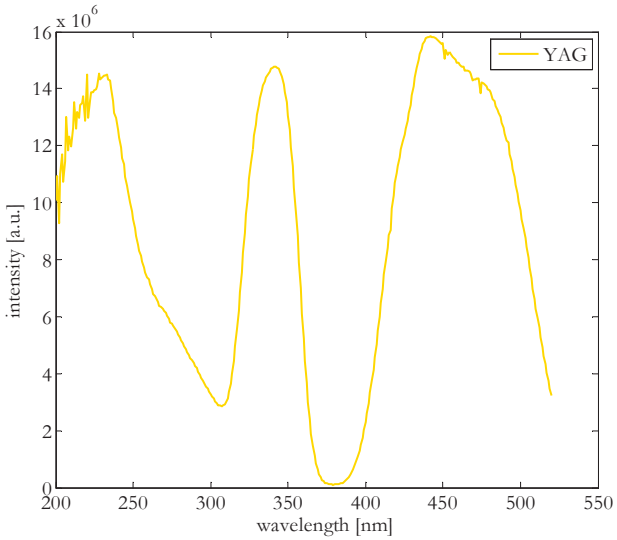

Fig. II-4. Excitation spectrum of emission of YAG:Ce^{3+} for different wavelengths absorbed.

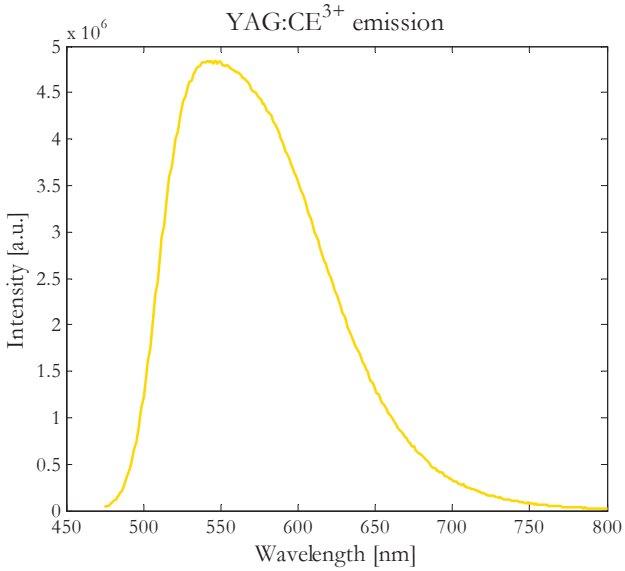

Fig. II-5 YAG:Ce^{3+} emission.

excitation spectrum, by looking the emission at 550 nm is presented.

Due to the characteristics of YAG emission, it can be noticed that the maximum of emitted light corresponds to 440 nm. Nevertheless, it is possible to get a yellow light by exciting a material with a source in a range 200 nm to 370 nm and starting from 390 nm. However, the emission will be not optimal.

The emission of the material after excitation by 445 nm is presented on the Fig. II-5. The band is around 550 nm. We can observe a small asymmetry which corresponds to the ground state doublet of Ce^{3+} ($^2F_{5/2}$ and $^2F_{7/2}$), noticeable on the energy level diagram.

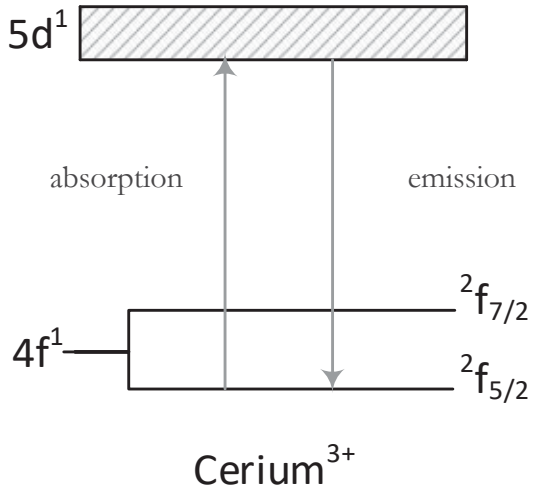

Fig. II-6. Energy level diagram showing the excitation and emission of cerium in YAG.

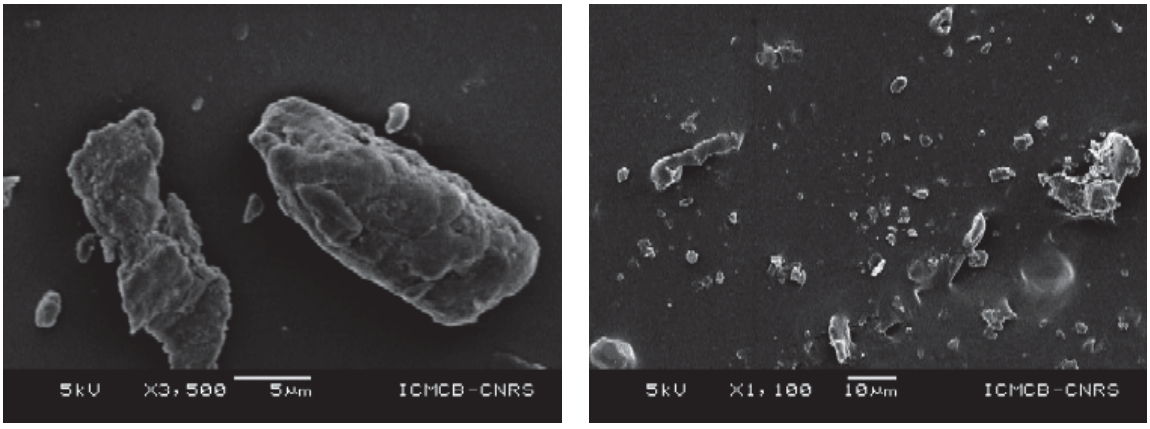

Fig. II-7. SEM pictures of phosphor particles of YAG.

Fig. II-6 shows a schematic energy level diagram for cerium. The ground state for cerium is $4f^1$. Excited by photon, electron from $4f^1$ goes to $5d^1$ (excited state). Orbital 5d is

an orbital external. Its energy is influenced by host material: YAG ($Y_3(AlGa)_5O_{12}$). As mentioned before, the wavelengths of excitation and emission can be easily modified, by modification of certain atoms.

The density of used phosphor powder is 4.8g/cm^3, the size of the particles around 18 μm. On Fig. II-7 the pictures done by SEM (Scanning Electron Microscope).

1.6 GYAG:Ce^{3+} with Nitride in silicon

This phosphor sample contains two types of compounds: GYAG doped with Ce^{3+} and Nitride doped with Eu^{2+}. GYAG is similar material to YAG, but has modified elements ($Y_3Al_5O_{12}$) to decrease the crystal field (related to the electronic cloud surrounding the 5d ions [53]) around the cerium and to increase the energy between ground state and excitation state.

Fig. II-8. GYAG: Ce^{3+} with Nitride

Nitride phosphors has received significant attention in recent years due to its encouraging luminescent properties: excitability by blue light, high conversion efficiency, possibility of full color emission, low thermal quenching, high chemical stability and high potential to use in phosphor-converted lighting.

Nitride compounds are a large family of nitrogen-containing compound that are formed by combining nitrogen with less electronegative elements. Covalent nitrides can be considered as a host lattice for phosphor because of their characteristic of an insulator or semiconductor and wide band gaps. Furthermore, the covalent chemical bonding in nitrides gives rise to a strong nephelauxetic effect, reducing the energy of the excited state of the 5d electrons of the activators. This results in long excitation/emission wavelengths and low thermal quenching, which cannot be achieved in conventional phosphors. From rare-earth ions with the 5d electrons unshielded from the crystal field by the 5s and 5p electrons when it excited state, the spectral properties are strongly affected by the surrounding effect (for example symmetry – see Fig. II-11, also covalence, coordination, bond length etc.) Because

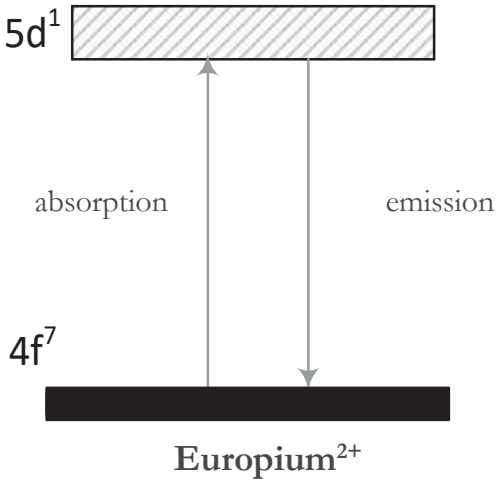

Fig. II-9. Energy level diagram showing the excitation and emission of europium in nitride.

of the higher formal charge of N^{3-} compared with O^{2-} and the covalence, the crystal-field splitting of the 5d levels of rare earth is larger and the center of gravity of the 5d states is shifted to lower energies (longer wavelengths). Consequently, nitride phosphors show longer excitation and emission wavelength. Moreover, the Stokes shift become smaller in a rigid lattice. A small Stokes shift leads to high conversion efficiency and small thermal quenching of the phosphor. [54]

On Fig. II-10 we can find the optimum wavelength for excitation. For GYAG (a) the best wavelength excitation would be 445 nm, for nitride (b) it is more n-UV light of 395 nm.

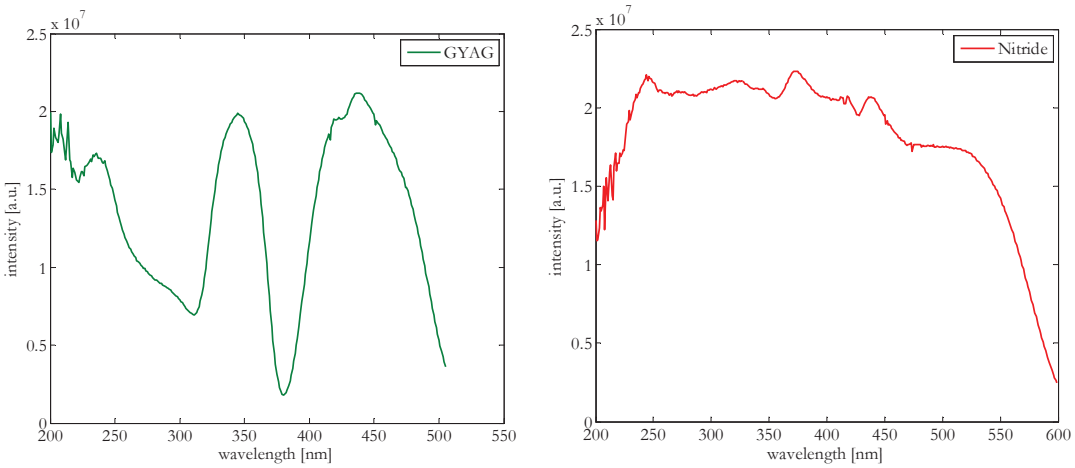

a) **b)**

Fig. II-10. Levels of emission of GYAG:Ce^{3+} and nitride:Eu^{2+} for different wavelengths absorbed.

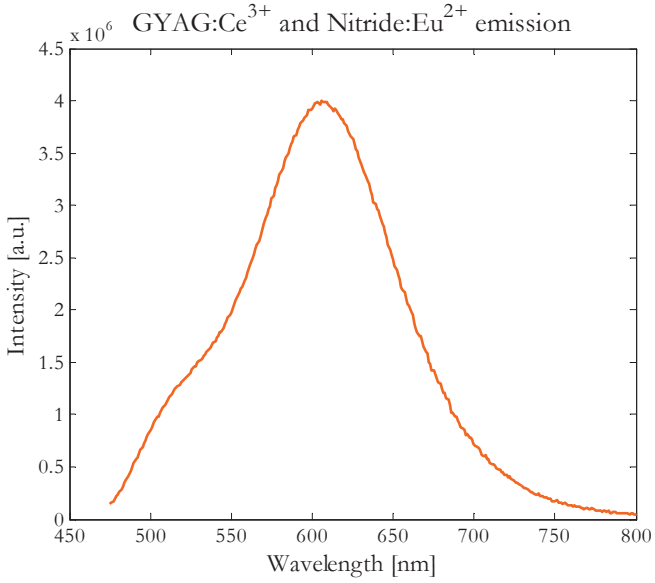

Fig. II-11. GYAG:Ce^{3+} and nitride: Eu^{2+}emission.

From the emission on Fig. II-11 we can observe, as mentioned before, symmetry in europium emission, which corresponds to the band of 625 nm. Band of 528 nm corresponds to emission of cerium. What characterize GYAG is also its shorter wavelength green range emission than in classical YAG. Mixing GYAG (yellow-green) with nitride (red)

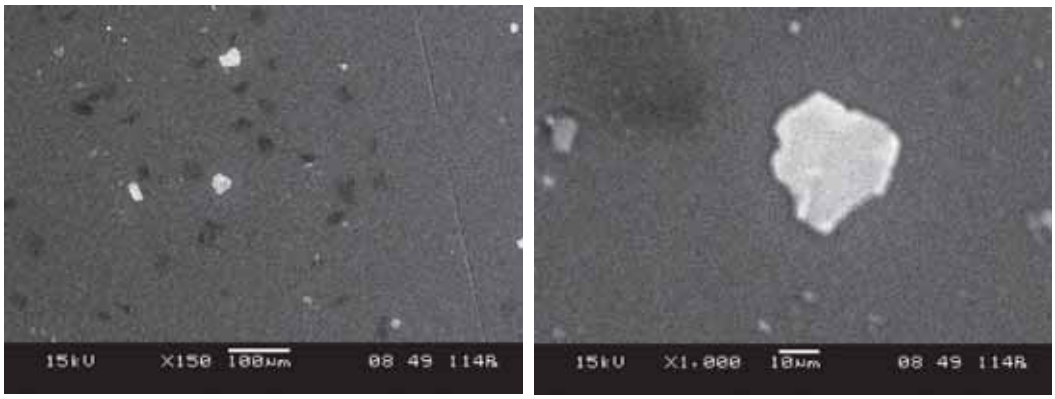

Fig. II-12. SEM pictures of phosphor particles of GYAG and nitride.

allows us to obtain wide-spectrum source of light, which may lead to high CRI value.

On Fig. II-12 we can observe the particles of phosphor under SEM microscopy. Their size is 13 µm.

1.7 Phosphor on glass

Due to degradation process of organic resin such as silicon while aging (see Chapter III), inorganic color converter such as phosphor ceramic, phosphor-in-glass (PiG) or phosphor on the glass are starting to replace conventional color converters, especially for high power and high brightness applications. Phosphor ceramics are sintered phosphor powder which can guarantee high conversion efficiency [55]. However, to make the transparent ceramic plate high temperature over 1600°C and high pressure are required, resulting in high production cost. Phosphor on glasses are simple mixtures of phosphors coated on transparent glass powders which can be sintered at temperatures lower than

Fig. II-13. Sample of phosphor on glass

800°C [56].

Along with their easy fabrication process, their color coordination can be also easily controlled simply by varying the phosphors, mixing the rations and the thickness. Moreover, glass shows it superiority as encapsulant over phosphor-in-silicon (PiS) in terms of its physical/chemical performance, thermal stability (which can solve the problem luminous degradation and color shift) causing by yellowing and carbonizing under long-term heat radiation coming from diode. [57] [58]

The samples of phosphor coated on the glass used in this study are, provided by Intematix: CL-750-R45-XT, CL-840-R45-XT, CL-750-R45-XT.

The emission of the light after blue laser diode excitation is presented on Fig. II-14

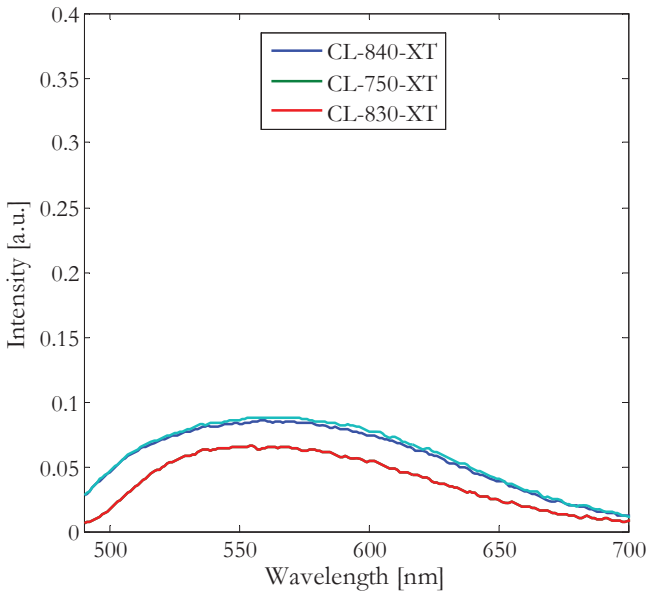

Fig. II-14. Emission of PiG samples.

To verify the type of dopant of these commercials phosphors, we used Holographic Monochromator Cornerstone 130 1/8 equipped with a xenon lamp. We sent different wavelengths, with step of 10nm, from 400 nm to 480 nm. Total spectrum of emission was measured by spectroradiometer Specbos 1201, placed after the sample, radiated by light from xenon lamp.

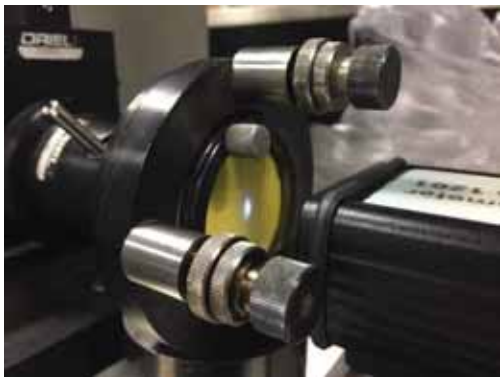

Fig. II-15. Experimental setup for emission by different wavelengths excitation.

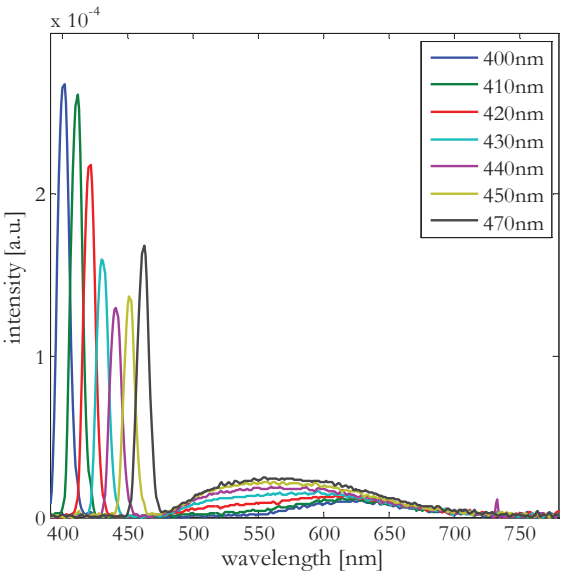

Fig. II-16. Excitation by different wavelength of CL-830-XT

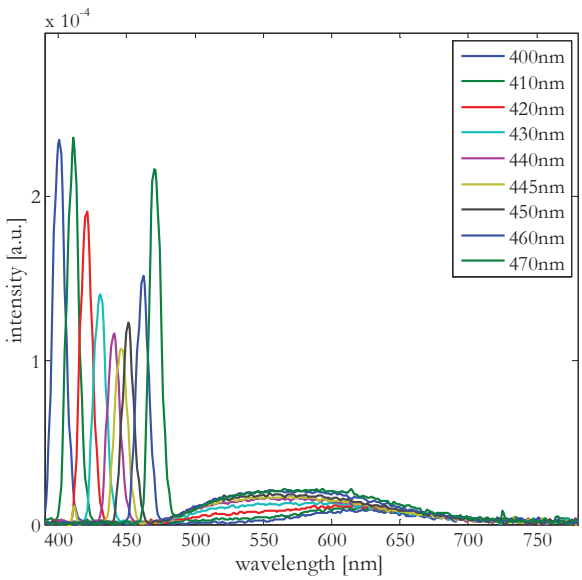

Fig. II-17. Excitation by different wavelength of CL-840-XT

On Fig. II-16 and II-17 we can see the results after excitation by different wavelength on different sample. Nevertheless, results are similar. When excitation wavelength is 400-410 nm we do not observe emission between 500 and 550 nm, whereas at higher wavelengths, emission appears. This phenomenon justifies the presence of cerium as dopant. Moreover, emission between 600 and 700 nm is characteristic for europium in nitrides. The presence of the cerium is also seen in the peaks of the source. Intensity is high for low wavelengths, which means low absorption of this wavelength. At 450 nm the intensity of source peak is lower, which means that energy has been absorbed by cerium. Indeed, the samples are mixed of YAG:Ce^{3+} and Nitride:Eu^{2+}. [59][60][61][62] However,

the level of absorption and emission are different. This difference comes from different chemical composition of host material.

2. White light

The light of the blue laser passes through the phosphor, causing yellow emission of light. Not all the blue light is absorbed by the yellow phosphor (efficiency of the phosphor plates is around 70%), the remnant of the blue light is mixed together with yellow light and can be perceived as a white light for human eyes.

2.1 Transmission

A LD-based phosphor-conversion white light source was assembled by using InGaN laser diode from OSRAM 1.6W (ref. TB450B) and Ce^{3+} doped YAG and GYAG mixed with Nitride:Eu^{2+}. The multiple-quantum-well (MQW) active layers of a laser diode are composed with two pairs of InGaN wells that were designed to emit blue light around 450 nm. The measurements were performed in an optical sphere, where as an output the spectro-radiometer Specbos 1201 was put. In front of spectrometer we placed a phosphor

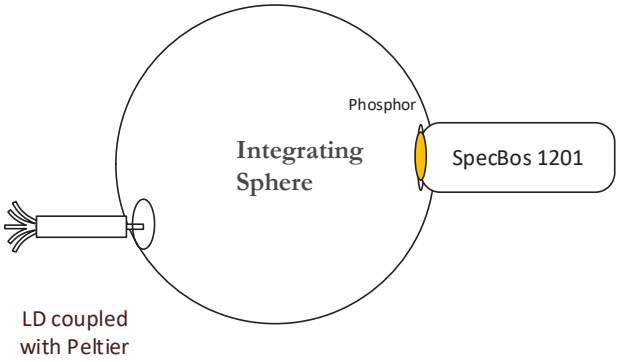

Fig. II-19. Schema of experimental setup.

Fig. II-20. Spectrometer attached to the sphere and the sphere used in this experiment.

plate. This let us to keep a phosphor in a distance from a diode, to avoid heating of material. The diode with its module was put as an input of the sphere. Laser was thermally coupled with Peltier module, which was connected to PID temperature controller TEC 2000 from ThorLabs. The sensor AD590 was placed under the stem of a laser to measure its temperature. The spectrometer allowed us to measure spectrum of light, CRI (Color Rendering Index), CCT (Correlated Color Temperature) and chromaticity coordinates.

Before measuring the white light parameters, the output characteristics of LD itself were measured under continuous-wave operation with varying temperature of LD. The operation temperature was adjusted by a controlled module to 20°C, 30 °C and 50°C respectively. The optical power was measured by power meter. The laser diode was itself,

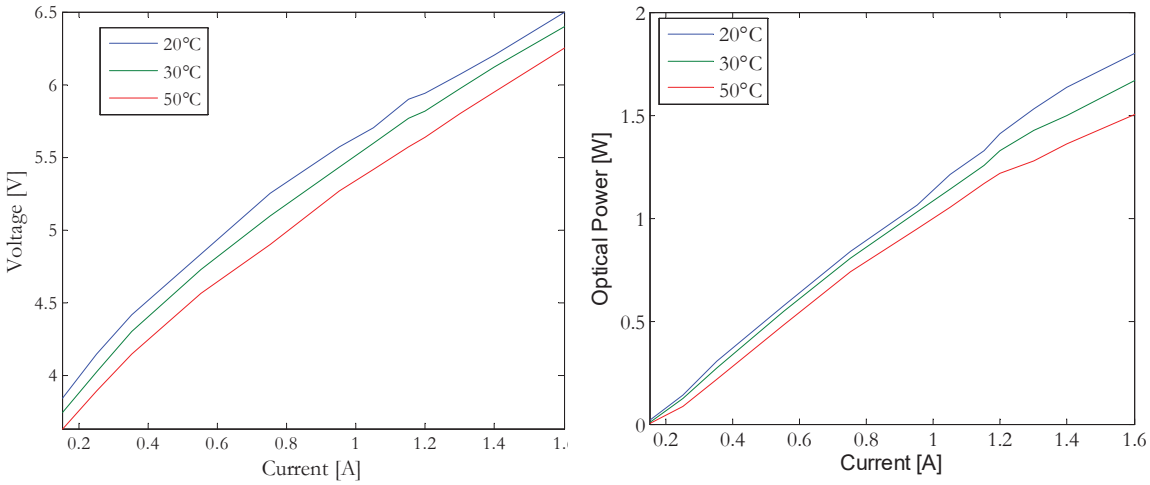

Fig. II-21. Characteristics V-I and P-I of LD

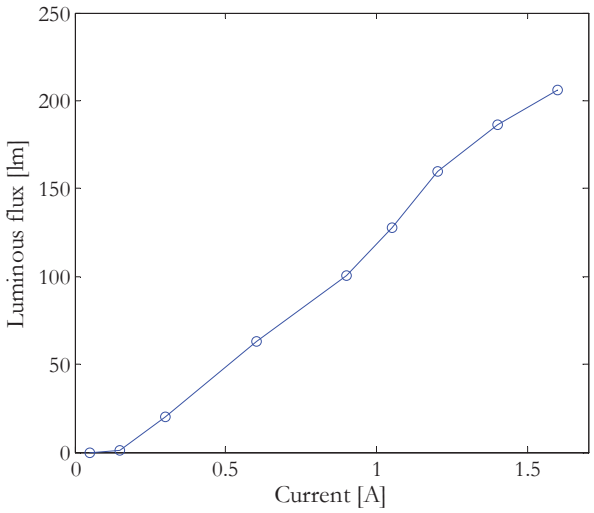

Fig. II-22. Luminous flux in function of current for LD.

without any focus module. The II-21 shows voltage as a function of current and the dependency of optical output power as a function of current.

Characteristics V-I for different values of the temperature are not linear – a little slope can be observed. Moreover, with rise of the temperature, the value of voltage drops. More explanations about this phenomenon can be found in Chapter III. Good linearity can be observed on Fig. II-21 for characteristics of output power versus current. Note, that optical output power does not decrease even at the high injection current (>0.8). This is strong contrast to the case of usual white LEDs, where efficiency begins to decrease substantially as injection current increases. This efficiency droop phenomenon has limited high-power and high-efficiency operation of LEDs.

Typical luminous flux-current curve is shown on Fig. II-22. Here, the operation temperature of LD was 30°C. The features of flux-current current basically reflects the curve power-current.

2.1.1 Results – YAG phosphor

Figures below present the spectrum of the light emitted by a laser and a phosphor. All graphs were normalized to the peak of 445 nm, which corresponds to light not converted, coming from a laser diode. The purpose of this normalization was comparison of

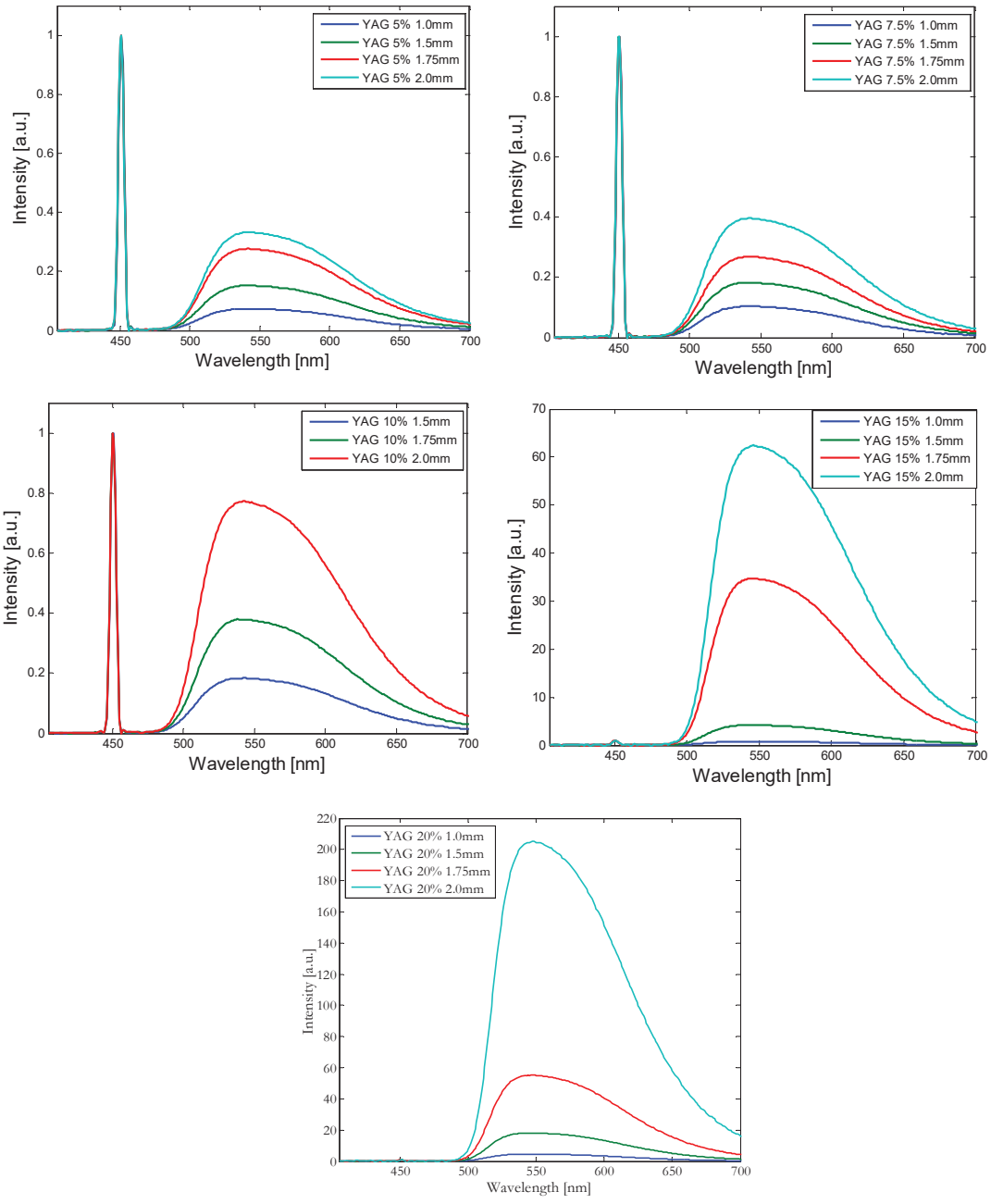

Fig. thick

Fig. II-23. Full spectrum emission phosphor conversion by YAG:Ce^{3+} and blue laser diode for different concentrations of phosphors in the silicon resin

phosphor's emission. Fig. II-23 presents conversion of the light by YAG of different concentration and thickness.

On Fig. II-24 we show the CIE chromaticity coordinates for samples of 1.5 mm for different concentration. In Table II-2, the CCT is mentioned. All the spectrums were measured, while the diode was supplied by a current I=0.6A, optical power P=0.5 W and its temperature was fixed at 30°C. The broad spectral region from 500 nm to 700 nm corresponds to emission of cerium. The increase of the intensity with thickness is due to excess amount of phosphor in the package.

Light converted by YAG:Ce^{3+} is characterized by its yellowish color (Fig. II-24) and warm color temperature. The CRI variates with concentration of phosphor in the silicon (Table II-1). The differences of CRI between the same concentration and different thickness doesn't exceed value of 10, so it was decided to present maximum CRI obtained with different concentration. CRI of YAG becomes very low for concentration of 15% and 20% due to high yellow peak and disappearing of blue peak. The reason of not very high CRI in general is quite narrow spectrum emission of YAG.

Table II-1. Color Rendering Index for different concentration of YAG phosphor in silicon.

Concentration of phosphor	**5%**	**7.5%**	**10%**	**15%**	**20%**
CRI	65	65	60	45	35

Table II-2. CCT of YAG in different concentrations and thicknesses.

Concentration of phosphor	**5%**	**7.5%**	**10%**	**15%**	**20%**
Thickness	CCT [K]	CCT [K]	CCT [K]	CCT [K]	CCT [K]
1.0mm	9058	6592	5320	4160	3951
1.5mm	5383	5102	5100	3941	3850
1.75mm	4660	4676	4440	3788	3804
2.0mm	4520	4431	4193	3816	3734

Table above shows the Correlated Color Temperature obtained for different concentrations and thicknesses. In spite of samples with low concentrations and thickness (YAG5% and YAG 7.5% for 1mm), the Correlated Color Temperature of source is warm. These two values of cold Correlated Color Temperature are due to low amount of the

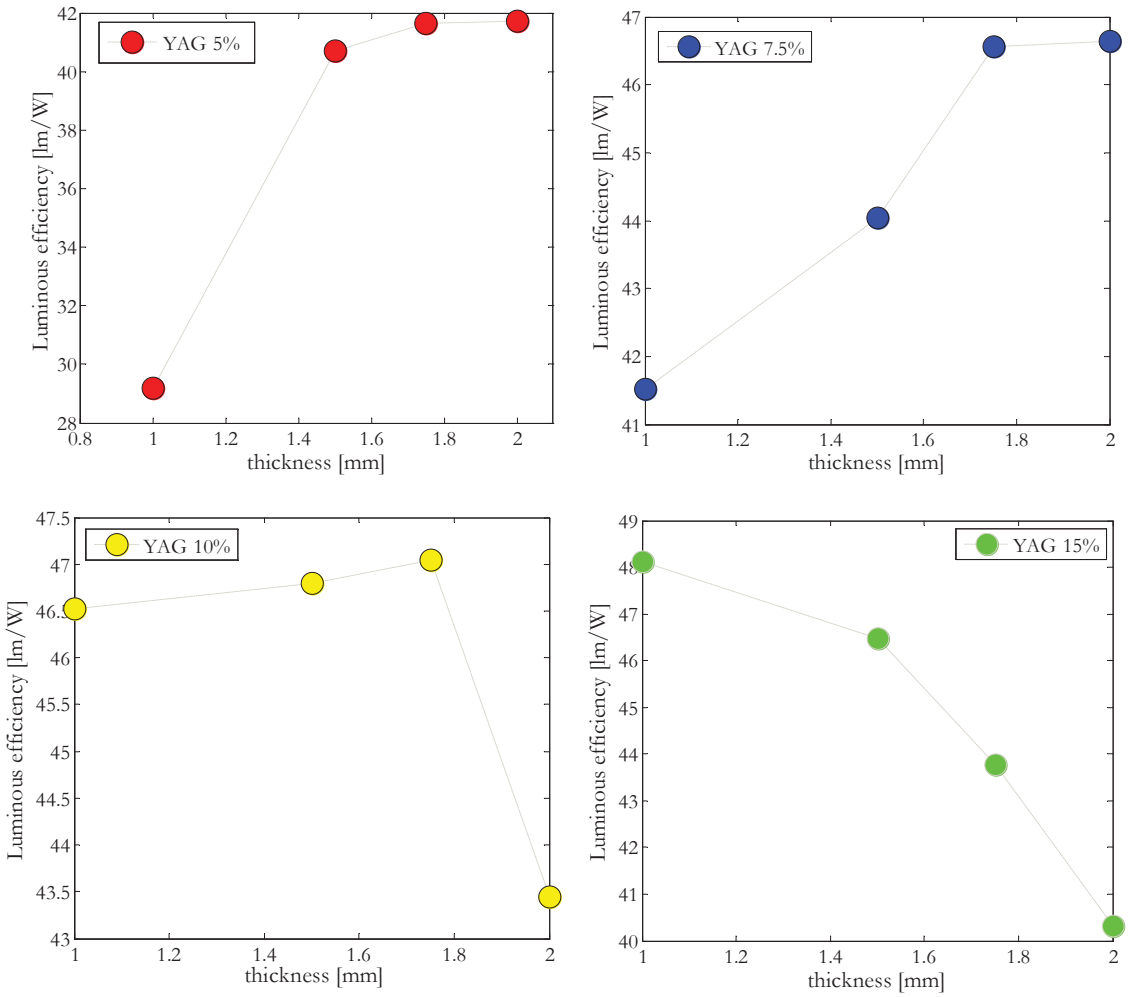

Fig. II-25. Luminous efficiency for the different thicknesses for different concentrations of the samples.

phosphor.

In the same integrating sphere, for the value of driving current 1.5A of a laser diode, we measured the luminous efficiency of the light system. On Fig. II-25 we present the obtained values. The highest luminous efficiency obtained with blue laser diode coupled with YAG was 48 lm/W. The calculations were based on electrical power of laser diode and the value of luminosity measured in the integrating sphere. Considering, that the maximum theoretical efficiency of white light is ~300 lm/W, and >100lm/W efficiency of high-efficiency white LEDs [36], obtained power is quite low. There is several reason. First, power-conversion of laser diode is not very high. Nevertheless, this issue could be easily

resolved by using a high power blue laser diode. Second, there is energy loss during wavelength conversion. The Stoke shift loss is estimated to be around 20%. [36]

From the evolution of luminous efficiency, we can notice its increasing with thickness for 5,7.5 and 10% concentration, whereas it decreases for 15%. Explanation of this behavior is described in paragraph 3.2 of this chapter.

2.1.2 Results – GYAG with Nitride phosphor

Below, on Fig. II-26 the full emission spectrum of GYAG and Nitride is presented. Rise of concentration of the phosphor in the silicon resin lead to rise of the emission. However, the emission of Nitride part (625 nm) increase much more, than part of GYAG (528 nm). The

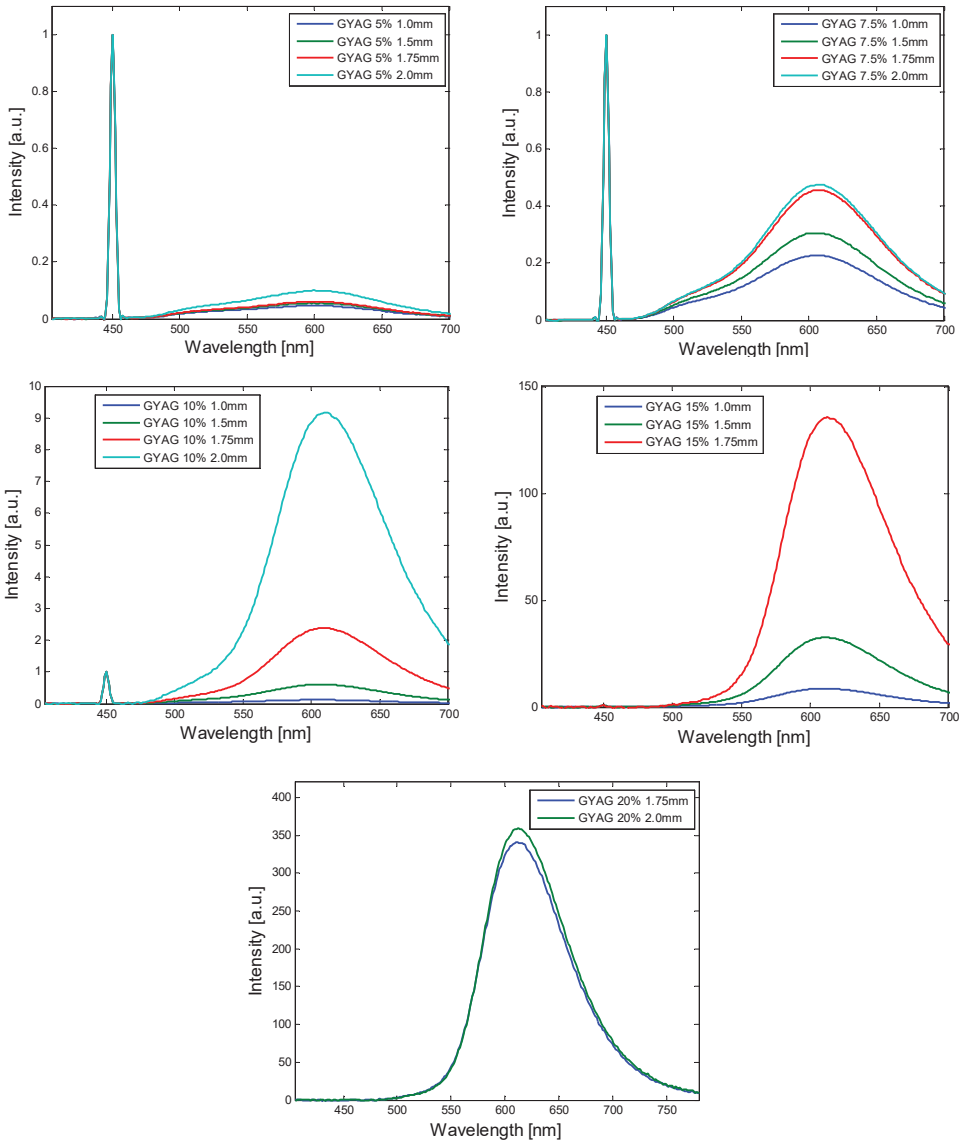

Fig. II-26. . Emission spectrum of GYAG with Nitride for different concentrations

reason of higher emission energy in case of Nitride was already described.

Table II-2. Color Rendering Index for different concentration of GYAG with Nitride phosphor in silicon.

Concentration of phosphor	5%	7.5%	10%	15%	20%
CRI	86	83	80	60	50

The CRI obtained for this material is very satisfying and exceed 80 for most of the concentrations of phosphor in silicon. However, the Color Rendering Index for samples with contain 15% and 20% of phosphor is lower due to very high emission of red phosphor and disappearing of blue peak. From CCT it can be noticed, that the light generated by the source based of GYAG and Nitride is very warm. Starting from 7.5% concentration, the light resembles the color given by a flame of candle. Also CIE chromaticity coordinates, due to the red phosphor, have a tendency to go into warm, red color.

Table II-3. CCT of GYAG and Nitride in different concentrations and thicknesses.

Concentration of phosphor	5%	7.5%	10%	15%	20%
Thickness	CCT [K]	CCT [K]	CCT [K]	CCT [K]	CCT [K]
1.0mm	4700	2691	3208	1850	1995
1.5mm	4500	2511	2228	1685	1775
1.75mm	4174	2277	2039	1552	1421
2.0mm	3400	2276	1716	1377	1389

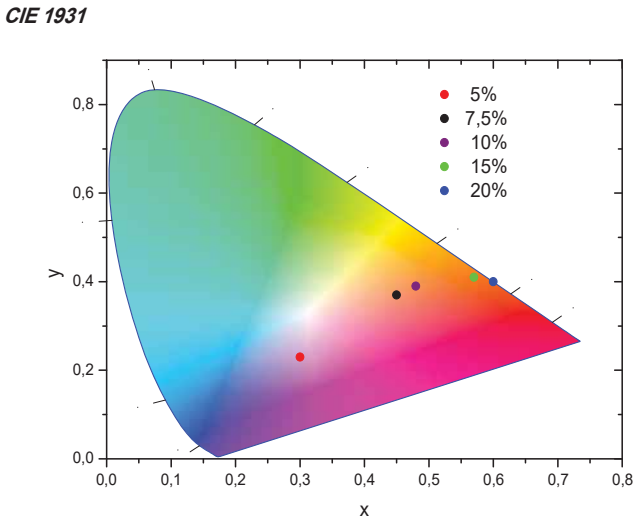

Fig. II-27. CIE chromaticity coordinates for different concentration of GYAG and Nitride in silicon resin for thickness 1.5mm.

The maximum luminous efficiency obtained for a light system with GYAG and Nitride is lower than the one with YAG and it is equal to 38 lm/W.

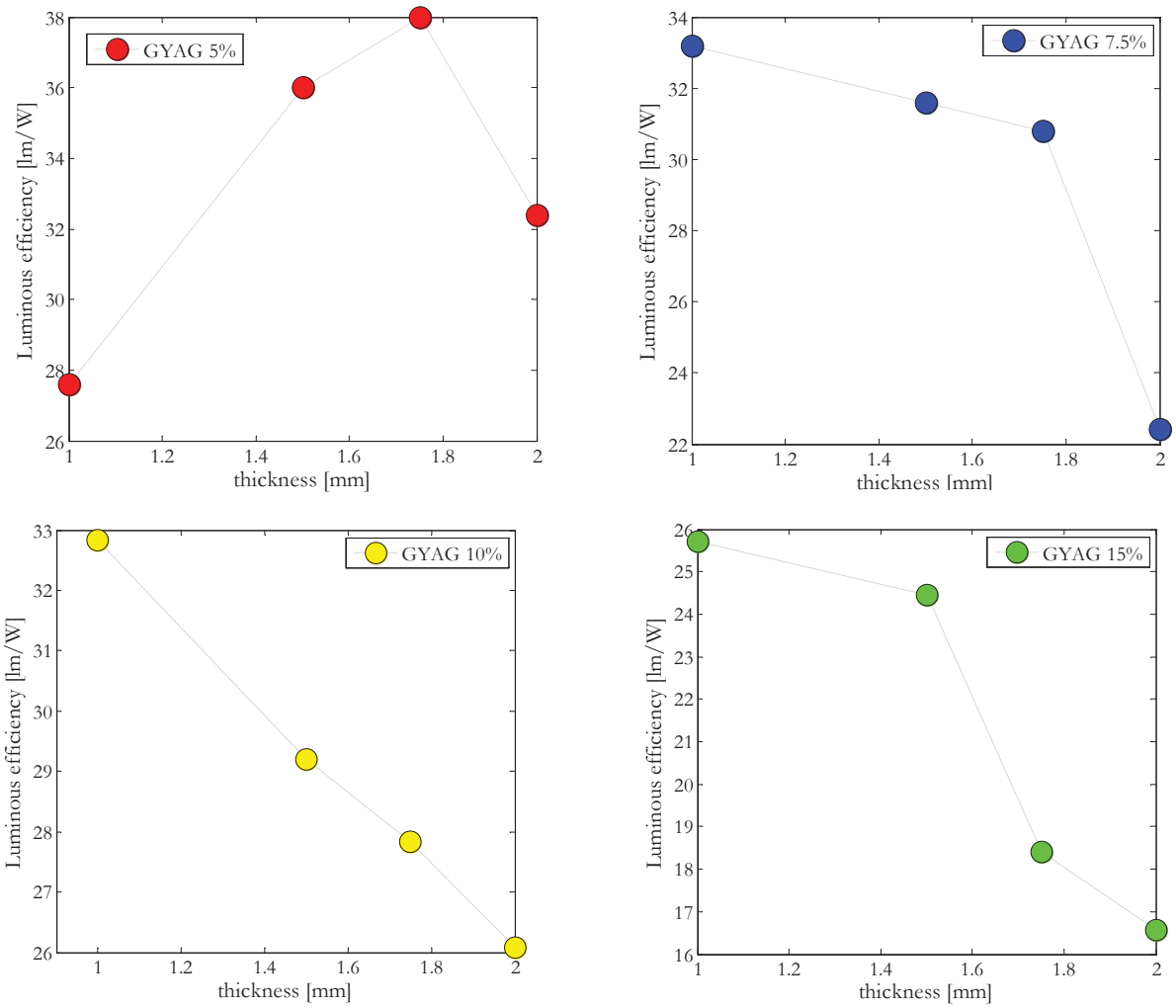

Fig. II-28. Luminous efficiency for the different thicknesses and concentrations of GYAG and Nitride.

2.1.3 Results – phosphor on glass

Subsequently, after measurements of phosphor in silicon, the spectrum and other light's parameters were measured for phosphor on glass.

From the spectrums on Fig. II-29 we can observe, that efficiency of the conversion was less than 20%. Probably it results from low concentration of the phosphor on the glass. Nevertheless, the Color Rendering Index is quite high – Table II-4 – its level is caused by two dopants – cerium and europium.

Although, CRI obtained with a mixture of GYAG and Nitride was higher, due to optimized concentration of the phosphors in the resin, which led to better conversion ratio.

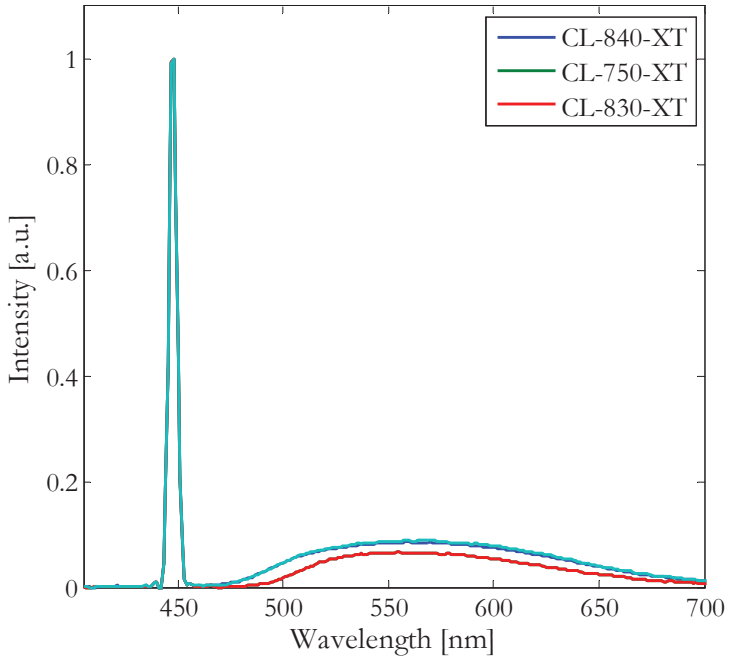

Fig. II-29. Spectrum of three phosphors: CL-840-XT, CL-750-XT, CL-830-XT.

Table II-4. Color Rendering Index for different phosphors in glass

Phosphor Reference	CL-840-XT	CL-750-XT	CL-830-XT
CRI	78	71	78

Table II-3. CCT of phosphor in glass.

Phosphor Reference	CL-840-XT	CL-750-XT	CL-830-XT
CCT [K]	6449	8922	6199

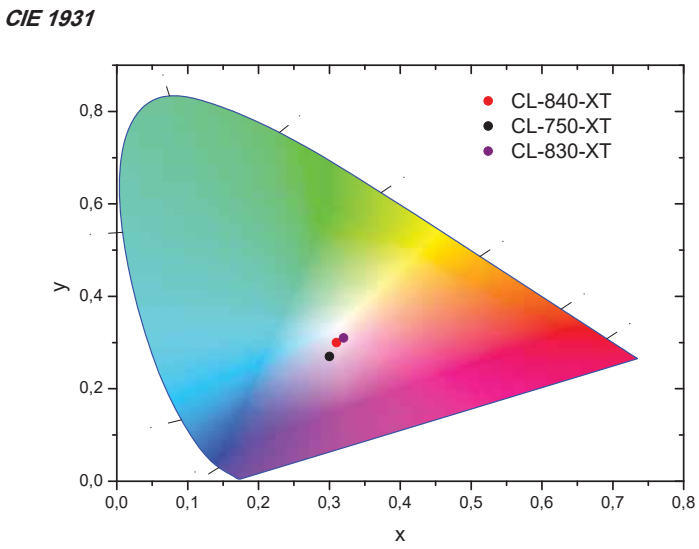

Fig. II-30. CIE chromaticity coordinates for phosphors in glass.

CIE chromaticity coordinates were very close to desired chromaticity of light (around 0.3, 0.3). Moreover, due to better heat dissipation, which lead to lower operating phosphor temperature (commercially used phosphor with blue LEDs have an operating temperature of 150°C [63]), the coordinates should be less susceptible on variations. CCT (Table II-5) appeared to be cold due to big blue peak of a laser diode, which was not fully converted by a phosphor. Luminous efficiency was around 85 lm/W for CL-840-XT and CL-830-XT and

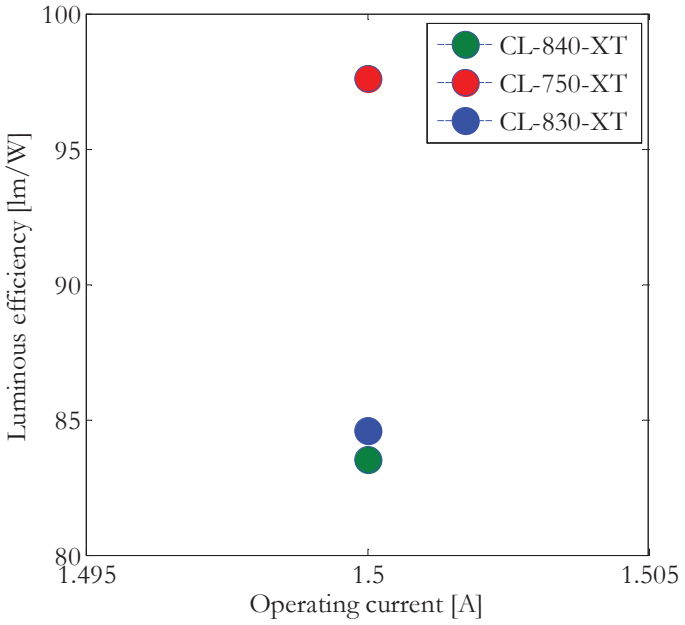

Fig. II-31. Luminous efficiency for PinG.

97lm/W for CL-750-XT. High luminous efficacy confirm stability of Phosphor on Glass and superiority at this point on organic resin. The luminous efficacy obtained by LD and this phosphor is similar to the one, obtained by commercial LEDs.

2.2 Reflection

Some types of the phosphors have possibility to operate in reflection mode which would allow to protect the human's eyes from direct contact with a blue light coming from a laser. Long direct exposition of the eyes on the blue light may cause macular degradation and lead to permanent vision loss. Adult human eye is very effective in blocking UV rays from reaching the light sensitive retina, at the back of the eyeball. On the other hand, all visible blue light passes through the cornea and lens, and reaches the retina. [64][65] For these reasons, so far, the pc-WLD solution are based on reflection mode. [66][67]

In this paragraph the results of the experiment performed in reflection mode are described.

2.2.1 Results

An integrating sphere spectroradiometer setup was used to measure the total spectral flux emitted by a sample illuminated by a blue laser diode in reflection. The laser beam enters to the integrating sphere and illuminated the sample put on the opposite side of the sphere (Fig. II-32). The spectro-radiometer is connected to the port at 90°. The sphere has a $BaSO_4$ coating with a high reflectance. The measurements were performed using GYAG and Nitride phosphor, with a concentration of 10% and thickness of 1 mm due to its excellent CRI value.

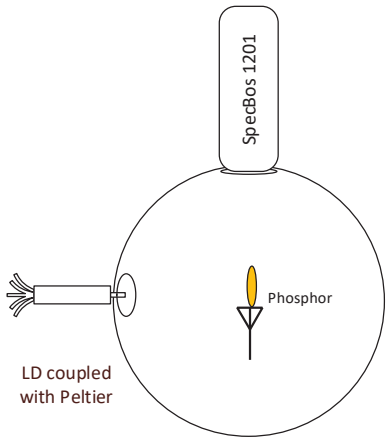

Fig. II-32. Experimental setup for reflection.

As predicted, the chosen material operates in reflection mode. However, the results show that peak of 445nm (blue light) is three times higher than in transmission. After

normalization to 445 nm it revealed that when the light is only reflected, we have more blue light as an output of a light source and less light is converted by phosphor.

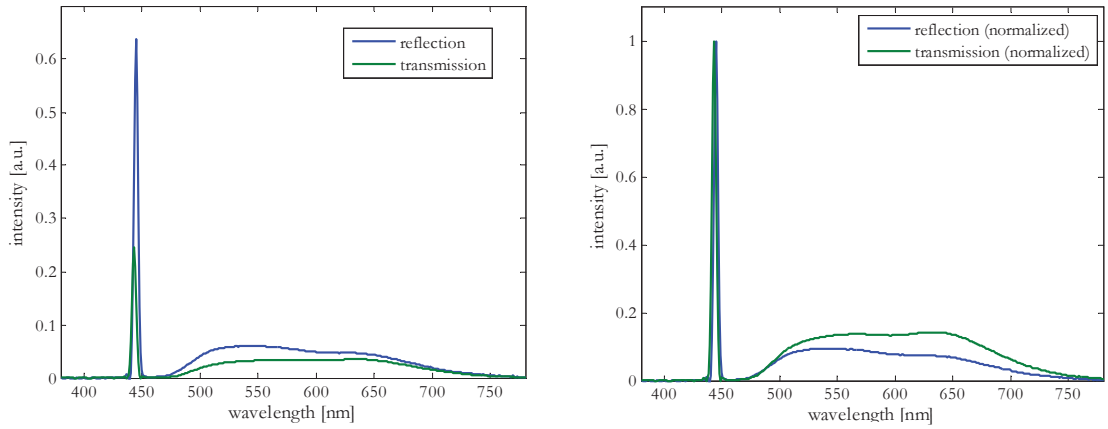

Fig. II-33. Results from transmission and reflection not normalized (a) and normalized to 445 nm (b).

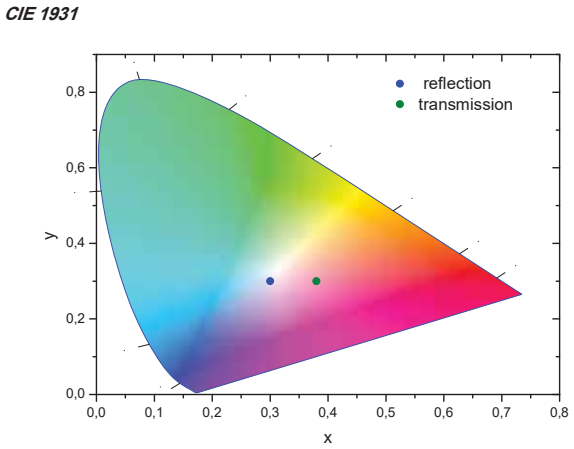

Fig. II-34. CIE chromaticity coordinates for reflection and transmission.

The CIE chromaticity coordinates in reflection were 0.3, 0.3, compering to 0.38, 0.3 in transmission, which result in desired value of chromaticity. The CRI was unchanged and was equal to 80. [6]

3. Optical power dependencies

In this paragraph the dependency of the optical power on thickness and concentration of phosphor is presented. Part of these study was presented on the conference SPIE Photonics West 2018 in San Francisco and published in Journal of Photonic for Energy. [68] [7]

3.1 Thickness and concentration

Phosphor plays very important role in the phosphor converted method to the luminous efficacy. The most crucial factors are not only geometry, particle size, the thickness and location but also concentration of the phosphor in the silicon resin. As well known the phosphor concentration includes some obvious effects on the performance of the device (Mie scattering) [69]. Also the aspect of placement and shape of phosphor is important. Studies show, that from conformal coating, dispensing and remote package, it is the remote phosphor that have more light output and higher efficiency compared with other package types. [70][71][72] However, the light output of white phosphor-converted source depends on the thickness and concentration. Below, on Fig. II-35 and II-36 we can find the results of the measurements for YAG and GYAG and Nitride, performed as in transmission setup, for different thickness and concentration.

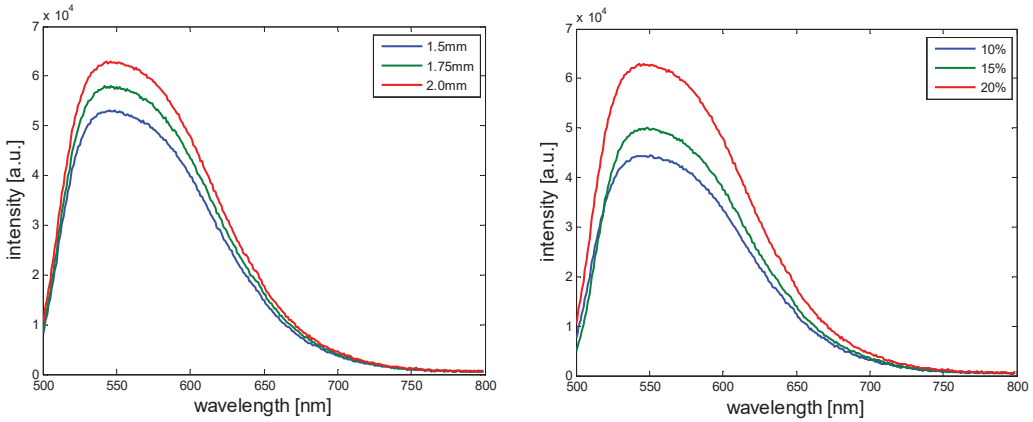

Fig. II-35. Light converted by YAG: Ce^{3+} for different thickness and concentration of plate.

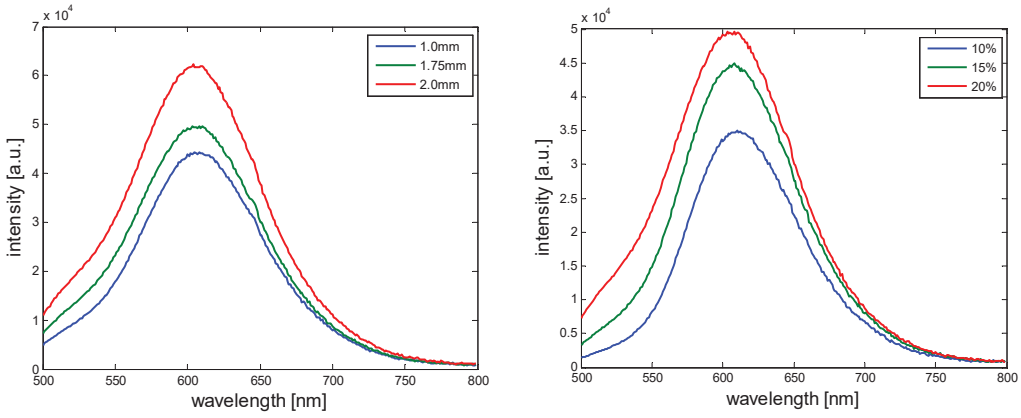

Fig. II-36. Light converted by GYAG and Nitride for different thickness and concentration of plate.

Increasing concentration or thickness leads to increasing of the light emitted by phosphor. Usually, these two parameters are treated independently. However, they might be

not considered in this way. Particles number may be a key parameter, which can be modified by changing the thickness of the plate or material concentration in resin. [5]

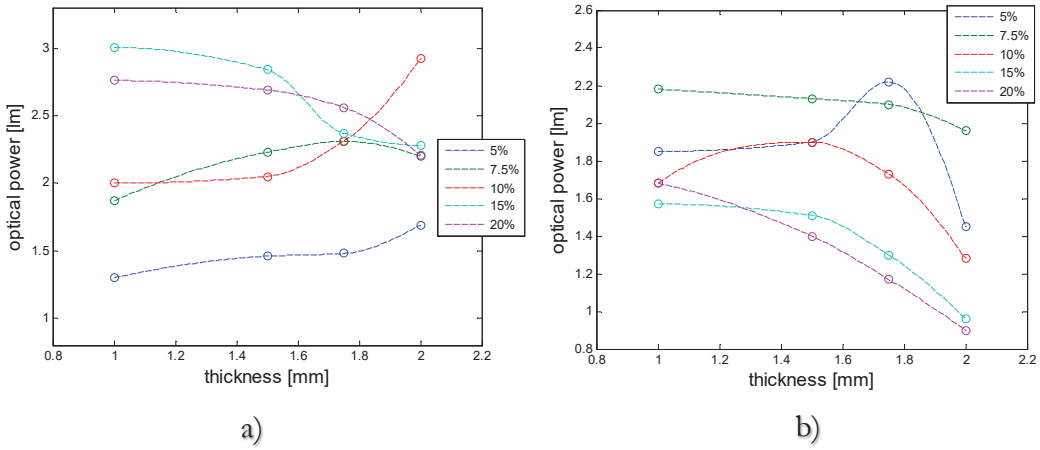

Fig. II-37. Output power of source and YAG (a) and GYAG and Nitride (b) plates with different thickness and concentration dependency.

The dependency of the output power on the different thickness and concentration are presented on. Fig. II-37. The same blue laser diode under the value of current I = 0.3 A was applied as common excitation source for all the phosphor plates in this measurement. We observed that the output power changed in different combinations.

For YAG (a) in cases for the lower concentrations, the optical power increased as the thickness of the phosphor plate increased (5%, 7.5% and 10%). In contrast, for the cases of higher concentration, the light power decreased as the thickness increased. (15% and 20%). For GYAG (b) plates the increase of the optical power with thickness was noticed only for the plate of 5% concentration.

From both figure we can assume that the optical power increases with the thickness for different concentration, until it obtains some maximum, that can be emitted by phosphor. After reaching optimal value, the power decreases with thickness. This phenomenon is strictly connected with another parameter – number of particles.

3.2 Number of particles

To see the relation between concentration and thickness, the number of particles in each plate was calculated. The equations used for calculations were proposed by [5].

3.2.1 Calculation of particles number

The assumption made for the calculation is that shape of particles is spherical and they are uniformly distributed across the volume of the plates. The diameter of a yellow and green phosphor particle is d_1=13 μm. The density of the phosphors is ϱ_{pho}=4.8 g/cm^3 and the density of the silicone resin – ϱ_{sil}=1.04 g/cm^3. The nitride phosphor has density ϱ_n=3.1

g/cm^3 and the diameters of particles d_2=15 μm. The weight of the silicon resin is 0.73g. In the experiment itself – all of the phosphor plates are made in flat cylindrical shape. That indicates the area of sample equal to A=0.0167 cm^2. The volume of the phosphor particle in the phosphor plate is:

$$V_{pho} = \frac{A \cdot h}{[1+\frac{\rho_{pho}+\rho_n}{\rho_{sil}}\left(\frac{1}{w_{pho}}-1\right)]} \quad (2)$$

where h indicates thickness and w_{pho} denotes the concentration of the phosphor by weight and is calculated from:

$$w_{pho} = \frac{W_{pho}+W_n}{W_{pho}+W_n+W_{sil}} \quad (3)$$

where W_{pho}, W_n, W_{sil} are weight of phosphors, nitride phosphor and silicon, respectively. Let N_{pho} be total particle number that is the sum of the number of phosphor particles N_{dj} with different diameters d_j:

$$N_{pho} = \sum_{j=1}^{k} N_{dj} \quad (4)$$

Where N_{dj} is related to the total particle number and their percentage, which can be written:

$$N_{dj} = N_{pho} \times p(d_j), \quad j=1,2\ldots k. \quad (5)$$

Finally, the number of particles N_{pho} is obtained:

$$N_{pho} = \frac{V_{pho}}{\sum_j^k \frac{\pi}{6} \cdot {d_j}^3 p(d_j)} \quad (6)$$

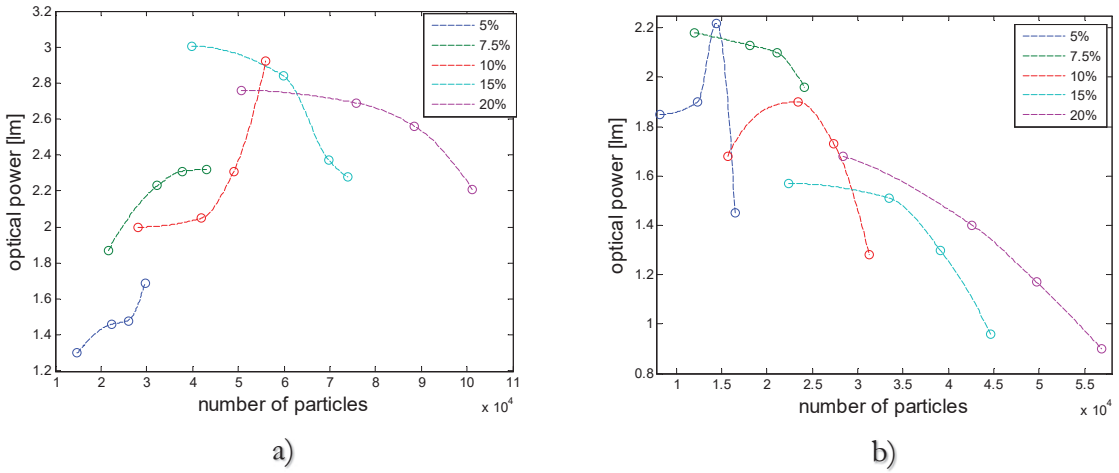

Fig. II-38. Optical power dependency on number of particles for different concentrations for YAG (a) and GYAG and Nitride (b).

Figures II-38a and b present the dependency of optical power on number of particles for different concentrations. The analogy with dependency on thickness of phosphor plate can be noticed. Optical power emitted by YAG increases until it reaches maximum (sample

of concentration of 15%), then it decreases. Optical power at the output of system with GYAG and Nitride plates increases only for lowest concentration (5%), then, it decreases. We can notice that probably too high number of particles of phosphor in silicon resin causes decreasing of output power. Moreover, we also find that it could exist an optimal particle number of the phosphor for the maximal output power ($4e10^4$ for YAG and $1.4e10^4$ for GYAG and Nitride) of the phosphor for maximal light output power. This value should correspond to the most proper condition for the phosphor particles uniformly suspending in the silicone resin. If there are not enough particles all the light is seldom to be scattered by more other particles. It causes easy escape for the light from the plate, such that the output flux increases When the number of the particles is higher than the optimal one, the phosphor particles are more like too dense in the resins. In this case all the light becomes difficult to escape out of the phosphor plate such that the output flux decreases.

The particles number can replace the concentration and thickness in exploration of phosphor excitation. It is believed that the process of collision between blue photons from laser with phosphor particles is much more essential in the exploration of phosphor excitation.

Interesting part of studies on particles number dependency is its relation with CCT and CIE chromaticity coordinates.

3.2.2 Dependency on CCT and CIE coordinates

The spectro-radiometer Specbos 1201 allows us to measure Correlated Color Temperature and chromaticity coordinates.

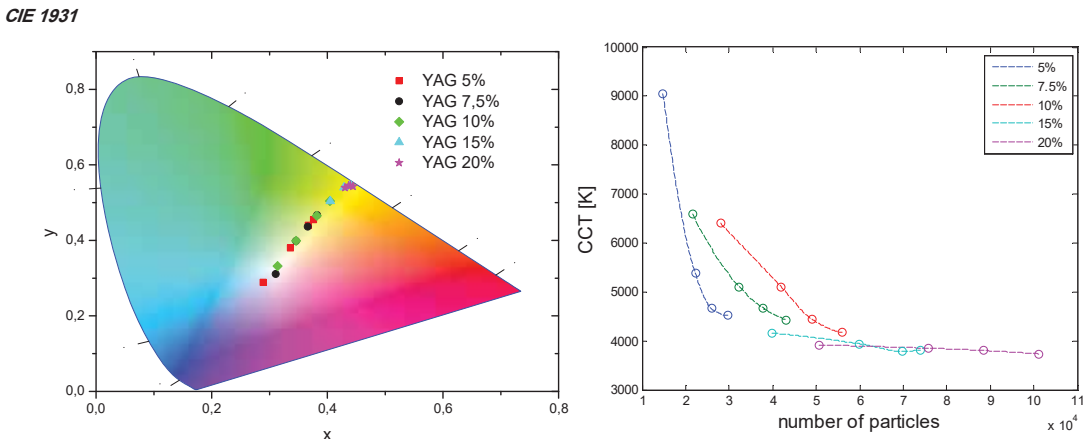

Fig. II-39. CCT and CIE coordinates dependency on particles number for YAG.

Table II-4. CIE chromaticity coordinates of YAG.

	YAG 5%	YAG 7.5%	YAG 10%	YAG 15%	YAG 20%
1.0mm	0.29,0.29	0.31,0.33	0.32,0.37	0.4,0.5	0.43,0.54
1.5mm	0.34,0.38	0.35,0.4	0.35,0.4	0.43,0.54	0.44,0.54
1.75mm	0.37,0.44	0.37,0.43	0.38,0.46	0.44,0.54	0.44,0.55

2.0mm	0.38,0.45	0.38,0.47	0.4,0.5	0.44,0.54	0.44,0.54

On Fig.II-39 we can observe CIE coordinates for different concentration of YAG in silicon resin and also dependency of CCT on number of particles. From the coordinates we can observe, that the more concentrated material, the less changing in coordinates for the same concentration and different thickness. Table II-7 presents the exact values of the CIE coordinates. For 5% we can notice big variation of coordinates. On the other hand, the values for 20% of the concentration are almost the same. This phenomenon can be also noticed in the dependency of CCT on particles number. CCT reduces as the particles number increases, until it gets to optimum. When the particles are too dense, the CCT almost saturate – and we do not observe variation of coordinates.

Nevertheless, the saturation of CCT is true only for plates of YAG. For plates where the GYAG with nitride were incorporated, the CCT seems to not to saturate (Fig. II-40). In fact, when the computed CCT falls below 2500K, the discrepancy between our system

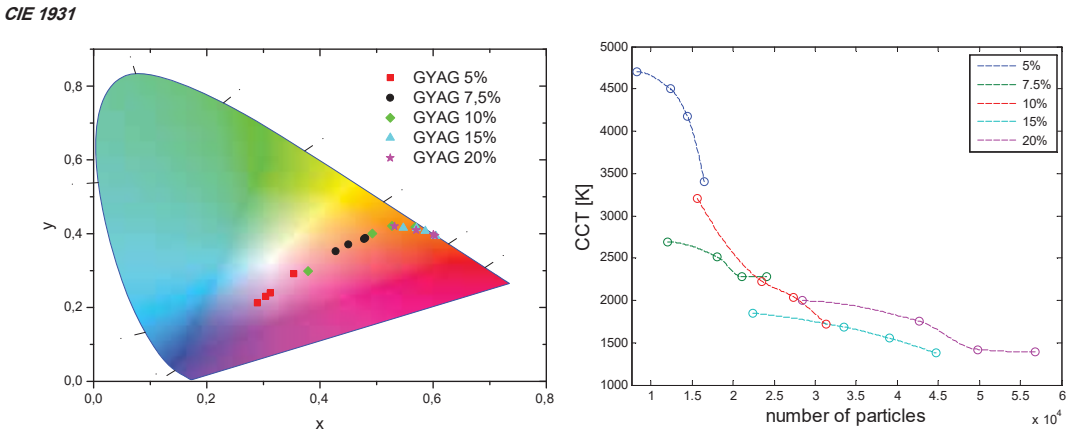

Fig. II-40. CCT and CIE coordinates dependency on particles number for GYAG.

spectrum and a black body becomes too important, leading to poor accuracy on the final result. We are thinking that the CCT is not the appropriate metric in such cases. Lack of CCT saturation after obtaining optimum of particles in silicon leads to variation of CIE coordinates for all the concentrations.

Table II-5. CIE chromaticity coordinates of GYAG.

	GY +N 5%	GY+N 7.5%	GY+N 10%	GY+N 15%	GY+N 20%
1.0mm	0.29,0.21	0.43,0.32	0.38,0.3	0.55,0.42	0.53,0.42
1.5mm	0.3,0.23	0.45,0.37	0.49,0.4	0.57,0.41	0.58,0.41
1.75mm	0.35,0.29	0.48,0.39	0.53,0.42	0.58,0.41	0.6,0.4
2.0mm	0.31,0.23	0.48,0.39	0.57,0.42	0.6,0.49	0.6,0.4

4. Conclusions

In this chapter we described the source of the light based on blue laser diode 445nm and suitable phosphor. In the study we used 2 types of phosphor incorporated into silicon resin and 3 samples of phosphor coated on the glass.

The materials based on silicon matrix we prepared by ourselves in laboratory ICMCB in Bordeaux. The preparations were prepared by a method sol-gel. Basically we mixed, obtained from Intematix, phosphor powder with a silicone gel, subsequently we cooked it in proper temperature.

Brief explanation of principle of light emitting by each phosphor has been described. The emission is based on two ions: Cerium $^{3+}$ in host materials - YAG and GYAG (yellow and green emission) and Europium^{2+} in nitride (red emission). Each of the material has its optimum of absorption exact wavelength, to emit maximum of light. With a blue laser diode of 445nm we are closer to optimum of GYAG emission. However, the methods of possible modifications in emission were described (for example: adding an element in host material)

Due to thermal issues of silicon as a matrix of phosphor, its yellowing process, as an alternative, the phosphor in glass was offered. PiG is also interesting alternative for ceramic phosphors which production is expensive due to high temperature of cooking. In this study we used commercial phosphors. To verify their doping, the experiment with monochromator was ran. Based on different wavelength excitation we were able to defined the general composition of phosphors: YAG doped with cerium mixed with Nitride doped with Europium.

After description of material properties, the pc-white light parameters were studied. All the measurements were performed in the integrating sphere. Firstly, the parameters of a laser diode were investigated. The optical power in function of current, increase linearly, regardless the temperature. Moreover, we do not observe, characteristically for LEDs, decrease in optical output power for high injection current. The optical power of the laser diode for the operating temperature of 20°C was 1.75W, for 50°C it dropped to 1.45W. The issues of this phenomenon of temperature variation are described more precisely in Chapter III. The luminous flux of a laser diode, without phosphor was about 210 lm.

Subsequently the studies on white light source based on a blue laser diode and each phosphor were performed. Investigation shows that source based on YAG has average CRI value due to narrow emission between 500-650nm. CCT obtained for very low concentration and thickness was high which leads to cold Color Temperature and its caused by low efficiency of conversion blue-to-yellow. After increasing phosphor concentration in silicon resin we got warm color of the light. The maximum luminous efficacy of the light source we obtained was 48 lm/W. On its value the influence had Stoke losses and power-conversion of a laser diode.

Source based on GYAG and Nitride shows excellent CRI value due to emission of two dopants: cerium and europium. With this mixed of phosphor we covered almost all

spectrum of the visible light what led to the value of Rendering Index of 83. CCT is more orientated to very warm color. The luminous efficiency of the light system was little bit lower than the one of YAG – 38 lm/W. It is assumed, that the reason of lower efficiency are bigger Stoke's losses, than in case of YAG.

Result obtained from conversion of blue light from a laser by a PiG are very promising. The luminous efficacy was at the level of the efficacy obtained today by commercial LEDs The CIE chromaticity coordinates shows that the light has perfectly white color. Moreover, similar to GYAG with Nitride, the two dopants - cerium and europium in the matrix cause that the emission of the elements cover almost whole range of visible light and gives very good CRI value, which is around 80.

The studies in reflection mode were also performed, however, the amount of blue light was 3 times higher than in transmission.

The investigation on replacing thickness and concentration by particle number as a parameter were also done. It revealed that for each phosphor we could find the optimum number of the particle which lead to the highest luminous efficacy and optical power possible to generate by a source of light. When there are not enough particles in the silicon, the light is seldom to be scattered by more other particles. However, when there is too much – the light is trapped in the phosphor plate and output flux decreases.

We found also the dependency of the particles number on CCT. However, this dependency is valid only for the CCT from a range 3000-6000K. The discrepancy between our system spectrum and a black body becomes too important, leading to poor accuracy on the final result. We are thinking that the CCT is not the appropriate metric in cases out of this range.

Chapter III

Mechanisms of Aging

Table of contents

Mechanisms of Aging **89**

1. Aging of semiconductors **90**

1.1 FEM Analysis 90

1.1.1. Steady State 92

1.1.2 Transient State 94

1.2 Influence of temperature variation on white light 95

1.3 Aging of laser diode 98

2. Aging of materials **100**

2.1 Aging by laser irradiation 100

2.1.1. YAG:Ce^{3+} aging process 101

2.1.2. GYAG:Ce^{3+} with Nitride aging process 102

2.1.3. FTIR analysis after irradiation 102

2.1.4. Silicon aging process 104

2.1.5. Glass aging process 105

2.2. Aging by artificial sun 106

2.3. Aging by blue LEDs 109

2.4. Temperature distribution on different phosphor plates 111

3. Conclusions **115**

1. Aging of semiconductors

To achieve obtaining a reliable and long-life source of light based on laser diode and phosphor, the aspect of semiconductor degradation also should be considered. So far, a great effort has been made to understand the failure mechanism of LDs. [73][74] While optical and electrical analysis of InGaN is necessary, thermal characteristics also play important role in a laser degradation. [75][76]

The thermal conductivity is very important from the point of view of thermal characteristics. Well-chosen substrate material could have small thermal conductivity in high temperature, which may lead to better heat convection and thermal dissipation (for example sapphire). In this paragraph we will focus on thermal analysis performed in ANSYS Workbench software of a blue laser diode OSRAM 1.6W

1.1 FEM Analysis

Analysis of thermal characteristics for InGaN laser have been carried out by using a three-dimensional thermal conduction model. Steady and transient temperature distribution of LDs were calculated by finite element analysis method. The following heat conduction equation was numerically solved [74]:

$$c_p \rho \frac{\partial T}{\partial t} = \nabla(k \nabla T) + S \quad \textbf{(7)}$$

where T is the temperature, c_p is specific heat, ϱ is the density, k is thermal conductivity and S is the heat source density. For steady state conditions the specific heat and density are equal to zero. At boundaries, heat flux q_c caused by natural convection heat transfer and q_r caused by heat radiation were considered using following equations [77]:

$$[k \nabla T]_n = q_c + q_r \quad \textbf{(8)}$$

$$q_c = \alpha(T - T_f) \quad \textbf{(9)}$$

$$q_r = \epsilon \sigma (T^4 - T^4{}_f) \quad \textbf{(10)}$$

where $[k\nabla T]_n$ is the heat flux component normal to the boundary, α is the heat transfer coefficient, ϵ is the emissivity of surface, σ is the Stefan-Boltzmann constant and T_f is the ambient temperature. In the numerical calculation, equation (7) was solved in three dimensions by the finite difference method with controlled volume. Boundary conditions were given as follows: α=0 and ϵ=0.1 for boundaries not in contact with a heat sink and α=∞ for boundaries with the contact with heat sink.

In semiconductors the heat generation is mainly located in active layer and p-cladding layer. In simulation parameters active layer and p-cladding layer are heat generators. Their values were calculated based on lumped element model:

$$Q_c = IV \quad \textbf{(11)}$$

$$I = WLJ \tag{12}$$

$$V = \frac{hJ}{\sigma} \tag{13}$$

where Q_c is a heat generation, V the voltage drops, J, the density of current, W the stripe width, L the cavity length, h the height of the layer and σ the electrical conductivity. On Fig. III-1 the schematic chip of the laser diode is presented. Fig. III-2 shows the model designed in software for thermal analysis.

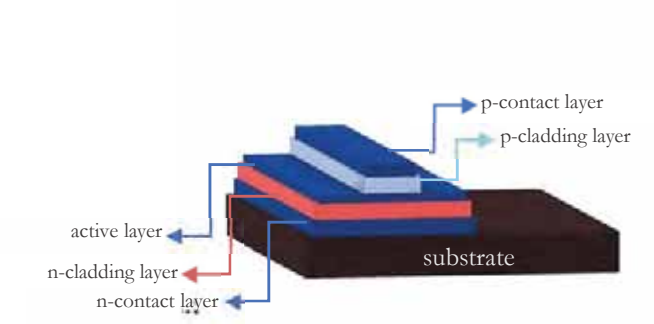

Fig. III-1. Schema of the chip of the laser diode used for thermal simulation.

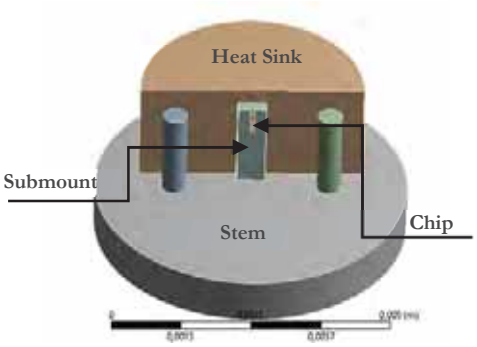

Fig. III-2. Schema of a laser diode used for thermal simulation.

InGaN chip is mounted on the AlN submount in a TO56 package. The submount is attached to Kovar heat sink. It is supposed that LD operates at I=1.5A.

In Table III-1 the specific heat, thermal conductivity and the density for 25°C of each material are presented, used in this simulation. [78]

Table III-1. Material parameters at 25°C.

Component	Thermal Conductivity [W/m·K]	Specific Heat [J/kg·K]	Density [kg/m^3]
Stem	46	460	8000
Heat sink	46	460	8000

Submount	285	600	3230
Substrate	130	490	6087
N-cladding layer	20	490	6087
N-contact layer	20	490	6087
Active layer	70	490	6087
P-cladding layer	20	490	6087
P-contact layer	20	490	6087

1.1.1. Steady State

Operating on high value of temperature can lead to reduction of life of semiconductor. To obtain a long lifetime of a laser appropriate cooling is required. The important factor to extend diode operation is junction temperature not exceeding 100°C. [79]

Based on the thermal conductivity of materials, the distribution of the temperature on the diode was simulated [80]. The conditions of simulation on Fig. III-3 present temperature on the different elements of the diode, without any cooling module or radiator

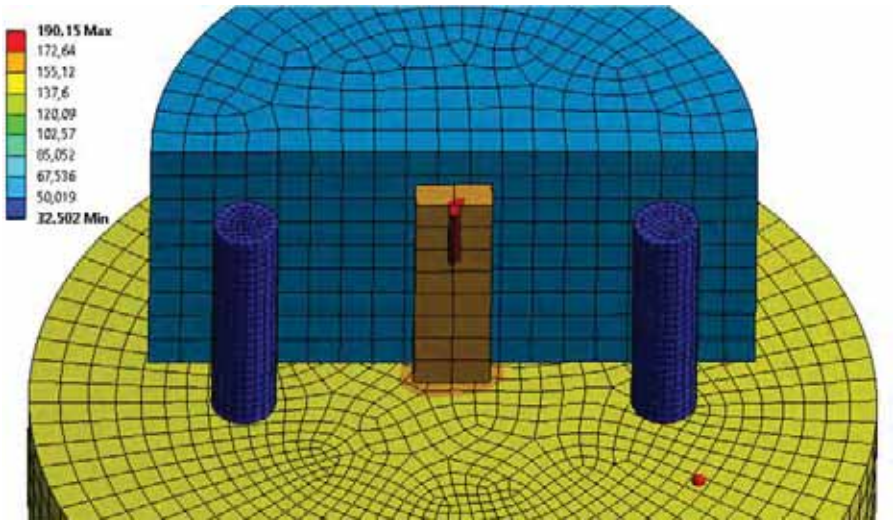

Fig. III-3. Distribution of the temperature in steady state without temperature control.

attached.

The maximum temperature reached on the chip of the diode was 190.15°C. This value exceeds recommended value of junction temperature almost twice. The heat dissipation for a packed semiconductor is mainly by conduction. From the heat source, through the substrate, finally to heat sink. Heat can be also removed by convection via a gas, as in surrounding air. Although effective heat transfers from source to ambient is an aim, it is more usual to define heat dissipation by considering inverse of the heat flow – thermal resistance between these two points. It is calculated from the equation:

$$R_{th} = \frac{\Delta T}{Q_{total}} \quad \textbf{(14)}$$

where ΔT is a difference of the temperature between junction and ambient, Q_{total} is a total heat generation. In the condition without any temperature control the calculated thermal resistance was 46K/W. However, the thermal resistance value calculated by this equation is a lumped value and will differ from depending on the spatial distribution of the heat source.

The temperature on the stem reaches 137.6°C. Considering that the temperature is dissipating via heat sink, the temperature of stem should be lower. It is suggested that the material of stem should be modified (for example to diamond or sapphire), which should give better results.

Subsequently, the simulation representing thermal coupling with temperature controlling module was performed. To simulate these conditions, the temperature on the stem was fixed on 25°C and 55°C respectively. Fixing these values on the stem corresponds to capture of the temperature, which is placed right under the stem.

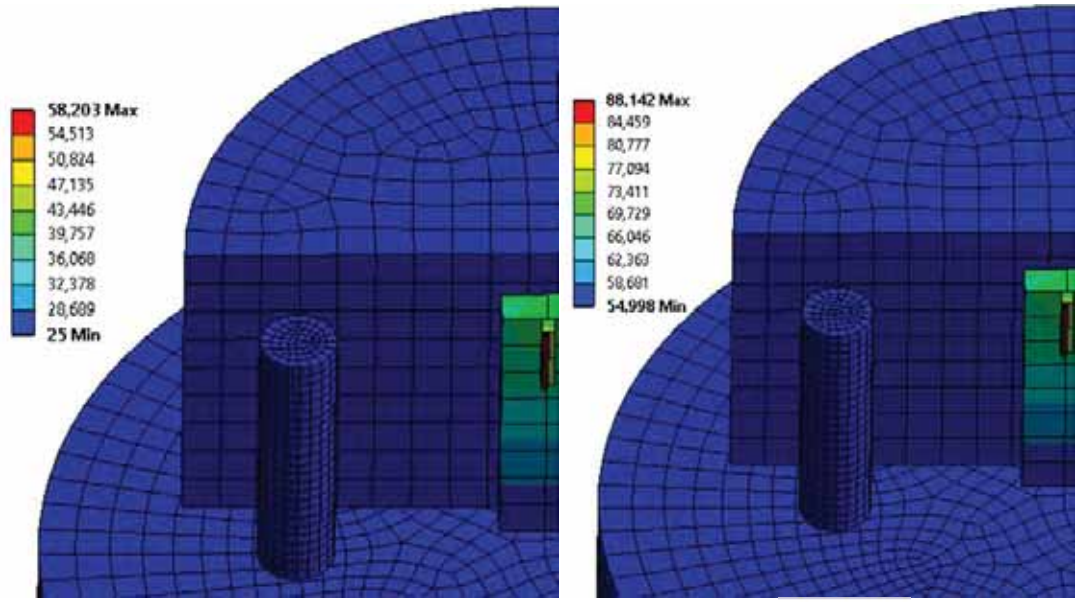

a) b)

Fig. III-4. Distribution of the temperature for 25°C (a) and 55°C (b).

Figure III-4 shows the results of the simulation. The junction temperature was less than 100°C and didn't exceed 58.2°C and 88°C for 25°C and 55°C respectively.

We calculated the thermal resistance for the case of 25°C and it resulted in 15.5 K/W. Studies show [74][79], that decreasing the connected area at the bottom of the stem will increase the thermal resistance. Also connecting a diode from lateral surface is enough to keep thermal resistance low. No connection, or connection only to pins lead to increasing the thermal resistance even three times (46K/W).

1.1.2 Transient State

For the same conditions (I=1.5A, parameters of materials in Table III-1), the transient simulation was performed. On Fig. III-5 the characteristic temperature from time on the hottest place (active layer) in the diode, without any temperature control, is presented.

In few milliseconds the temperature in active layer increases to 120°C. This corresponds to stabilization of current value at the level of 1.5 A. However, after the current stabilized, the temperature still rises, but with smaller slope. In the same time, the voltage decrease, due to higher thermal resistance, which lead also to drop of intensity of the light.

Adding cooling module hold the temperature at the constant level. It let also to keep the electrical parameters constant. On Fig. III-6 we can observe the evolution of the temperature in time for the temperature regulation at 25°C. The slope rises slowly, and doesn't exceed 65 °C.

The important factor for a good solid state lighting source is stability of a laser diode. The proper cooling module should be able to keep the temperature at the constant level. Changing the value of the operating temperature leads to changing the electrical characteristics. (see Fig. III-7)

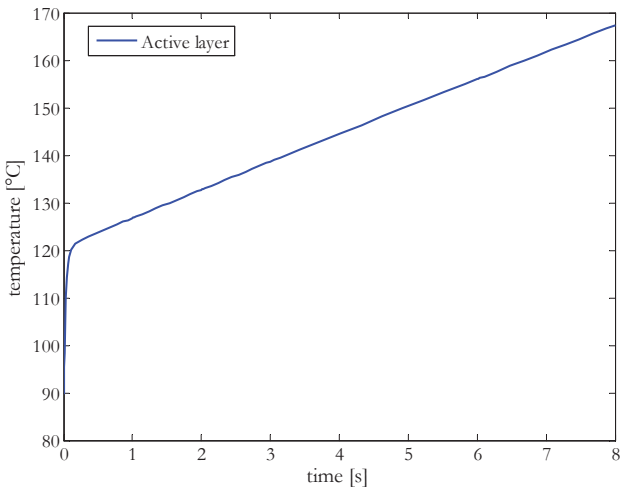

Fig. III-5. Characteristic of temperature in time evolution in active layer without cooling module.

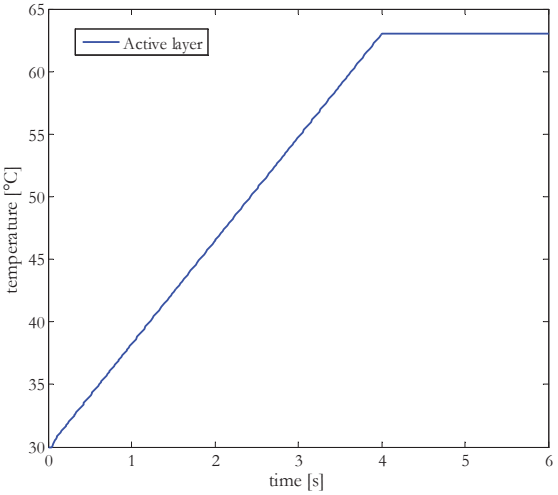

Fig. III-6. Characteristics of temperature with diode in the temperature regulating mode.

But not only the electrical characteristics are affected. Due to temperature variation, we observe also variation of the wavelength and light intensity. On Fig. III-8 the spectrum of blue LD for different diode's temperatures was presented. When the temperature increases, the shift into higher wavelengths can be observed. Moreover, when reaching the 55°C, the intensity of the light decreases about 30%. This shift obviously has influence on the light

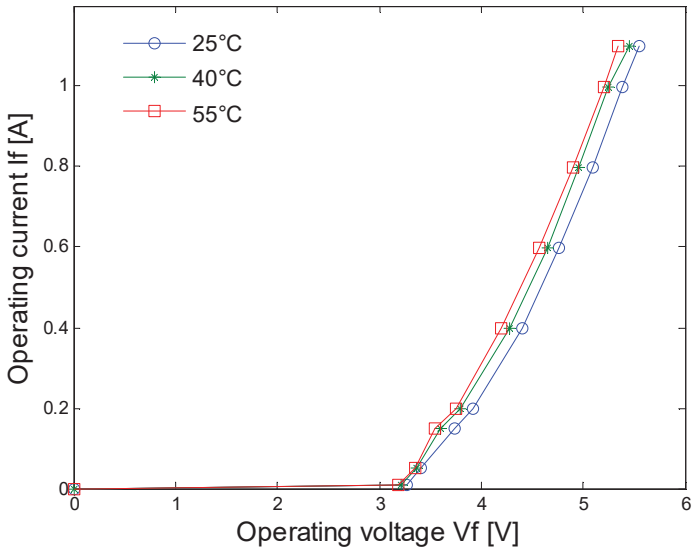

Fig. III-7. Electrical characteristics for different temperatures.

emission by material.

1.2 Influence of temperature variation on white light

In this paragraph the results of experiment of light conversion by phosphor for laser diode operating on different temperature level are presented. The measurements, as before, were performed in integrating sphere. The diode was supplied with a current 0.8A, and coupled with temperature regulation module. We fixed the temperature for three different values: 25°C, 40°C and 55°C respectively. The light of the laser diode enters to the sphere, and travers phosphor, which was put as an output, just in front of spectro-radiometer. The phosphor that we used, were the phosphors prepared by us in ICMCB laboratory, incorporated in silicon resin, described in chapter II – YAG doped with cerium and a mix of GAYG doped with cerium and nitride doped with europium. We chose the samples with thickness of 1mm each and concentration of phosphor 10% in silicon. On Fig. III-9 the converted light by our two phosphors is presented. To see the difference in amount of converted light by diode, we normalized the graphs to the maximum peak, which corresponds to blue laser diode emission. The intensity of converted light by YAG increase proportionally to the temperature, but this augmentation is not very significant. In contrary, for the light converted by mix of GYAG and nitride, it can be found that converted light decreased by 50%, only after changing the temperature by 15°. This variation is connected to the characteristics of light emission by materials. The optimal emission for cerium, when

the host material is YAG, can be found at 442 nm. When the host material is GYAG, cerium emission finds its maximal emission while excited by 437 nm. Europium emits maximum for excitation source also at 437nm. Our source emits the wavelength of 445 nm, when operating at 25°C.

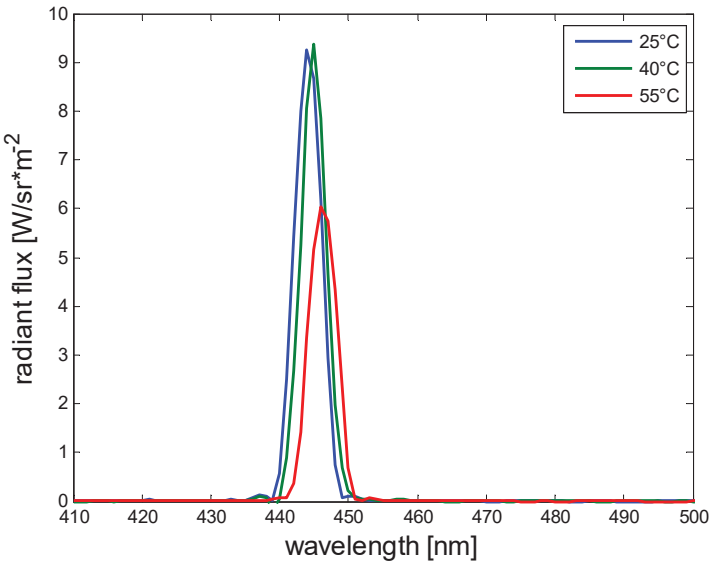

Fig. III-8. Spectrum of blue laser diode for different temperature**.**

However, when the temperature increases, our source changes its wavelength. For the temperature 45°C it shifts to 447 nm, for 55°C – to 449 nm. From Fig. III-10 we are able to explain the spectrum presented on Fig. III-9. When we take YAG material, we can notice that on its emission level characteristic, just before 450 nm we have small peak in emission. This small peak would explain the not very significant augmentation in emission during

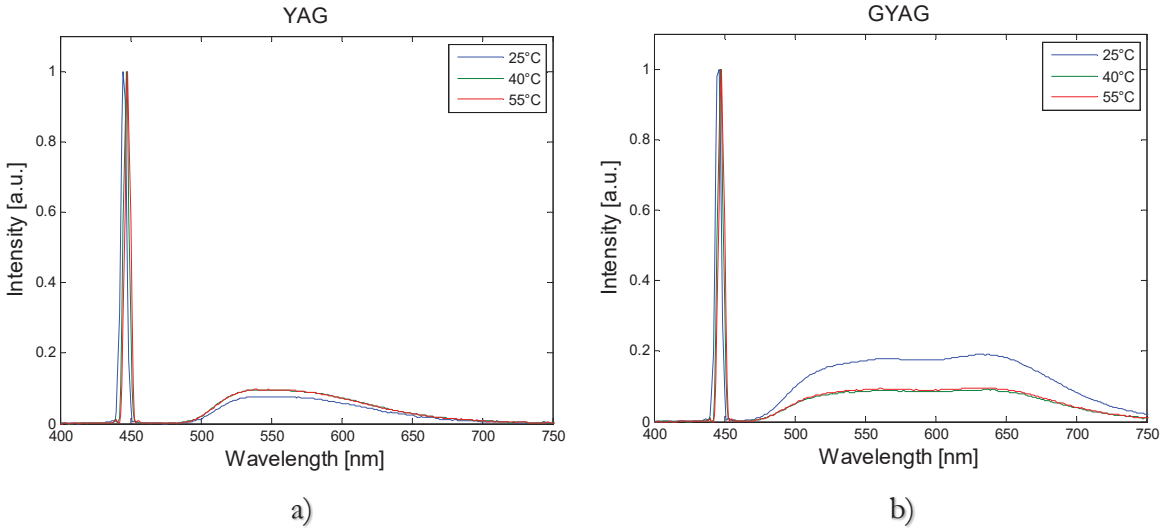

Fig. III-5. Spectrum of converted light by YAG (a) and GYAG (b) for different temperature.

conversion by YAG for 55°C. Situation for GYAG and nitride is easier – we can observe

only drop in emission after 445 nm. Due to this drop, the emission decreases. However, there can be another aspect which will cause this variation which reproducibility of measurements. Beam of the light doesn't really pass by the same amount of particles, which

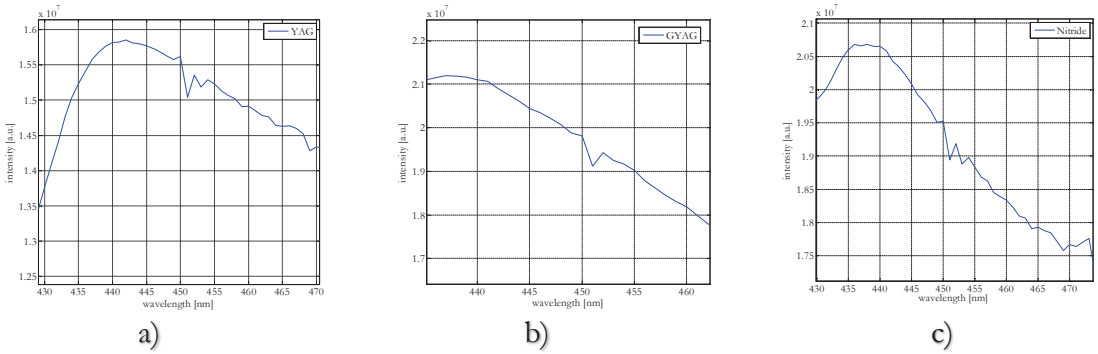

Fig. III-6. Level of the emission by different excitation wavelength for YAG (a), GYAG (b), nitride (c).

are also not homogenously spread.

The consequences of emission variation are not only in emission of a light itself. If the emission of converted light drops, at the output of our light source we find more blue light. It is caused by the drop of the efficiency of the phosphor emission. In emission characteristics we are not anymore at the maximum, which means that more blue light passes through plate. Rise of blue color can cause perturbation of human circadian rhythm [81][82][83], which can be dangerous to health.

The spectro-radiometer allows us to measure not only spectrum of the light, but also parameters as CCT, CRI or CIE chromaticity coordinates. For different values of the temperature we measured all of them. The Table III-2 presents Color Rendering Index, Table III-3 shows CCT and Fig. III-11 CIE chromaticity coordinates.

Table III-2. Color Rendering Index for different temperature.

Temperature	YAG:Ce^{3+}	GYAG:Ce^{3+}+ Nitride:Eu^{2+}
25°C	65	85
40°C	65	84
55°C	65	84

Table III-3. Correlated Color Temperature for different temperature.

Temperature	YAG:Ce^{3+}	GYAG:Ce^{3+}+ Nitride:Eu^{2+}
25°C	6653	3927
40°C	6354	4974
55°C	6254	4794

For CRI, we do not observe big difference. However, CCT and CIE chromaticity coordinates varies. In case of YAG, the color gets only a little warmer, and in case of GYAG and Nitride we observe shift into blue, which can have more serious consequences for our health.

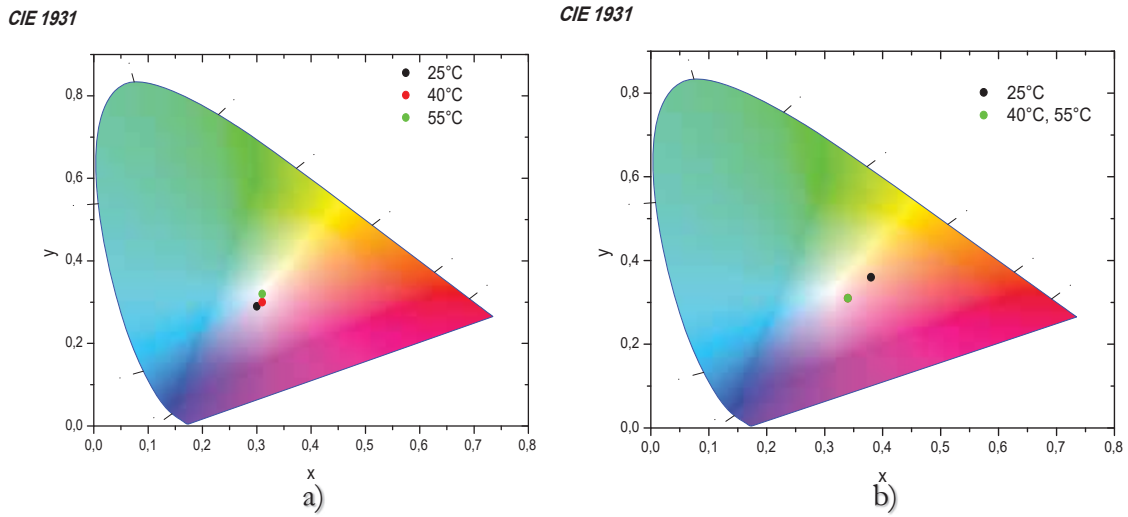

Fig. III-7. CIE chromaticity coordinates for YAG (a) and GYAG and Nitride (b).

1.3 Aging of laser diode

Degradation of a laser diode as a source of light is a very important aspect. Phosphors properties show, that small changing in a wavelength can cause for example shift from warm to cold light. The influence of the high temperature, on the other hand, can lead to

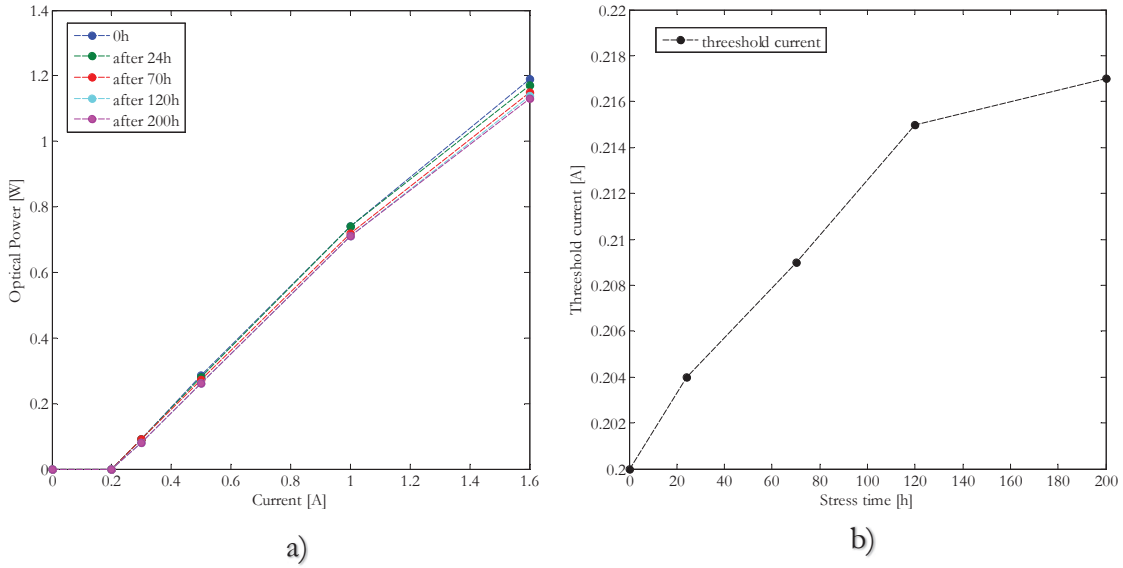

Fig. III-8. Optical power evolution for different current after stressing (a) and evolution of threshold current (b).

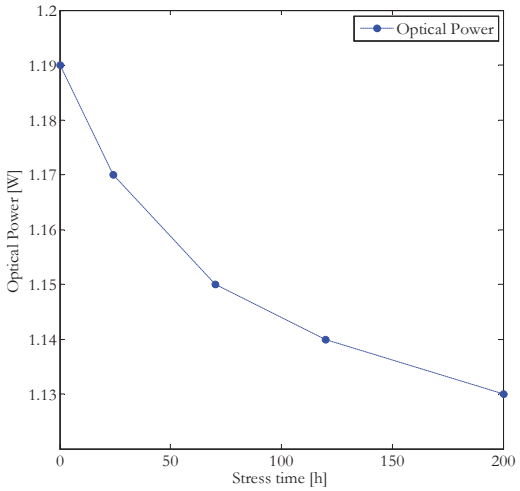

Fig. III-9. Decrease of optical power for current 1.6A.

decrease of intensity. Nevertheless, all these variations could be predictable and easy to adjust and control. The process, which can cause more difficulties is aging of laser with time.

To accelerate the aging process, we supply our laser diode with a "stressing" current of 1.7A for the period of 200 hours. The temperature indicated by controller was 45°C. At the same time, we were checking optical power for different values of current, and also the threshold current. The diode was supplied by Keithley Power Supply to provide high precision in measuring the threshold current.

On Fig. III-12a we summarize the results of the optical characterization of representative InGaN laser submitted to stress. As a consequence of constant current stress, LD showed a gradual increase in threshold current with no strong variation in slope of efficiency. Threshold current presented on Fig. III-12b was found to increase according to the square-root of stress time. It revealed that the threshold current increase about 10% of its beginning value. On the other side, the optical power after 200 hours of stressing decreases 3% (Fig. III-13) A similar behavior was previously described for InGaN-based laser diodes and is considered to the signature that laser diode degradation process in related to the increase in the concentration of defects within the active layer due to a defect-diffusion process. [84]

Due to general degradation process in the chips of semiconductor, we decided to verify optical power evolution in LED, to compare with the one of laser diode. The blue Light-Emitting-Diode Dragon PowerStar from OSRAM was chosen. To avoid overheating, the diode was mounted on the additional heat sink. The temperature was measured by thermocouple and was around 50°C. We supplied LED with the stressing current of 1.1A.

On Fig. III-14 we present the result of stressing the Light-Emitting-Diode. The decrease of power is around 8%. It is 5% higher than in case of a laser diode. This difference can be caused by different powers of the devices and also different types of heat sinks. Regardless the values, the behaviors (shapes of the curves) are similar.

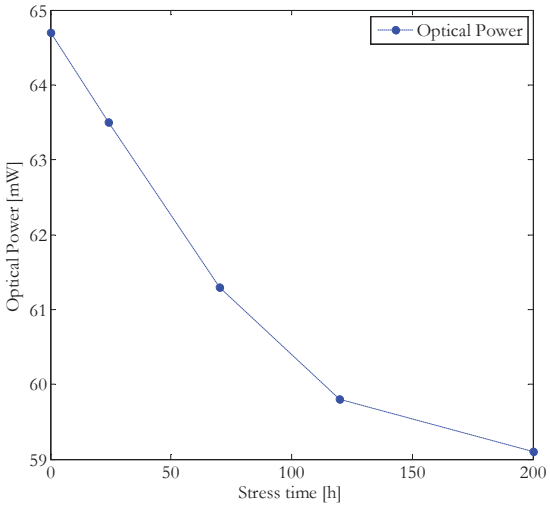

Fig. III-10. Decrease of optical power under stressing for Light Emitting Diode.

2. Aging of materials

Transparent silicon resins are generally used as an encapsulants for SSL sources. However, silicon resins have two disadvantages. One is that cured silicon resins are usually hard and brittle owing to rigid cross-linked networks. The other, is that epoxy resins degrade under exposure to radiation and high temperatures, resulting in chain scission and discoloration [85] Moreover, the color uniformity is also important issue. The usual consequence of a central and directional blue source combined with phosphor particles having an isotropic scattering is called yellow ring phenomenon [86]. The failure modes of encapsulant yellowing are decreased light output due decrease of transparency and discoloration. The basic causes of yellowing are: prolonged exposure to short wavelength emission, excessive junction temperature and the presence of phosphor [85]. Nevertheless, all these cases were described by aging a polymer in the oven under high temperature. We decided to age our phosphors, used for white light production, by laser irradiation, in the oven, and under the artificial sun.

2.1 Aging by laser irradiation

Our experiment was performed for 90 minutes. Again, the laser diode was set as an input of integrating sphere, but this time the phosphor was placed directly on the laser. We

aged YAG7.5%, YAG10% and YAG15% in thickness of 1.5 and 5.0mm. As an output, we put spectro-radiometer which allow us to observe the changes of the spectrum after 30, 60 and 90 minutes, respectively. Schematic experimental setup is shown on Fig. III-15.

2.1.1. YAG:Ce^{3+} aging process

On Fig. III-16 we can observe the converted light by the YAG phosphor. All the graphs were normalized to blue peak which correspond to laser light in order to compare the efficiency of the emission.

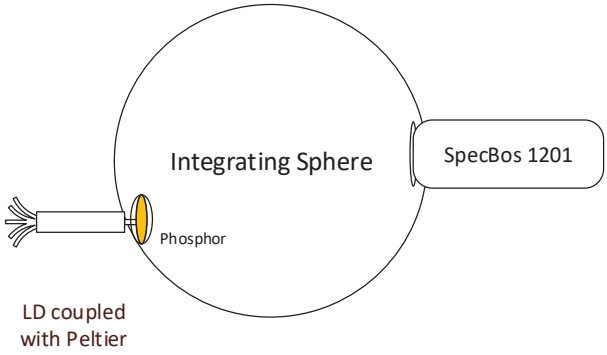

Fig. III-11. Schema of experimental setup for aging process.

The first observation let us conclude that laser irradiation caused decreasing of the conversion efficiency. However, it is more observed with the samples with low phosphor concentration. This lead us to assumption that it is silicon which is affected by irradiation and particles of phosphor might be understood as a heat sink. Moreover, from the shape of the figure, we can say that there are no structural modifications in phosphor component.

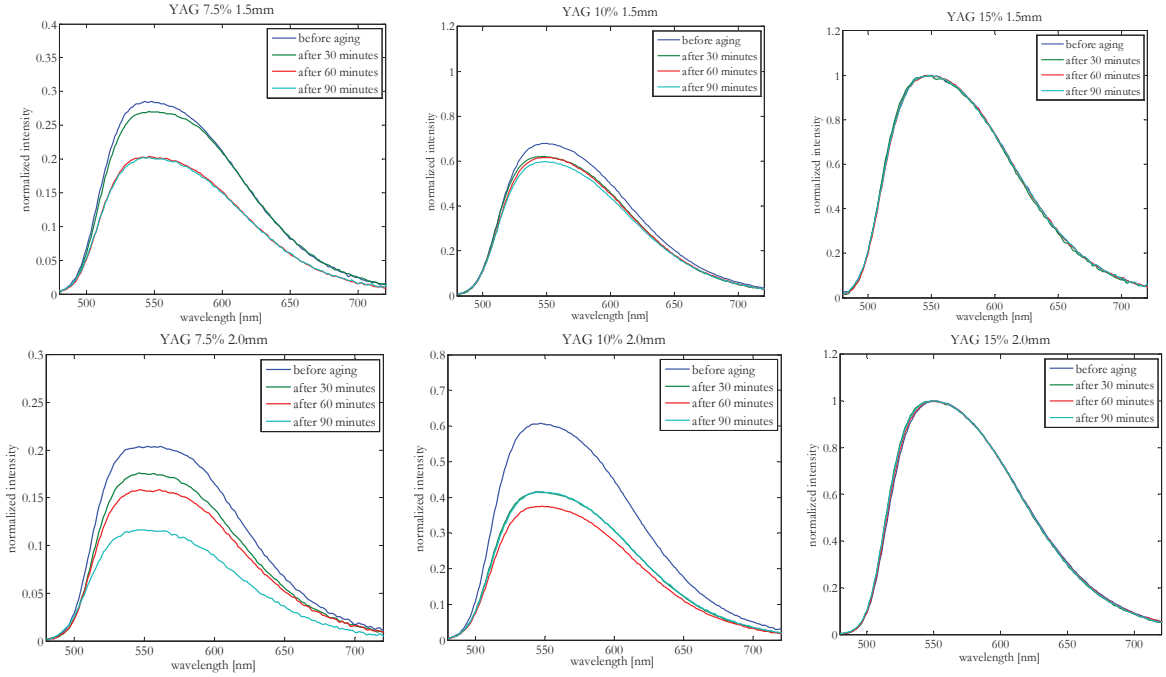

Fig. III-12. Effect of laser irradiation on YAG.

2.1.2. GYAG:Ce^{3+} with Nitride aging process

The same experiment was repeated with our mixture of GYAG and Nitride. The results are presented on Fig. III-17

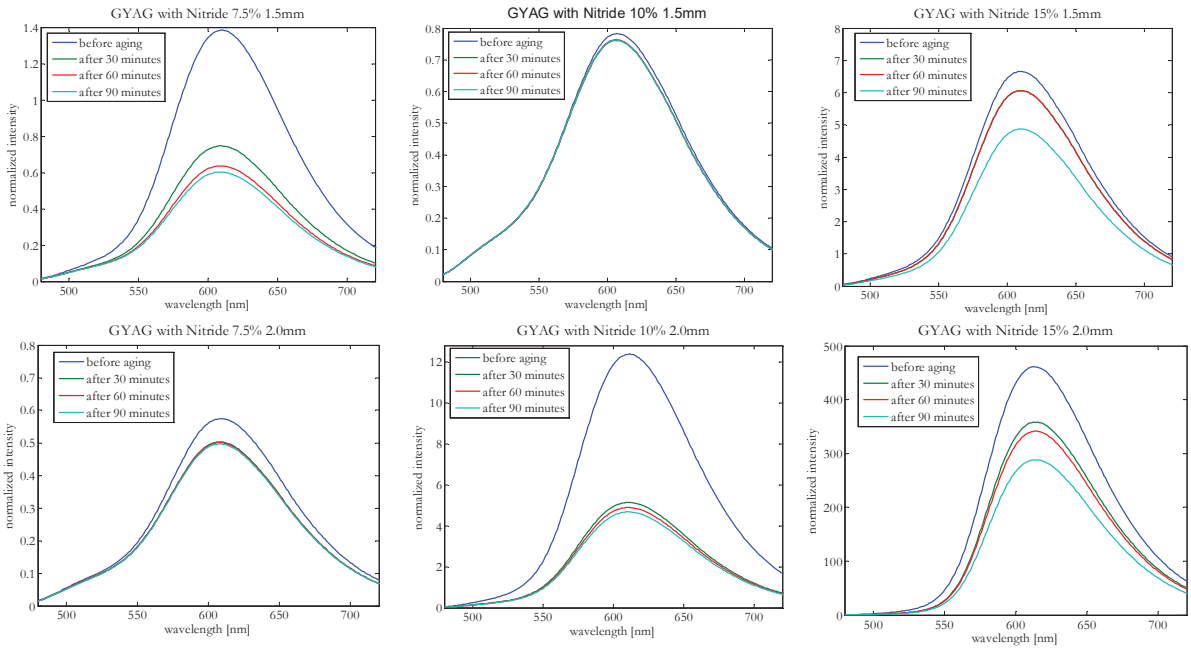

Fig. III-13. Effect of laser irradiation on mix of GYAG and Nitride.

Compering to results of YAG (emission with band at 550 nm), the drop of emission of GYAG part (525 nm) of mix GYAG and Nitride is higher. YAG has higher stability than GYAG.

However, the part of nitride in this composition with GYAG, decreases less (band at 650nm) due to its more covalent properties than GYAG. Indeed, nitride component contains nitrogen chemical bounds that are more covalent than oxygen bounds relevant of the YAG materials. This is due to the smaller electronegativity of nitrogen anion N^{3-}; 3, instead of 3.5 for oxygen anion O^{2-}. It induces a bond energy almost twice intense between nitrogen and neighbored cation (~940 kJ/mol) compared to oxygen and its neighbored cation (~500 kJ/mol), that are responsible of the chemical and physical hardness of the compound. In addition, it leads to a higher crystal field surrounding the luminescent cation, and to an intense nephelauxetic effect [87]. These two last phenomena are responsible of the high wavelength emission of nitride and low influence on a structure [68].

2.1.3. FTIR analysis after irradiation

To study the influence of irradiation on the structural level of the materials, the Fourier-transform infrared spectroscopy analysis was performed. For this study we used a spectroscope InfraRouge ATR Schimadzu Miracle 10, with the range of the wavelength 400 to 4000 cm^{-1}, with a step of 4 cm^{-1}. As a reference we used a zone not effected by a laser irradiation (so-called "Ref"). To investigate the changings performed in the material more

precisely, we compared the samples which were irradiated and stuck to the laser diode directly ("stuck"), with the one, where irradiation was performed from a distance of 2 cm. ("distance"). The whole measurement gives the information about all the Si-O-C-H mutual bonds that are into the silicone compound.

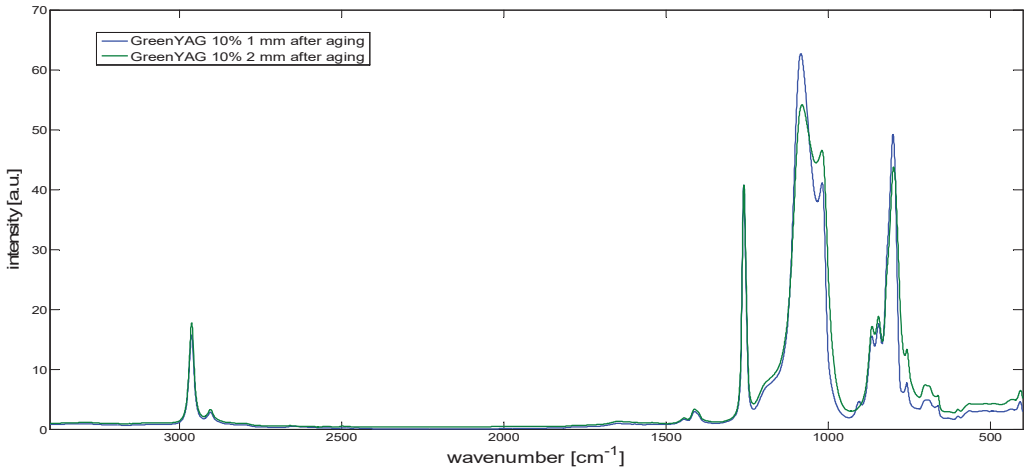

Fig. III-14. Example of full spectrum from infrared analysis.

The most relevant part is related to the band 2965cm^{-1}. It can be seen (Fig. III-18) that the band increases comparing to the reference value. This phenomenon is related to destruction the bond CH_2=CH_2, which can be found in silicon, and creation CH_3. After destruction of the bond, the free radicals are created which lead to theirs' recombination with the free particles of hydrogen causing creation of CH_3. [88]

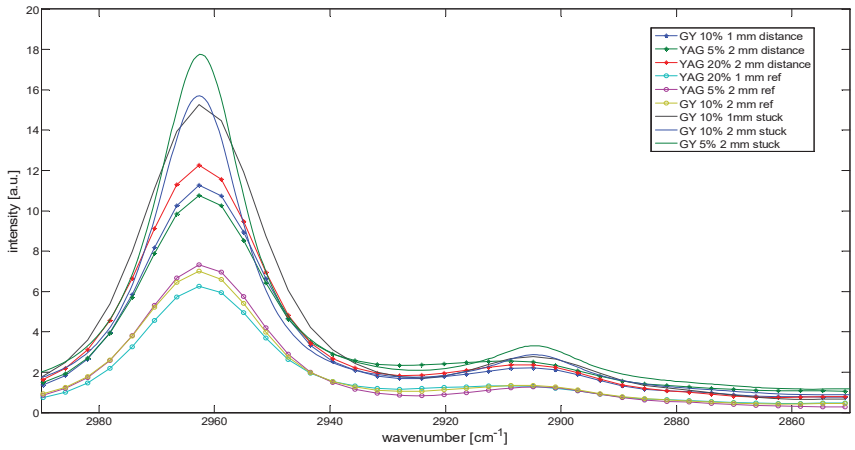

Fig. III-15. Infrared spectrum between 2900-2800 cm^{-1}.

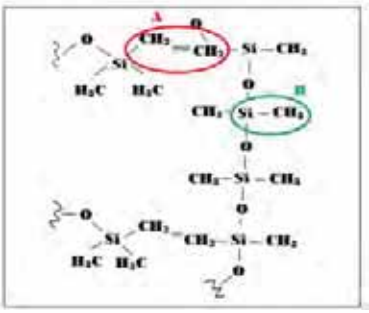

Fig. III-16. Degradation of bond CH2=CH2 (A) and recombining to create CH3 particles (B)

Additionally, the influence of positioning sample directly on the laser is more significant than in case of keeping a sample in distance. Moreover, in this study, we didn't observe the influence of phosphor concentration or thickness of a samples on an aging process by laser irradiation.

However, the optical properties of the phosphor can be modified, due to oxidation of the doping ions ($Ce^{3+} \rightarrow Ce^{4+}$), thermal extension or thermal quenching. [89][90] Oxidation as well as extinction increase with temperature. Oxidation is irreversible, whereas extinction disappears on the return to the room temperature. Nevertheless, oxidation can also occur due to humidity and reactions with free radicals of polymers. In addition, by increasing the temperature, a broadening of the emission band may appear, and a shift of the emission of the phosphor has to be highlighted [80].

2.1.4. Silicon aging process

Photodegradation of polymer materials usually take place by increasing the molecular mobility of the polymer molecule, which is made possible by raising the temperature and the introduction of chromophores as an additive or an abnormal bond into the molecule, both which have absorption maxima in region where the matrix polymer has no absorption band. [91] Photodegradation depends on exposure time and the amount of radiation. Thus even an exposure to visible light can cause the polymer be degraded [92][93].

Many epoxies can turn yellow when subjected to prolonged exposure to ultraviolet light as well as blue light. Discoloration results in a reduction of transparency and causes a decrease of light. Furthermore, degradation and the associated yellowing increases exponentially with exposure energy. [85]

To observe the effects of exposure of epoxy to high temperature we decided to accelerate the process. We put a polymer on the heating plate, to heat it to 200°C. On Fig. III-21 we can observe the transmission of silicon after being heated. The uniformed discoloration of silicone was assumed. Our preliminary studies seem to reveal a 16% of darkening on the blue side and 13% of darkening on the red side.

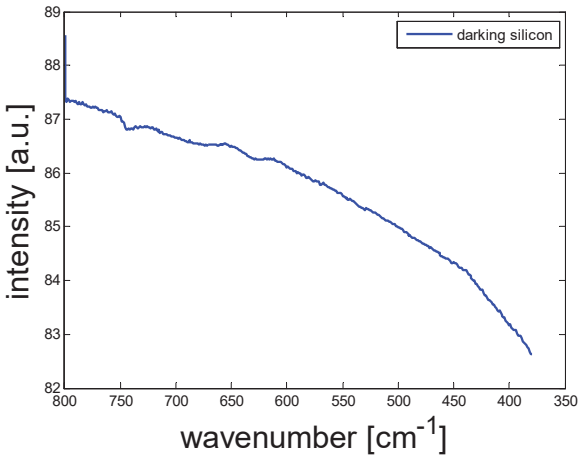

Fig. III-17. Darkening of silicon after heating to 200°C**.**

2.1.5. Glass aging process

Commercial red phosphors are hard to incorporate into glass due to chemical reactions between nitride and melting glass[94]. However, pasting a layer of phosphor on a piece of glass gives very good results (see Chapter II). Nevertheless, due to backscattering, absorption and reabsorption of the phosphor particles a significant portion of blue light from source and yellow light from phosphor layer were ultimately lost within the package [45]. Despite these small drawbacks, glass is very rigid material with high thermal conductivity.

In order to verify its rigidity, we irradiated the phosphor in glass CL-830-XT with a blue laser diode, supplied with maximum current I=1.5A. for 120 hours. With spectro-radiometer Specbos, we measured the parameters of the light before and after irradiation process.

On Fig. III-21 the spectrum before and after irradiation are presented. To compare the efficiency of the conversion, spectra were normalized to blue peak, which corresponds to

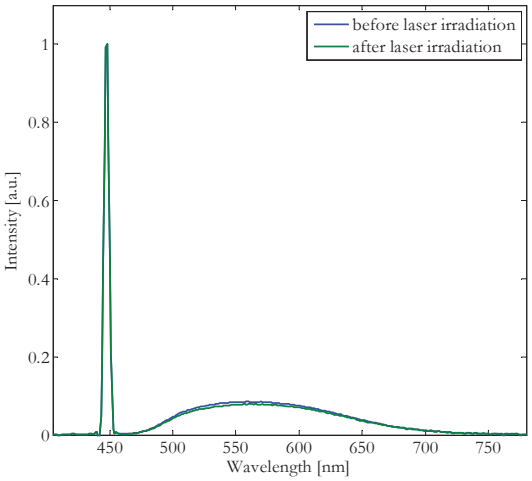

Fig. III-18. Spectrum before and after irradiation for 120h.

blue laser diode emission. Due to the curves, we can notice that the emission of conversion almost did not change at all. It means that probably neither phosphor nor glass was affected by this irradiation.

Table III-4. CCT and CRI before and after irradiation.

Before irradiation		After irradiation	
CRI	**CCT**	**CRI**	**CCT**
76	6449 K	76	6664 K

The CIE chromaticity coordinates are very similar. We can observe small shift into blue color due to insignificant decrease of conversion efficiency. CCT also move into colder

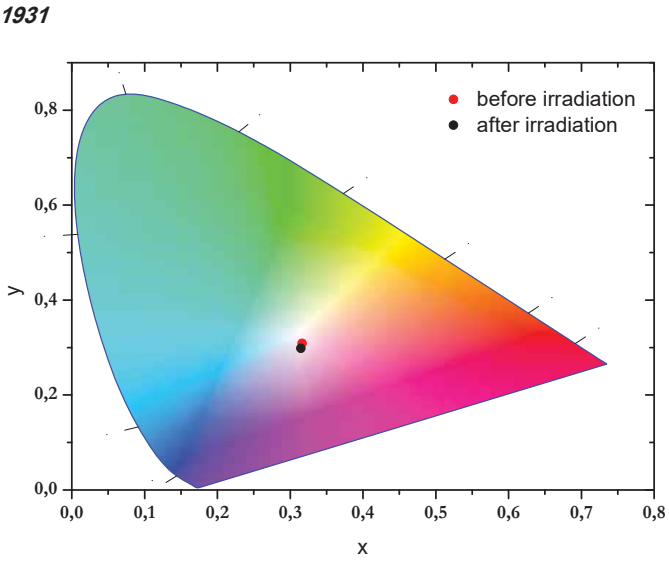

Fig. III-19. Chromaticity coordinates before and after irradiation.

colors (from 6449 to 6664K). CRI stays the same.

2.2. Aging by artificial sun

The phosphors are not influenced only by LEDs' or lasers' light, especially when used for outdoor applications. There is also an external influence from light of sun – in particular UV. We decided to degrade silicon and phosphor in silicon by artificial sun for 600 hours.

As an artificial sun we used a xenon lamp which generates not only visible light, but also can emits UV rays and infrared. The temperature under the artificial sun was 65°C. The optical power generated by this source was measured by Power Meter Newport Model 843-R and was equal to 98mW. The phosphor and silicon samples were placed below the lamp.

Fig. III-21. Experimental setup for aging the sample by artificial sun (xenon lamp).

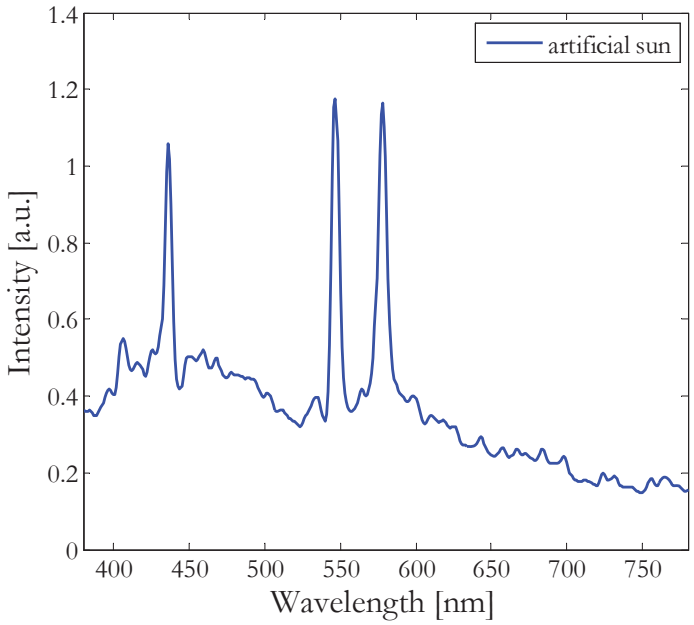

Fig. III-20. Spectrum of "artificial sun".

Experimental setup is presented on Fig. III-24.

On Fig. III-25 we present the spectrum of the lamp “artificial sun” taken by spectro-radiometer Specbos.

In paragraph about aging of silicon it was said that after heating the silicon to 200°C we could have observed changes at ends of spectrum. Irradiation of the laser caused decreasing of efficiency and modification in silicon structure. This experiment should show the influence of exposition to the visible light and ultra violet radiation on silicon and phosphor in silicon samples.

Two materials were aged: silicon Dow Corning® EI-1184 (thickness 1mm), and YAG: Ce^{3+} incorporated into this silicon (concentration 10%, thickness 1mm).

On Fig. III-26 we present the results of aging by artificial sun. For YAG, the results show the value of maximum emission by YAG and its evolution with time. For silicon, the

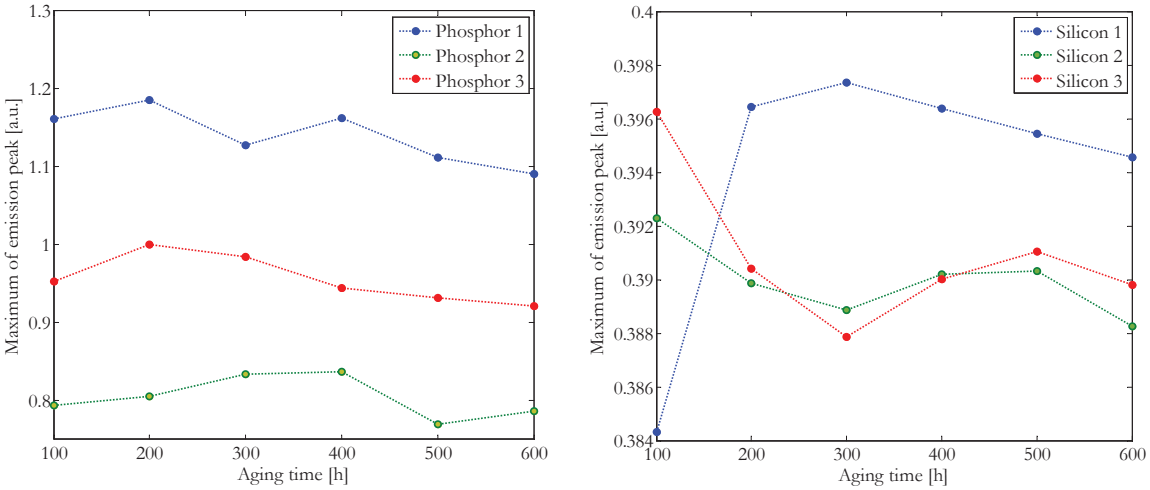

Fig. III-22. Emission after aging by YAG and silicon.

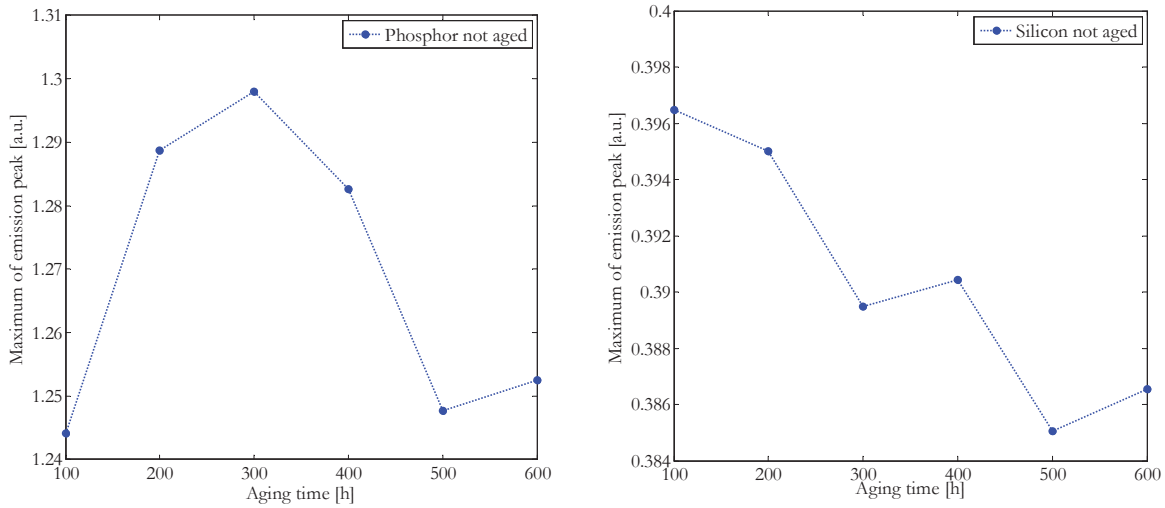

Fig. III-23. Phosphor and silicon not aged.

results show the blue light traversing the sample and its maximum value in function of time. To focus on efficiency of conversion the maximums of emission by phosphor are taken, when the spectra were normalized to blue peak. The emission of light traversing by silicon

is not normalized and represents real value of emission by a diode after passing by the silicon sample. To confirm our results, we performed our experiment on three samples of silicon and three samples of phosphor.

To better understand the behavior of aging, at the same time we were monitoring the spectrum of samples which were not affected by aging, but were closed in the box, without light access. The maximums of emission of phosphor and silicon in time evolution (not aged) are presented on Fig. III-27.

Due to bibliography research [45][95][96][97] we expected the efficiency drop in conversion by YAG material or emission by silicon. However, the results show that with and without aging, the maximum band's variation is not coherent. The amplitude of variation is less than 10%. Nevertheless, the typical aging process did not occur. The common drop of the emission is caused by very high temperature or humidity [97]. In our case the temperature of aging equal to 65°C was too low. The phosphor particles degrade due to temperatures that exceed 100°C. And it is the burning phosphor which heat silicon and cause its degradation (darkening, yellowing). The silicon without phosphor particles would be more resistive to the high temperature. Moreover, artificial sun emits UV radiation. Since we cannot observe obvious degradation, it means that there is no influence of ultraviolet on our samples.

2.3. Aging by blue LEDs

The blue light can have particular influence specially on the silicon. It may cause photodegradation and yellowing. To verify this thesis, we put silicon and phosphor samples under blue LEDs irradiation for 600 hours. The LEDs are mounted on the wall of box. The

Fig. III-24. Image of diodes mounted in the box for aging process.

samples were put under the diodes in a distance of 5 cm.

The measurements were performed every 100 hours. The optical power generated by LEDs was 8.6 mW. The spectra of the LEDs are presented on Fig. III-29. The results of

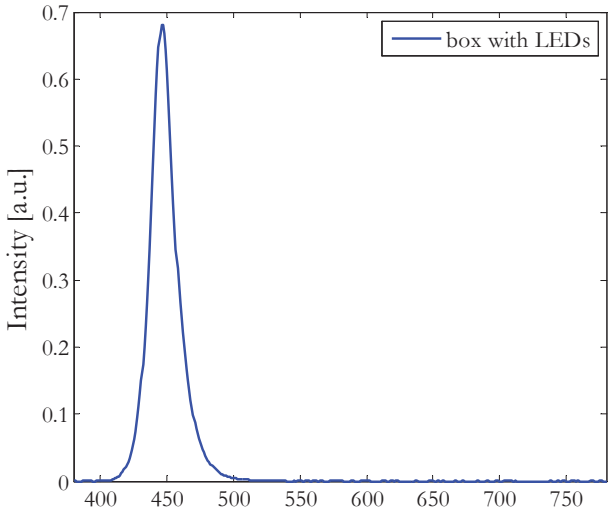

Fig. III-29. Spectrum of box with LEDs.

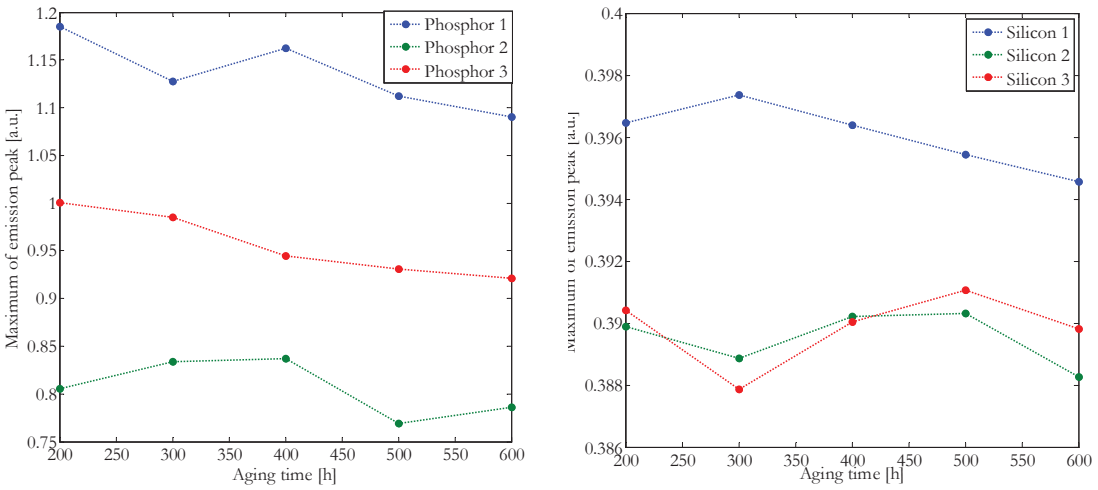

Fig. III-30. Evolution of maximum peak of emission of phosphor sand silicon.

the maximum peak of emission of phosphor and transition of the light via silicon are presented on Fig. III-30.

The results show similar tendency to this, after aging by artificial sun. This allow us to say, that blue or ultraviolet light has no big influence on aging of silicon or phosphor in silicon. The principle cause of aging is high temperature, which heat the phosphor particles what leads to burning the silicon around them. Moreover, silicon degrades slower, if it does not contain phosphor particles.

The explanation of evolution variations was found by measuring the spectrum of a source – laser diode, supplied by constant current 1.0A and 0.5A respectively. In spite of fixing the temperature on 30°C by temperature controller, we were verifying its real value.

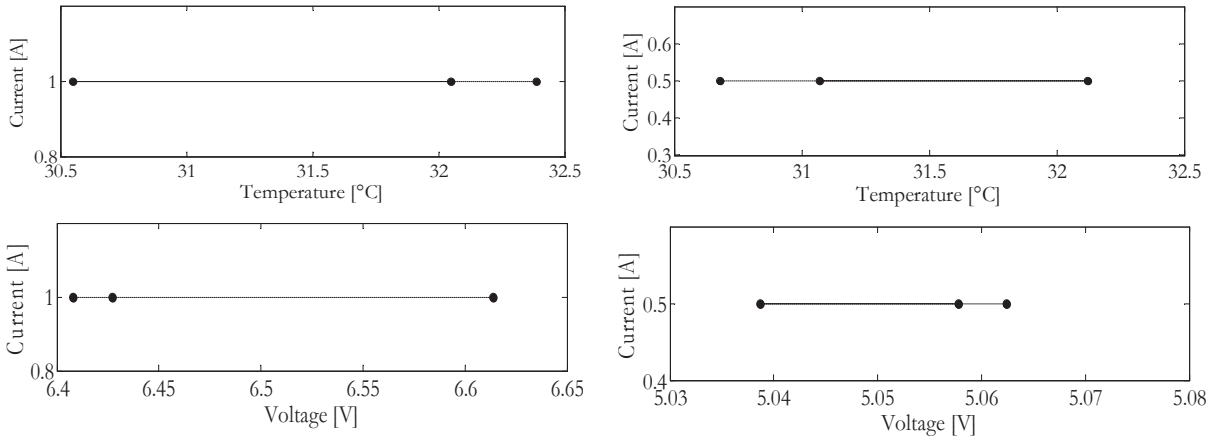

Fig. III-25. Variation of temperature and voltage for constant current.

The results show that the temperature changes around 2°C and the voltage varies 0.2V and 0.03 for 1A and 0.5A respectively. These parameters have direct influence on the intensity of the light emitted by a diode. Moreover, the measurements of the spectrum of the light for aged samples were performed at high value of current – the variations seem to be higher with higher current. Based on these measurements we can explain the variation of the maximum emission.

2.4. Temperature distribution on different phosphor plates

In source of light based on phosphor, the phosphor region is non-negligible heat source due to Stoke loss and the imperfection of phosphor conversion quantum efficiency. Moreover, phosphor is often mixed with transparent silicon matrix which has poor thermal conductivity. The temperature issues may even lead to carbonize of phosphor region, due

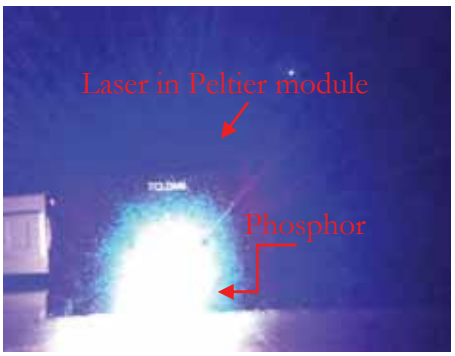

Fig. III-26. Experimental setup. Phosphor in silicon placed in front of laser diode in Peltier module.

to self-heating [96].

In our experiment we studied the temperature distribution on two types of phosphor plate: YAG doped with cerium in concentration of 20% in silicon matrix of the thickness of 2 mm and diameter of 10mm, and a mix of YAG and Nitride doped with cerium and europium, respectively, coated on the glass of thickness 3 mm and diameter of 45 cm.

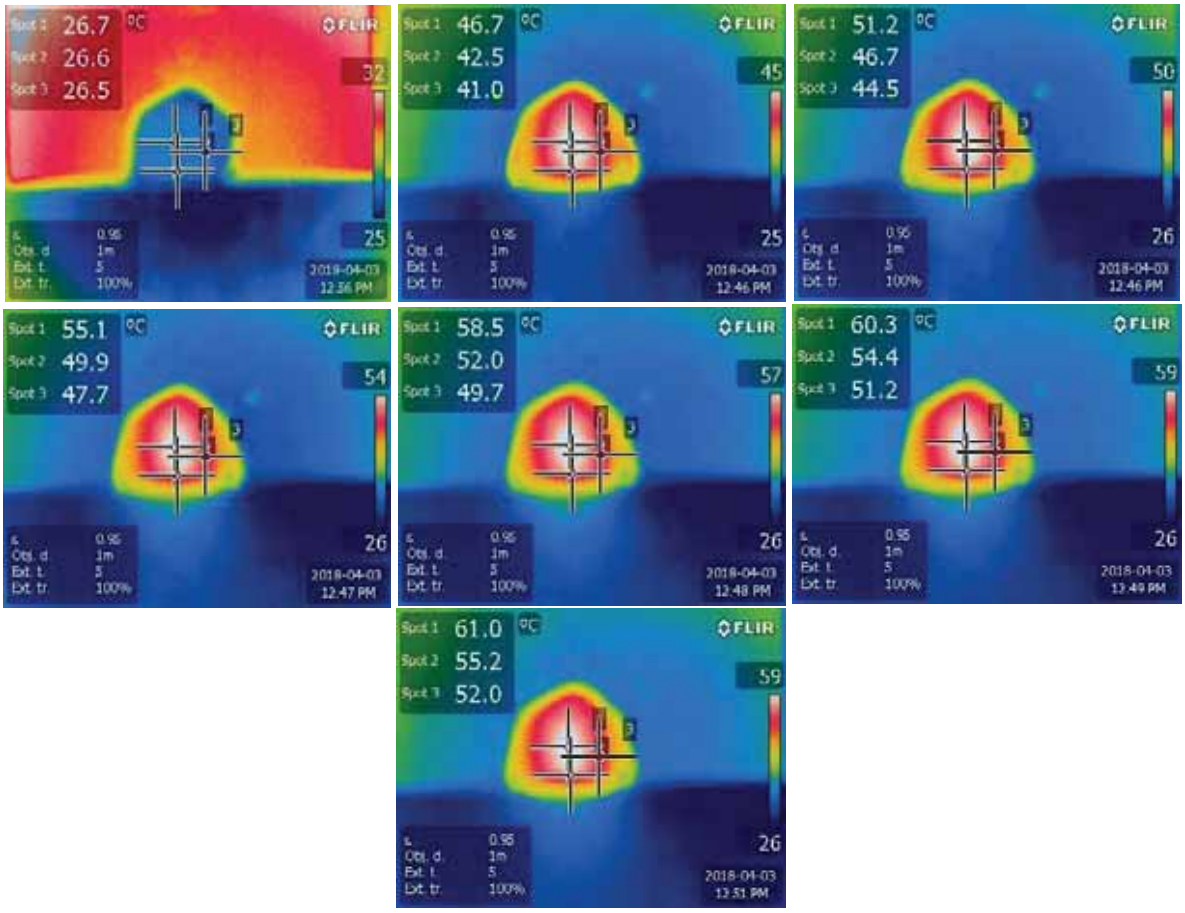

Fig. III-27. Distribution of the temperature on silicon in time evolution.

We supplied our blue laser diode with a high current 1.5A. The samples were placed in a distance of 50 mm from a diode, to avoid additional losses. The temperature was measured by thermal camera FLIR TG167 which uses the infrared technology. The measurement was taken in three places on the phosphor plate – in the middle (spot 1), on the bottom (spot 2) and on the side (spot 3). No optical equipment to focus beam of the laser was used.

The distribution of the temperature on silicon plate is presented on Fig. III-33

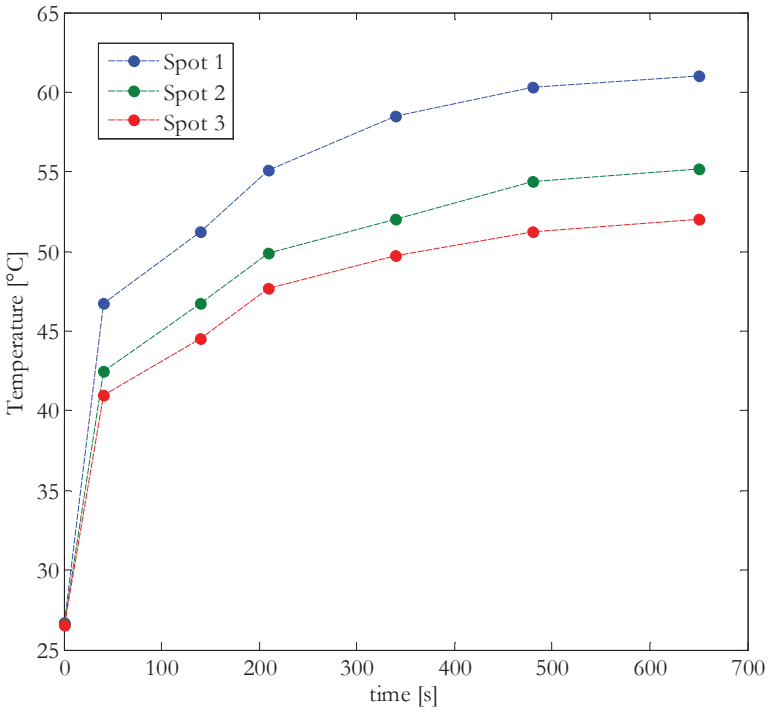

Fig. III-29. Temperature evolution in a function of time on silicon plate.

The first picture shows the distribution of the temperature when the diode is turned off. We can notice, that temperature of the three spots is similar and around 27°C. The red color behind with the value of 32°C is a laser diode in Peltier module, with temperature controller fixed at 30°C. After suppling a diode, the temperature on the phosphor changes. Nevertheless, we can observe that the highest value is in the middle of phosphor (and the middle of beam). The lowest value of the temperature is on the side of a sample, due to oval shape of a laser beam. After 640 seconds, the maximum value of the temperature was 64°C. The minimum, obtained on the side, was 52°C. The distribution of the temperature seems to be constant, which means that the irradiation constantly affects more intensively

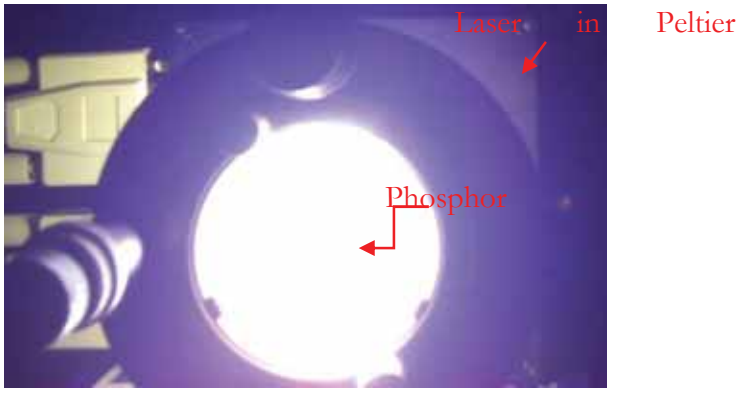

Fig. III-28. Experimental setup. Phosphor in glass placed in front of laser in Peltier module.

the same place. This may lead to not uniform darkening of the silicon.

Graph, presented on Fig. III-34 shows the evolution of the temperatures on different spot in time. The temperatures on different spots are increasing proportionally. After 300 seconds the slope starts to saturate slowly.

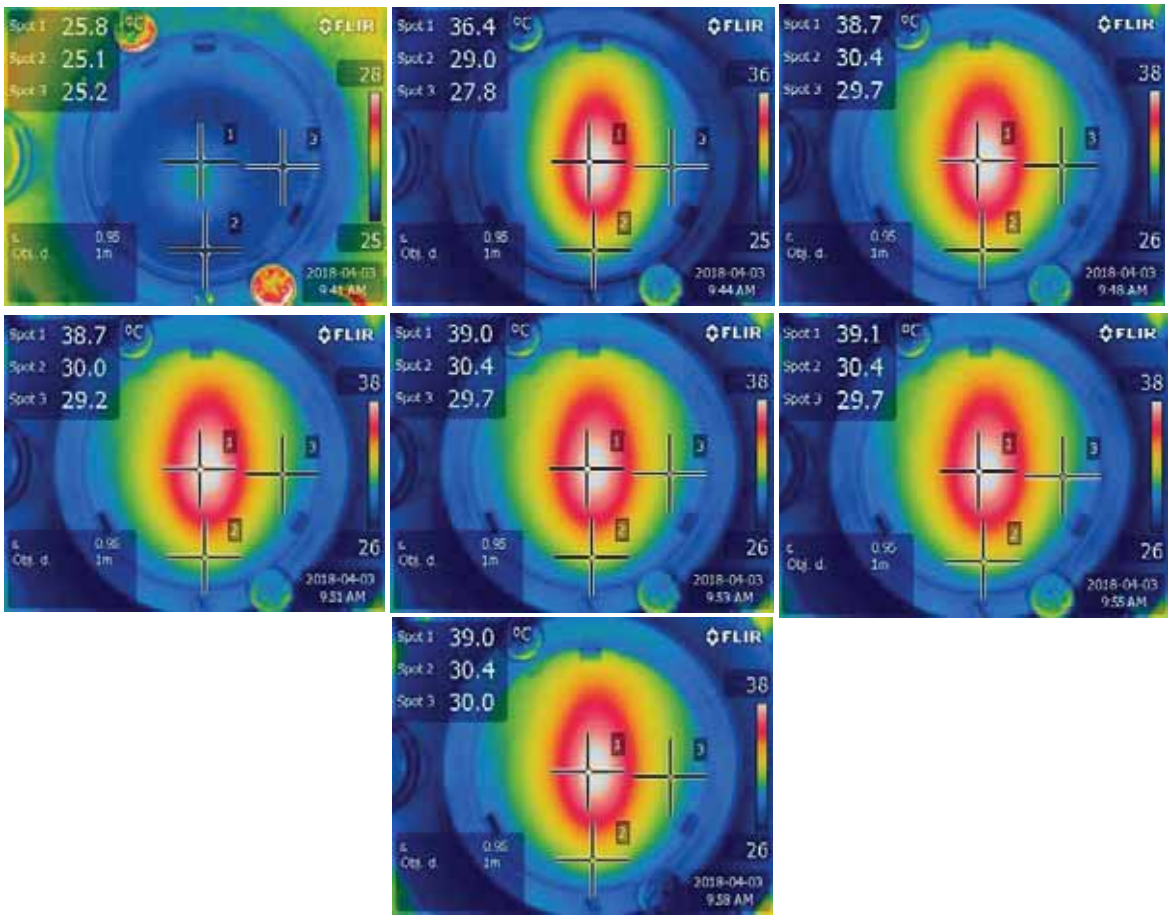

Fig. III-30. Distribution of the temperature on phosphor on glass.

Subsequently, we have done the same for the phosphor in glass sample. However, we left them for 2 times longer under laser irradiation, to confirm the saturation of the temperature. On Fig. III-36 we can again notice the characteristic oval shape of light distribution. The maximum value of the temperature we obtained was around 40°C, and represents the spot 1. Temperature on the bottom and on the side was around 10°C lower. On Fig. III-37 we represent the temperature evolution in time. It stabilizes after 400 first seconds and seems to saturate.

The exposure to high energy radiation cause lower stability of silicon resin. Moreover, due to long thermal stress, higher thermal conductivity and thermal quenching, the significant reduction in luminescent is observed.

The samples do not exist in the similar form (size difference) so the mechanism of thermal quenching of luminescence does not remain the same. However, in bibliography

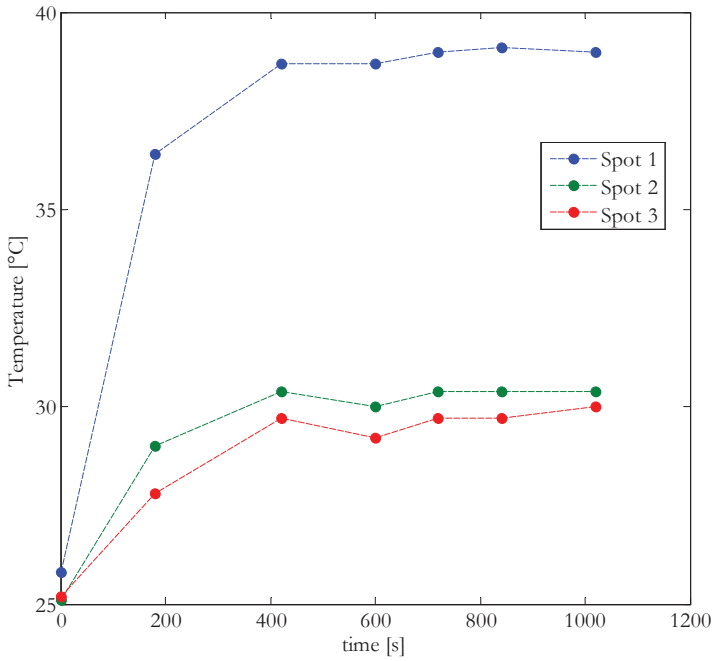

Fig. III-31. Temperature evolution in a function of time on phosphor in glass.

[98] we found that the thermal conductivity of the phosphor-silicon system can be found 10 times that of the phosphor in glass. The higher thermal conductivity of the Phosphor on Glass thus can effectively reduce the rate of the heat flow and reduces the rate of phonon assisted nonradiative transmission in phosphor This is a considerable advantage of the system based on glass over the conventional resin-based system, when considering the high operating temperature of potential system.

3. Conclusions

In this chapter the different aspects of aging of the source of light based on semiconductor and phosphor were described.

First type of aging occurs in semiconductor. Due to high temperature in active layer, while suppling a diode, the additional heat sink is necessary. We performed a simulation in FEM software to show the distribution of the temperature inside of the diode. Our analysis was run for a case without additional heat sink, and with a temperature controller and Peltier module for cooling. In steady state results revealed that the temperature can achieve 190°C. Transient state shows, that we reach 120°C inside of the diode in milliseconds, if we do not apply additional radiator. We also showed the values of the temperatures on the chip, while controlling a temperature on different level: 25°C and 55°C. Moreover, we

calculated the thermal resistance of a diode and we found out that it can increase even three times without cooling module.

To fulfill these studies, we verified how the temperature of the diode can influence on the emission of light after conversion by a phosphor. We noticed, that intensity of the diode is lower for 55°C than for 30°C, which lead to lower intensity of a converted light. Moreover, when the diode heats, its wavelength moves to the higher values. By checking the absorption and emission of different materials we show that variation in wavelength can lead to variation in light parameters – especially dangerous case is when we start to convert less blue light, what can cause damages to our eyes.

Another interesting aspect is decrease of optical power which leads to decrease of intensity. Decrease of intensity cause decrease of light conversion. Nevertheless, after 200h of working under stressing current the optical power decreases only about 3%. We also found out that with a time, the threshold current increased about 10%. We compered our results with aging of a blue Light Emitting Diode. We found similar behavior, however, LED's optical power decreased more.

Another type of aging in a SSL concerns phosphors. We tried to aged our materials in different ways.

First type of aging was a laser irradiation. We left a silicon sample with phosphor for 90 minutes just in front of laser diode, which was working under maximum optical power. Studies revealed that YAG is sustainable and resistant phosphor, however nitride is more covalent and shows better resistance to aging. Shape of emission did not change, which led us to conclusion that there are no structural changings in phosphor.

However, the emission after irradiation dropped. Infrared analysis proved destruction of the bond $CH_2=CH_2$ in silicon and creation new one – CH_3. Additionally, the optical properties can be modified by the oxidation, thermal extension or thermal quenching. In our case, after aging silicon sample, without phosphor inside, on heating plate (200°C), we saw darkening phenomenon.

Due to darkening issues of silicon we tried phosphor in glass which supposed to be more ridged and have higher thermal conductivity. As before with phosphor in silicon, this time we irradiate with a laser diode, powered with the highest current possible, a sample of phosphor in glass. Regarding properties of glass, we decided to leave a phosphor under radiation for longer than time – 120 hours. Results revealed no aging process, no changing in spectrum or in light parameters. Moreover, the temperature distribution, examined by infrared camera shows, that glass can better evacuate the heat that the silicon. Also, the temperature on the glass finally saturates, while on the silicon constantly increases.

Aging under artificial sun (xenon lamp), which emits UV light proved that without heating a samples in silicon into very high temperature (>100°C) we are not able to decrease the conversion of a phosphor. Similar conclusion was made after aging by blue LEDs. The variations of the emission are the influence of small variation of light emitted by diode.

Chapter IV

White Light Based on n-UV Laser Diode

Table of contents

White Light Based on n-UV Laser Diode 119

1 Near-UV laser diode 120

2 Blue phosphors 121

3 BAM: Eu^{2+} 124

3.1 Aging of BAM: Eu^{2+} 125

3.2 Optical power dependencies 126

3.2.1 Number of particles 126

4 White light 127

4.1 BAM: Eu^{2+} and YAG:Ce^{3+} 128

4.2 BAM: Eu^{2+} and GYAG:Ce^{3+} with Nitride 129

4.3 Phosphor mix 131

4.4 Filter application 133

4.5 Number of particles 140

5 Saturation effects on phosphor materials 142

6 Conclusions 146

1 Near-UV laser diode

Some applications required very high value of CRI. Museums, expositions or stages lighting, sources of light for medical purpose should be design with a CRI minimum 85. Unfortunately, the higher the CRI, the lower the luminous efficacy of SSL source is. [99] Source of light based on blue laser diode gives satisfactory results, however, after the time, the diode lose its optical power, or efficiency of material decrease, the value of CRI drops due to changes of blue peak. As an alternative, to obtain wider spectrum, independent from a laser light changes influence, the near-UV laser diode can be used.

To generate white light by n-UV laser diode two types of phosphors are needed – blue, that converts violet light to blue, and yellow – to convert blue light to yellow. The sum of these colors give a white light [100][101][102].

The laser diode used in this study was a n-UV GaN laser diode 405 nm, 500 mW from USHIO. The first measurements were performed to verify characteristics of a laser diode.

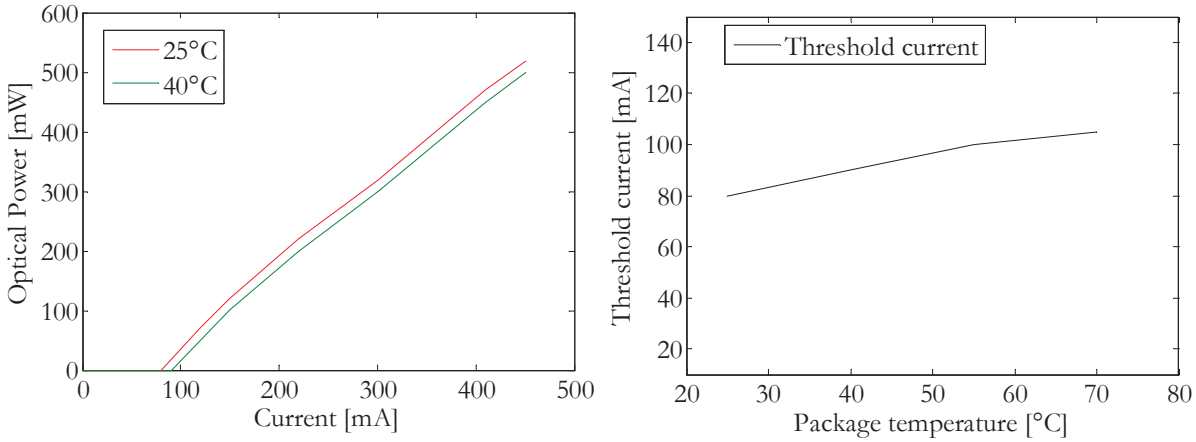

Fig. IV-1. Characteristics of optical power and threshold current for a violet laser diode.

The value of the threshold current for 25°C is around 80 mA and it increases, when the temperature rises. Between 25°C and 70°C the threshold current changes about 23%. In the temperature of 25°C the maximum optical power is achieved with the current of 450 mA. When the temperature rises, the maximum optical power drops about 20mW.

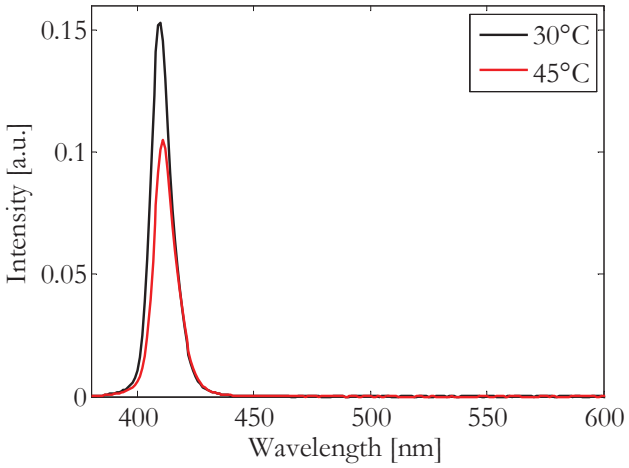

Fig. IV-2. Spectrum of laser diode 405 nm for different temperatures.

On Fig. IV-2 we present the sensibility of the wavelength to different temperatures.

We perform the experiment in the integrating sphere. The laser diode was coupled with Peltier Module, to dissipate the heat. It was also connected to temperature regulator, to control the temperature. We did the measurements for two different values: 30°C and 45°C. In both cases the diode was supplied with the forward current 0.5A. With the increase of the temperature the slight shift to longer wavelengths can be noticed. Moreover, the intensity of the light emitted by diode drops 33% compering between 30°C and 45°C.

2 Blue phosphors

To produce white light by using a violet laser diode, the blue phosphor is needed. We have produced three different phosphors compositions and incorporated them into silicon resin. Each sample has a thickness of 1mm and diameter of 15 mm.

The first type of blue phosphor is BAM ($BaMgAl_{10}O_{17}:Eu^{2+}$). The powder we used was offered by Philips company and can be found in discharged lamps. We also got commercially prepared BAM powder from Sigma Aldrich.

Fig. IV-3. Propositions of blue phosphors: BAM, RCA, Pba.

The second material is a calcium barium phosphate Pba ($Ca_6BaP_4O_{17}:Eu^{2+}$). It is reported that this phosphor has excellent thermal stability and stabilization of the ionic charge in the lattice, compared to other oxide phosphors. [103]

The third proposition is blue phosphor called RCA. It is a phosphor used by Thomson

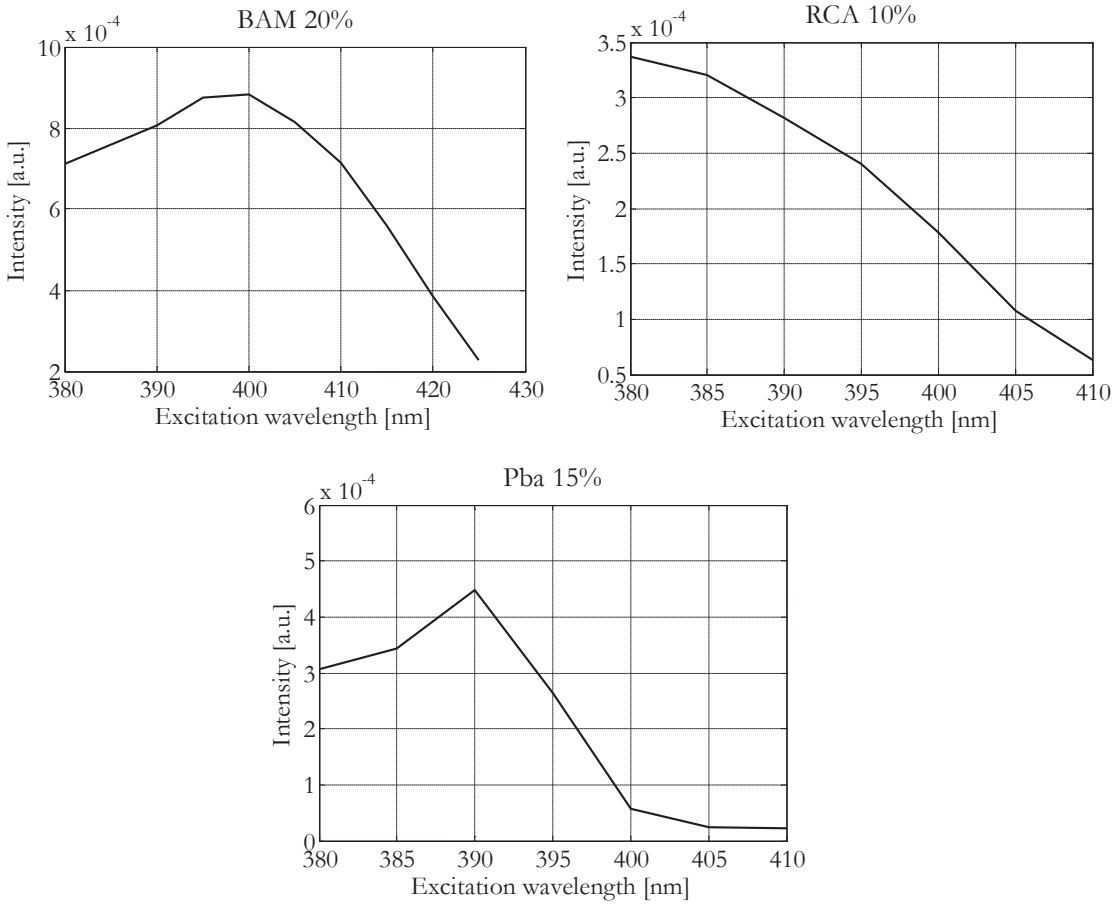

Fig. IV-4. Excitation by different wavelength for BAM, RCA and Pba.

in cathode screens. [104]

To choose the material with the most suitable properties for our application we used monochromator, to send different wavelength, to verify which material would absorb and emit the most and which energy.

From the excitation spectrum we can see that for the laser diode of 405 nm the most suitable material would be BAM. Its maximum intensity is at excitation of 400 nm. RCA and Pba are characterized by low emission at 405 nm. The maximum for Pba is around 390 nm and for RCA at 380 nm. Both of these materials would be better for UV source.

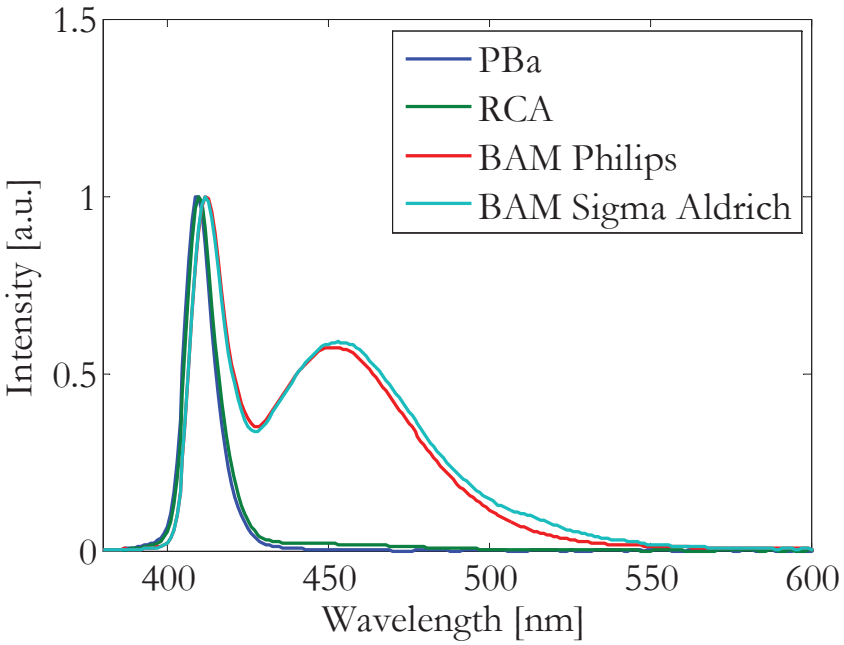

Fig. IV-6. Excitation spectrum by violet laser diode of different material.

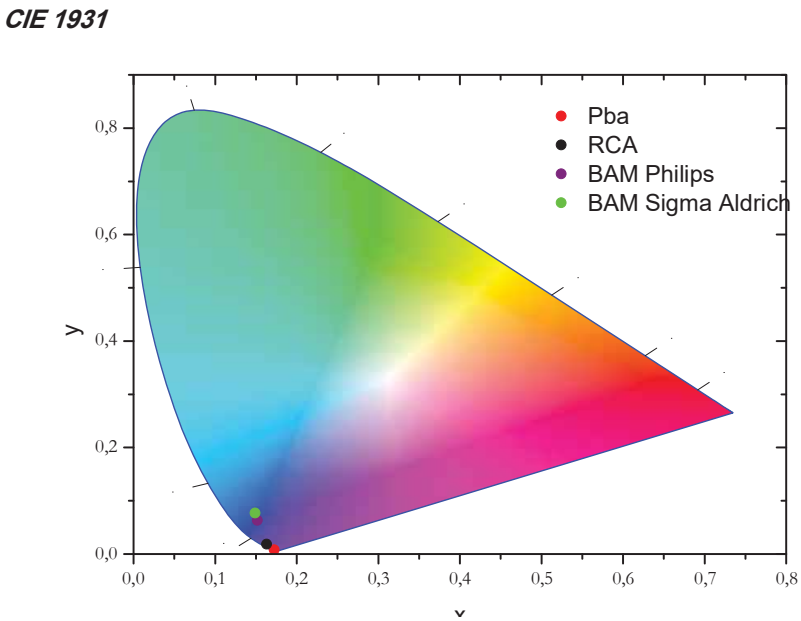

Fig. IV-5. CIE chromaticity coordinates of light emitted by diode nUV and blue phosphor.

In spite of these results obtained by monochromator, we decided to see the spectrum of emission, and color of the light, after conversion by all of these materials while excited by a violet laser diode.

As we can see on Fig. IV-5 the emission spectrum of Pba 15% and RCA 10 % are very weak. In contrary, the emission of spectrum of BAM (Philips and Sigma Aldrich – both in concentration of 20%) is quite high, and can be improved by increasing the concentration in silicon resin.

The shift between blue peak appears due to small temperature variation (which lead to voltage variation) during the measurements.

To see better the color of the light emitted by the material, after conversion, excited by nUV laser diode, we measured the CIE chromaticity coordinates. On Fig. IV-6 we find coordinates of light for Pba, RCA and two types of BAM. BAM materials can be found in the blue region, while Pba and RCA are more into violet.

3 BAM: Eu^{2+}

$BaMgAl_{10}O$ (BAM) powder doped with 10mol% of Eu^{2+} is a known commercial phosphor. Its blue emission resulting from allowed 5d to 4f radiative transition within the Eu^{2+} ion produces a broad band centered at 450 nm and covering about 400-520 nm spectral region. The emission can be excited with any wavelength from UV to near UV region, which makes the phosphor useful for fluorescent lamps and plasma display panels. Recently, another spectacular utilization for BAM has been proposed. Its properties were found to be attractive for the study of the UV environment on the surface of Mars. [105]

An important drawback of BAM is a partial oxidation of Eu^{2+} to Eu^{3+} as an organic binder is being burned off at about 500°C [106][107]. Nevertheless, as an application for solid-state lighting, these temperatures are not reached.[108] Unfortunately, nUV excitation partially degrades the powder phosphor performance in time of using: the emission moves to green and the efficiency decreases. The reason is again the Eu^{2+} to Eu^{3+} transformation simulated by the high energy photons and rather complex structural changes resulting from this effect. [109] Moreover, it is believed that the BAM host can damaged easily when external energy is introduced. [110]

The BAM, on which all the measurements were performed, were prepared from two types of powders: Philips and Sigma Aldrich. Phosphor were incorporated into silicon resin in 4 different concentrations: 10%, 20%, 30% and 40%. Each sample has round shape, diameter of 15 mm and thickness of 1mm.

We excited BAM material by violet laser diode 405 nm, 500 mW from USHIO. To stabilize the excitation wavelength, the diode was coupled with Peltier module, connected

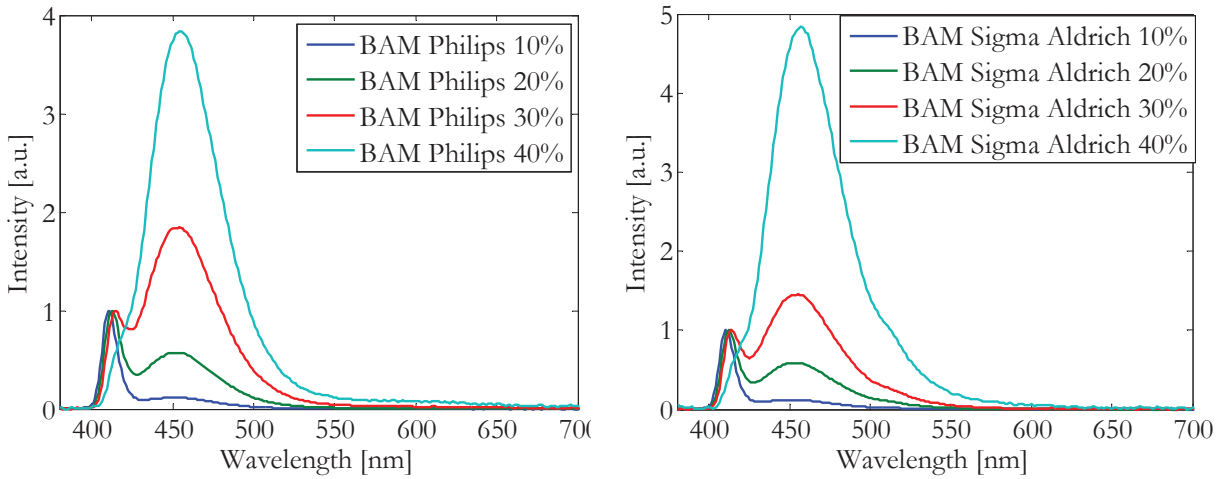

Fig. IV-7. Emission spectrum of BAM Philips and BAM Sigma Aldrich by violet laser diode.

with temperature regulator. The temperature was fixed at 30°C. The measurements were done in the integrating sphere, where as an input we put a laser and as an output – the radio -spectrometer Specbos, in front of which we placed the phosphor. The spectrum obtained is presented on Fig. IV-7.

The figures were normalized to violet peak 405 nm, to see the difference of amount of emitted light. The broad band at 450 nm corresponds to emission of Eu^{2+}. No emission is observed around 600 nm, which confirms no presence of Eu^{3+} in the lattice [111]. As expected, the maximum emitted light was obtained while using 40% concentration of phosphor in silicon resin. The powder provided by Sigma Aldrich seems to be more intensive, than the one from Philips, which can be a result from some small modifications in chemical composition.

3.1 Aging of BAM: Eu^{2+}

Degradation processes of BAM, while excitation by n-UV source, are typically loss of efficiency and shift to green region. Moreover, external energies, like heat, could also accelerate the aging process.

We irradiate the plate of BAM in concentration of 20% in silicon resin by violet laser diode. To increase the damages, the n-UV laser diode was supplied by maximum forward current possible I=0.7A, what gave it maximum optical power – 500 mW, for controlled temperature at 45°C. Additionally, we put the phosphor directly on the laser, to get influenced by its temperature. The aging process took 48 hours.

We measured spectrum of light by spectro-radiometer Specbos. Fig. IV-8 shows the results of aging. All the results were normalized to peak of violet laser diode, to compare

the amount of converted light. The first measurement was performed after 4 hours of irradiation. We can notice the drop of conversion efficiency around 25%. After 48 hours of aging the drop is around 40%, compering to state before aging.

Similar to results from aging of YAG and GYAG with Nitride in Chapter III, we can notice, that the shape of emission band does not change. This irradiation did not influence on structure of phosphor. However, the efficiency drop, compering to 20% concentration of YAG or GYAG and Nitride in silicon, is much higher. Moreover, the optical power of the laser used in this study is 3 times lower than the one used in irradiation of yellow

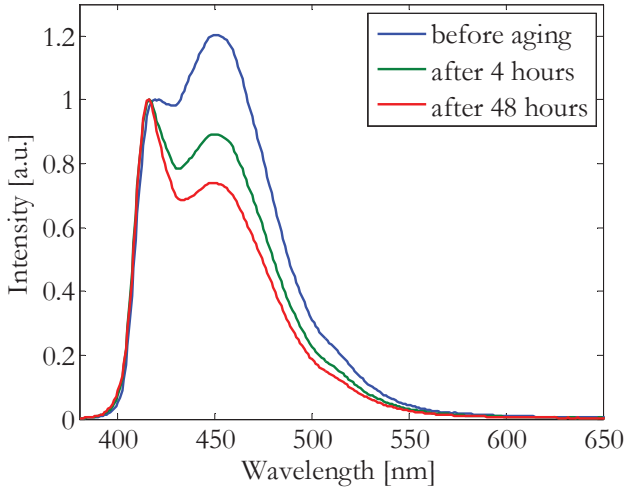

Fig. IV-8. Aging process of BAM.

phosphors. This lead us to the conclusion, that BAM is thermally more instable.

Heating and poor heat dissipation of phosphor particles provokes faster degradation of silicon. The efficiency drop comes from silicon material modification (chapter III, silicon aging), due to weak thermal properties of BAM phosphor.

3.2 Optical power dependencies

In this part, the correlation between concentration and particles number was study. Importance of this dependency was described in Chapter II.

3.2.1 Number of particles

Due to higher intensity and available datasheet of BAM powder from Sigma Aldrich we studied the particles number for this exact powder.

Again, it is assumed that the particles have spherical shape and are distributed uniformly across the volume of the round plate. The diameter of particles is d_l=9μm. The density of the phosphor ϱ_{pho}= 3.77 g/cm^3 [111], and the density of silicon resin is ϱ_{sil} = 1.04 g/cm^3. The weight of silicon resin is 0.73 g. Weight of phosphor varies, depending on its concentration. The area of a plate is equal to A=0.0167 cm^2.

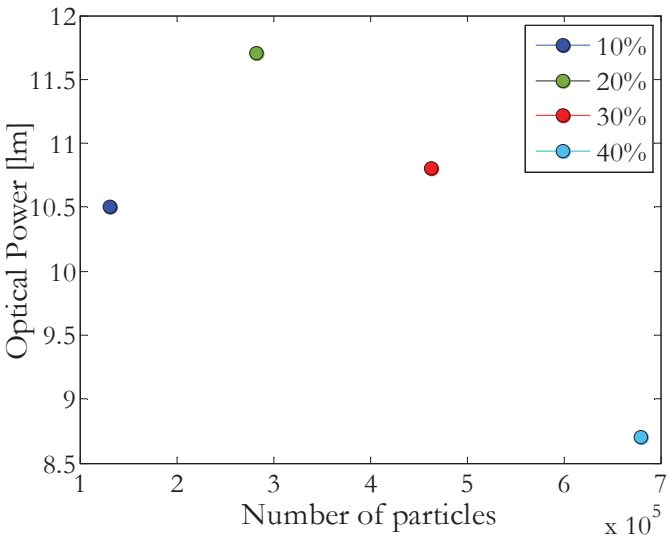

Fig. IV-9. Number of particles in dependency on optical power.

On Fig. IV-8 the optical power dependency on the number of particles is presented. As we can see, the optical power increases, until it gets maximum and it starts to decrease. These studies allow us to know the optimal number of particles in the silicon resin, to obtain optimal optical power. For BAM material, the optimum was found for 282261 particles, which corresponds to concentration of 20% in silicon. After this value we observe the drop of optical power.

4 White light

To obtain white light we used two phosphors – yellow one and blue one. We stuck together two samples of thickness 1mm. The violet light passes through blue phosphor, giving blue light, subsequently, blue light emitted by blue phosphor is converted by yellow one, which, with the residuals of blue light, gives a white color.

The experiment was performed in the integrating sphere. Two samples were placed on the spectro-radiometer, which was an output of the sphere. As an input, we placed a 405 nm laser diode, 500 mW, which was supplied by operation current 150 mA.

Fig. IV-10. Experimental setup. Spectro-radiometer as an output of an integrating sphere.

4.1 BAM: Eu^{2+} and YAG:Ce^{3+}

Firstly, we used combination of BAM and YAG. The concentration of BAM determines the conversion from blue to yellow. From the spectrum on Fig. IV-11, where all the graphs were normalized to peak of 405nm, we can see that the ratio of conversion from blue to yellow, for higher BAM concentration is much higher. Moreover, the conversion by YAG 15% are higher, than the one of YAG 10%. This was already explained in Chapter II, that by increasing the concentration, the intensity increases.

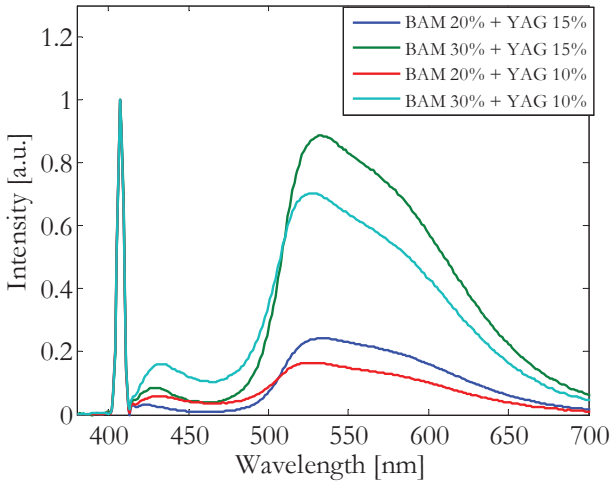

Fig. IV-11. Spectrum of converted light by laser diode 405nm and two phosphor's samples: BAM and YAG.

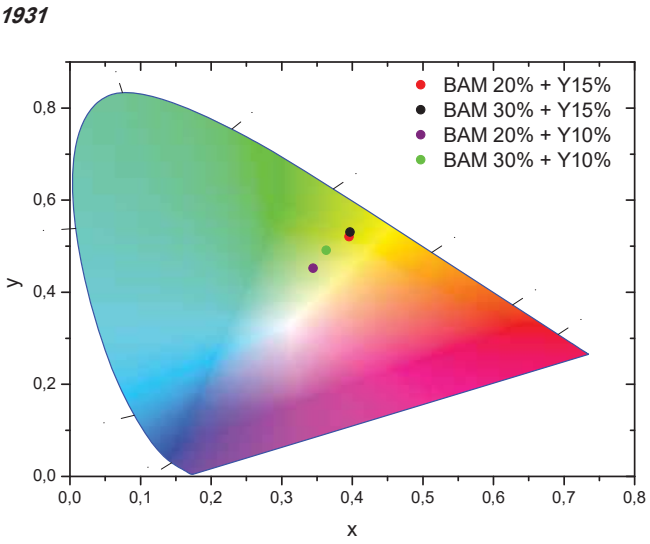

Fig. IV-12. CIE Chromaticity for BAM and YAG excited by 405 nm laser diode.

The CIE chromaticity coordinates graph shows that the color of the light obtained is yellowish. The less BAM and YAG we have, the closer to the blue we are. There is no big difference in the color between BAM20%+YAG15%, comparing to BAM30%+YAG15%. However, decreasing the concentration of YAG to 10% leads to shift into direction of blue. According to this results, we can say, that changing the concentration of BAM has less influence on the color, than in case of YAG.

The CRI obtained for a system with BAM20% reached 75. The CRI for BAM of 30% concentration was 68

4.2 BAM: Eu^{2+} and GYAG:Ce^{3+} with Nitride

To get wider spectrum of light we connected BAM material with a phosphor we used in previous studies: GYAG doped with trivalent cerium and mixed with Nitride doped with divalent europium. It allows us to get red light, due to emission of Eu^{2+}at 650 nm and yellow-green emission due to cerium.

On Fig. IV-14 we can see that almost all light of the laser (405 nm) was absorbed by phosphors. Actually, it is Nitride, which is able to absorb all the wavelengths (see Chapter II), and convert it to the red light. We do not observe this phenomenon with combination of BAM with YAG, because YAG does not absorb the wavelength below 410 nm, and BAM at 30% of concentration is not absorbing all the violet.

Due to high concentration of Nitride, the color of the light is very warm and red. However, obtained Color Rendering Index for the samples with GYAG and Nitride 7.5% was at the level of 85. The system, which contains GYAG and Nitride in 15% of concentration in silicon resin is definitely too red, which lead to drop of CRI to 65.

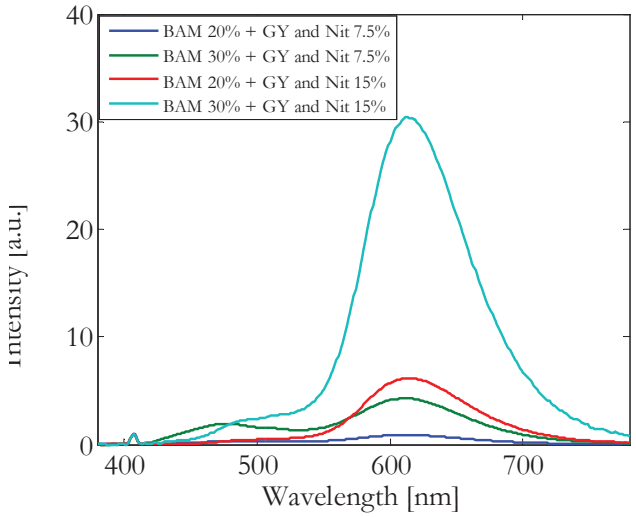

Fig. IV-14. Spectrum of converted light by a laser diode 405nm and two phosphor samples: BAM and GYAG.

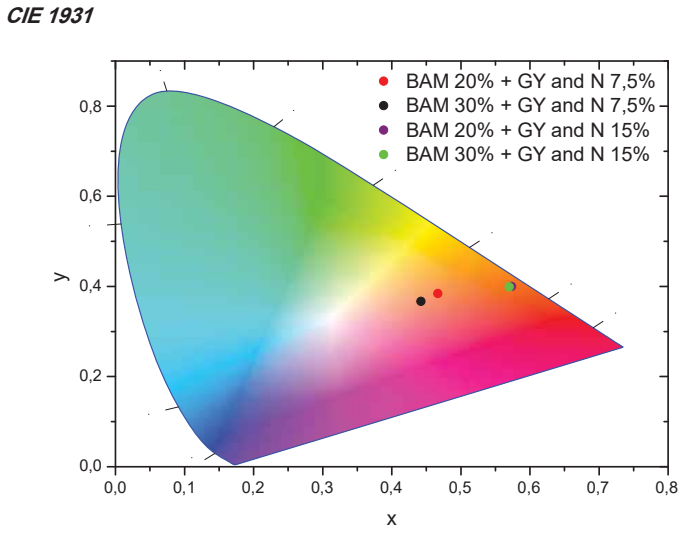

Fig. IV-13. CIE Chromaticity for BAM and GYAG with Nitride excited by 405 nm laser diode.

4.3 Phosphor mix

Due to extra losses caused by two layers of silicon (see Fig. IV-15), the mix of phosphor in one sample was decided to do. Instead of having two phosphor samples of 1 mm, we mixed the powders of YAG:Ce^{3+} and BAM:Eu^{2+} and incorporated them into silicon. We got a sample of 1mm in different concentration.

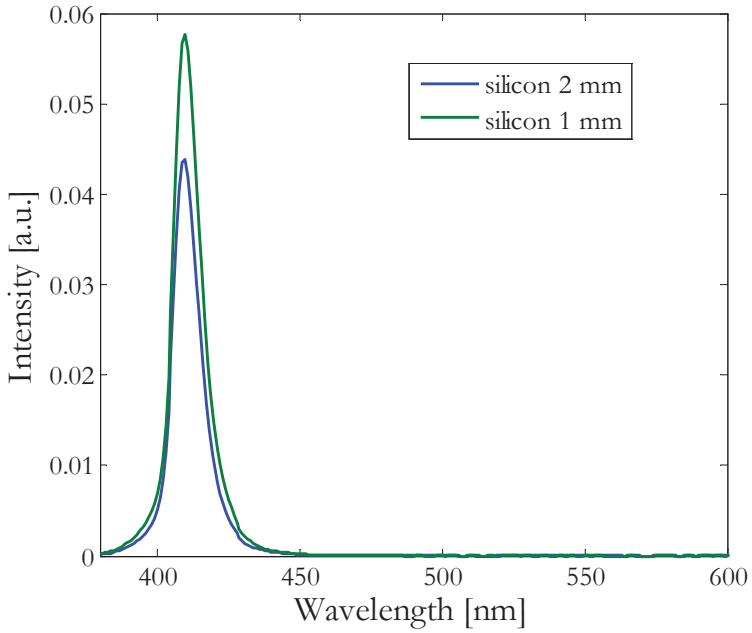

Fig. IV-16. Silicon resin of 1 mm and 2 mm and difference of the light intensity passing through.

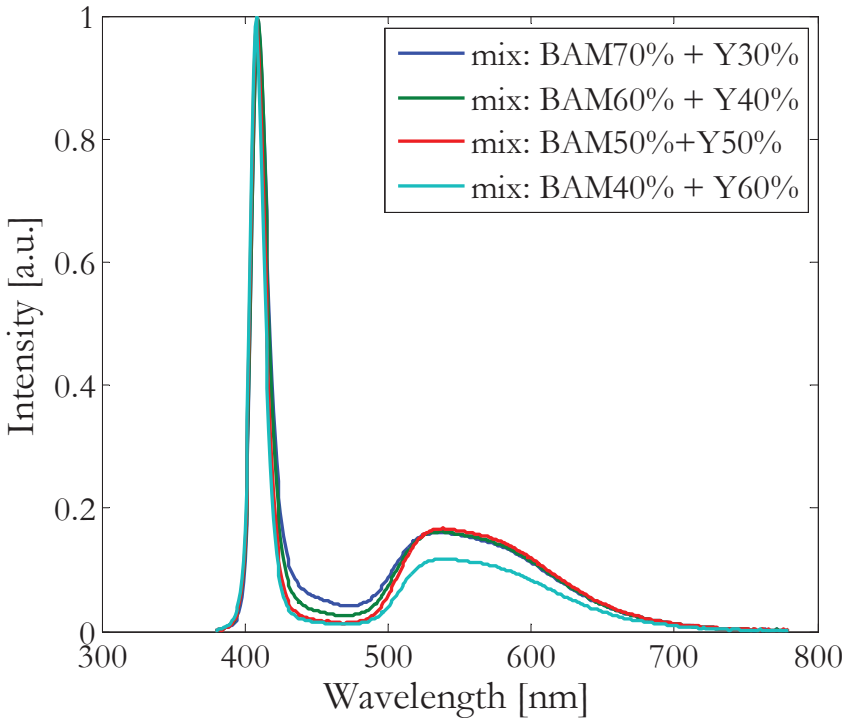

Fig. IV-15. Spectra of the light of different mixes.

The mix of two phosphors were prepared: BAM:Eu^{2+} and YAG:Ce^{3+} in ratio 7:3 in concentration of 10% in silicon, in ratio 6:4 in concentration 20% in silicon, in ratio 5:5 in concentration 10% in silicon and 4:6 in concentration 20%. The materials were excited by n-UV laser diode 405 nm, 500 mW, which was placed as an input of integrating sphere. The measurements were done by using spectro-radiometer Specbos. The laser was supplied by a constant current I=0.5A. The spectra presented on Fig. IV-16 shows the results of different mixes and Fig. IV-17 presents CIE chromaticity coordinates.

From the spectra, we can see, that most or all of the blue light, coming from BAM material, is converted by YAG. To obtain a full spectrum of a white light, little amount of blue is needed. In this case the mix containing 70% of BAM and 30% of YAG has a color of the light closest to white (what can be noticed on the CIE chromaticity diagram)

The CRI of the mixes is not very high. This can result from very high violet pick, coming from the laser diode, which is not fully converted by BAM material.

Table IV-1. CRI of mixed phosphor.

Concentration of phosphor	7:3 10%	6:4 20%	5:5 10%	4:6 20%
CRI	66	63	60	60

To improve the results of the white light parameters and to reduce visible big violet peak which may have bad influence on our eyes, the application of filter, reducing the violet light is suggested.

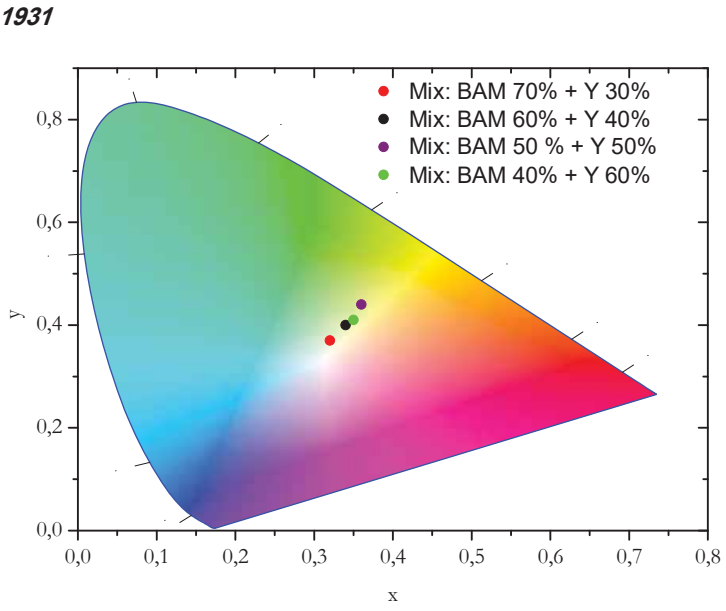

Fig. IV-17. CIE chromaticity coordinates of mixes of the phosphor.

4.4 Filter application

Blue and violet light are very dangerous to our eyes. They can easily damage our retina [112]. Moreover, exposure of biological chromophores to near-ultraviolet radiation can lead to photochemical damage. A lot of positive tests in this domain have been performed, that

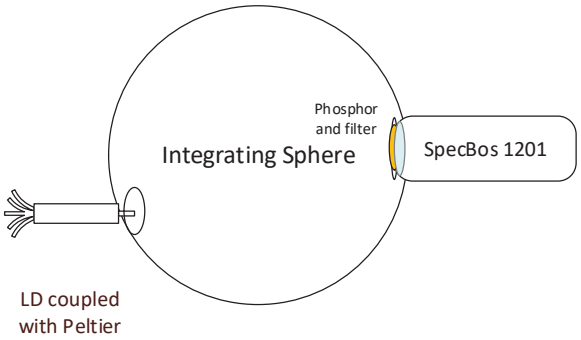

Fig. IV-18. Schema of experimental setup for measurements with the filter.

blue light (in this case blue light was defined as a light from spectrum from 390 to 500nm) is toxic to non-pigmented epithelial cells, confluent cultures of humans primary retinal epithelial cells, which were exposed to the blue light for up to 6 hours. [113][114]

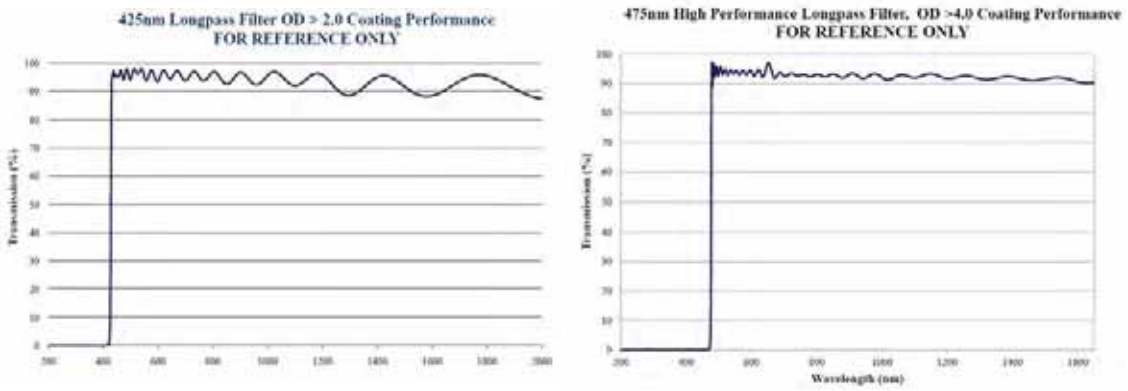

Fig. IV-19. Characteristics of transmission of filter 425 nm long pass and 475 long pass from Edmund Optics.

To design a reliable source of light, not only technical parameters have to be taken into consideration. The human's health is even more important. To make our light system safe to the eyes, we decided to use a filter. The long pass filter from Edmund Optics (OD 2) is cutting the light before 425 nm. Since small amount of blue light is necessary to have a good quality light, we decided to cut only the light not converted by the phosphors, coming from the laser diodes. We used it in our both system: with two phosphors samples and with one sample, where two phosphors were mixed. As a comparison we decided to use also long pass filter that cut blue light – it does not transmit the light before 475 nm. (Long pass filter 475 nm from Edmund Optics)

The measurements, to simulate a source of light with a filter, were performed again in an integrating sphere. The laser diode 405 nm in a Peltier was put as an input and supplied

with a current I=0.7 A, and as an output we put phosphor sample(s). To let the conversion of violet to blue, and then to yellow happened, the filter was placed just after the phosphor, before the spectro-radiometer.

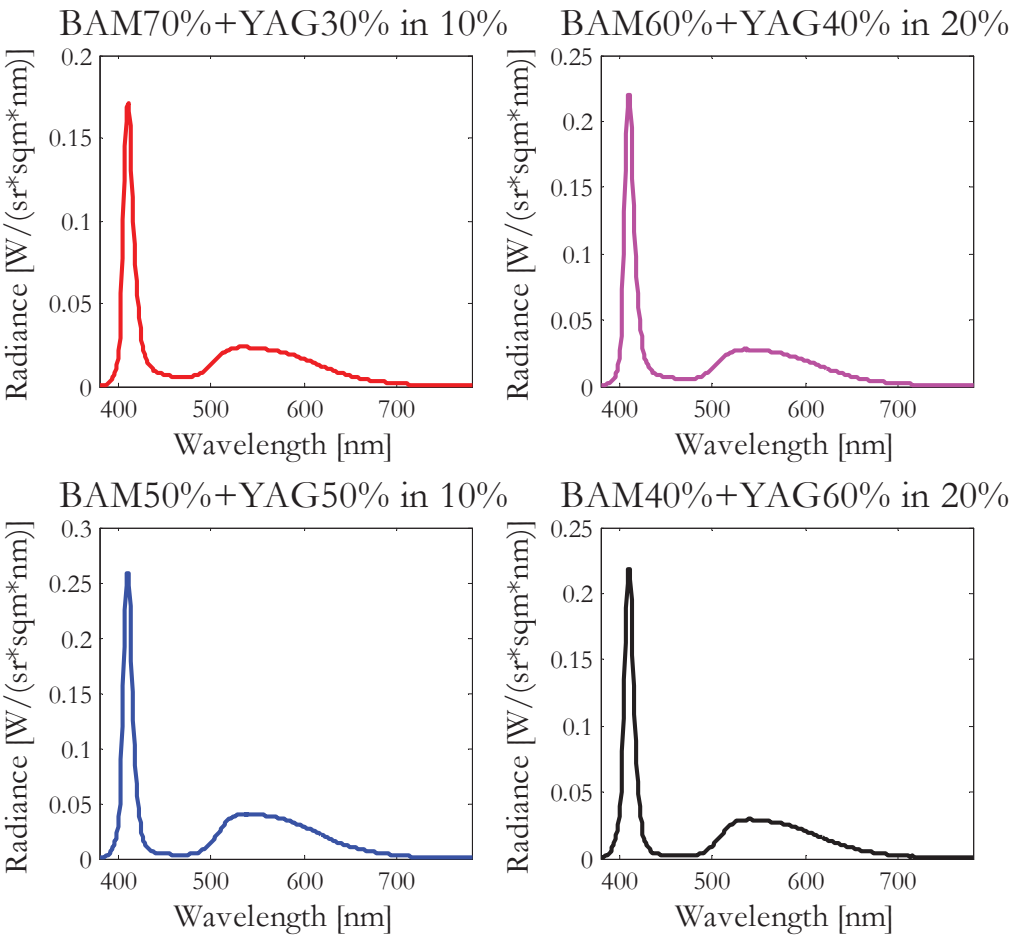

Fig. IV-19. Mixture of phosphors - spectra **without** the filter.

The first measurements were performed with a mixture of phosphors.

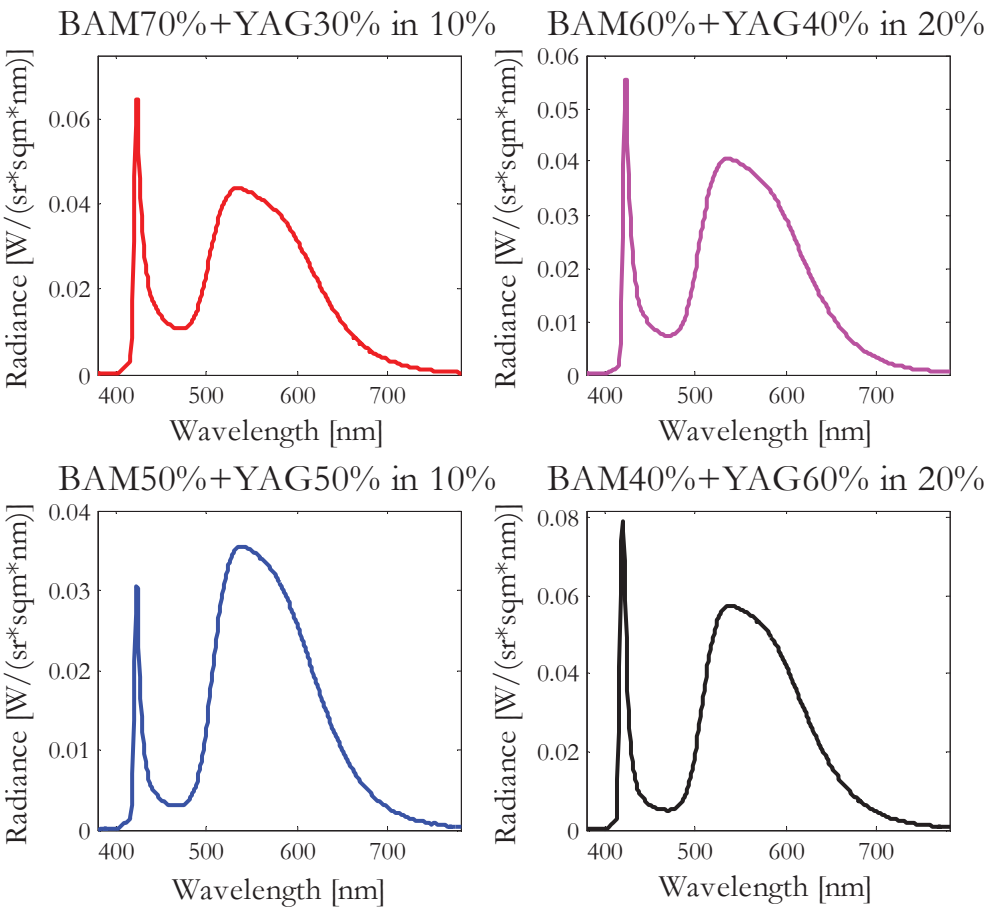

Fig. IV-20. Mixture of phosphors – spectra **with** the filter 475 nm.

Fig. IV-20 shows the results of the mixture without using a filter. We can observe that not all n-UV light was converted, and the intensity of converted light is around 5 times lower, than the intensity of 405 nm peak.

On Fig. IV-21 the spectrum after using the filter was presented. It can be noticed, that the n-UV peak was slightly cut. Moreover, we can notice that the ratio of the violet peak to converted light is lower. The intensity of the light changed also due to only 99% of transparency of the filter. As a comparison, the area under the violet peak and converted

Table IV-2. Areas under the violet peak and converted light peak.

With filter		Without filter		
Peak 405 nm	**Peak converted light**	**Peak 405 nm**	**Band converted light**	
0.0058	7.84	2.64	3.28	**B70% Y30%**
0.000504	7.751	3.59	5.15	**B60% Y40%**
0.0021	5.75	3.20	3.78	**B50% Y50%**
0.0044	8.413	3.12	3.69	**B40% Y60%**

light peak was calculated.

Table IV-2 presents the values of the area under the peaks. Clearly we can notice, that the area under the violet peak decreases 1000 times after using the filter. However, the area of the converted light increases each time. In general, the efficiency of the conversion with filter only seems to be higher. This phenomenon can be explained by lower general intensity and limiting the passage of the photons with the energy less than 425 nm.

Using the filter led to decreasing of intensity and changing the ratio between violet peak and converted light. The parameters of light: CRI, CCT and CIE chromaticity coordinates with and without filter were presented in tables IV-3 and IV-4.

Table IV-3. Parameters of the light **without** the filter.

Without filter	B7 Y3	B6 Y4	B5 Y5	B4 Y6
CRI	66	63	60	60
CCT [K]	5816	5559	4783	4817
CIE chromaticity	0.32; 0.37	0.33; 0.38	0.36; 0.43	0.36; 0.42

Table IV-4. Parameters of the light **with** the filter.

With filter	B7 Y3	B6 Y4	B5 Y5	B4 Y6
CRI	66	64	62	61
CCT [K]	5091	4826	4400	4423
CIE chromaticity	0.35; 0.45	0.36; 0.45	0.39; 0.49	0.39; 0.48

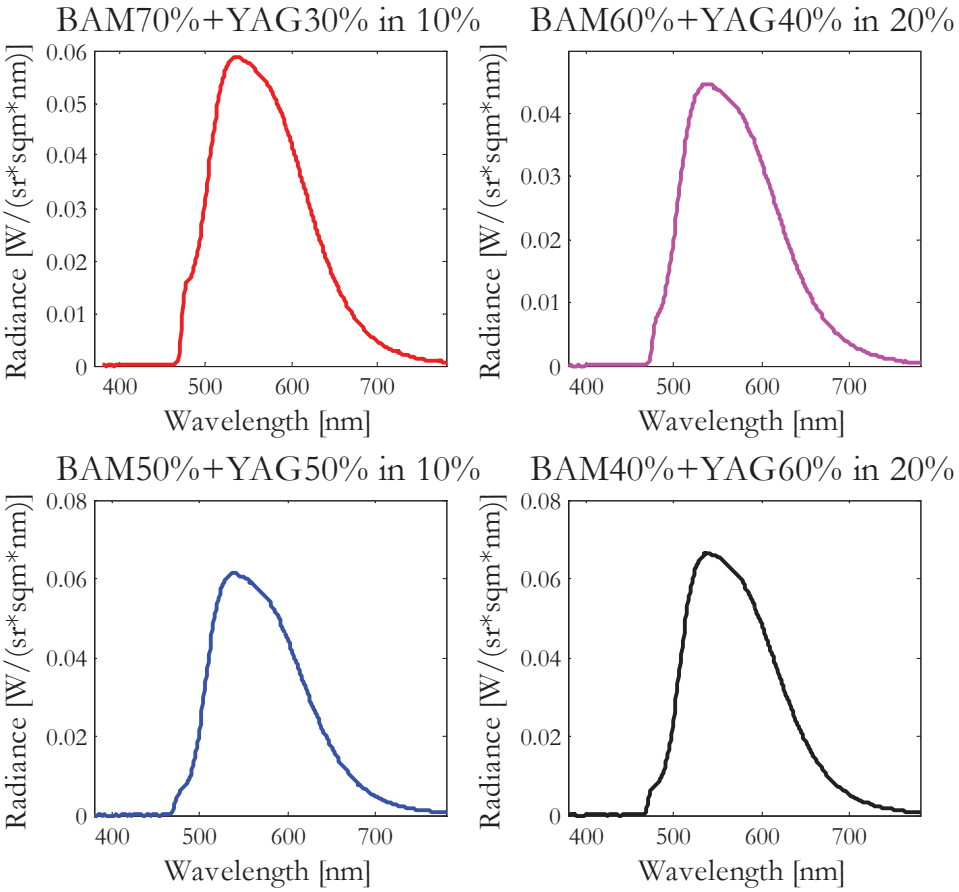

Fig. IV-22. Mixture of phosphors – **with** filter of 475 nm.

CIE 1931

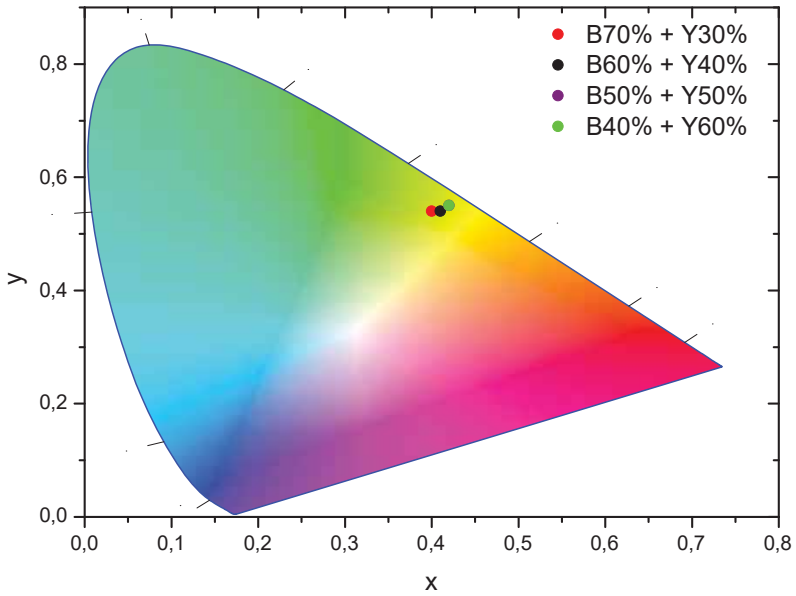

Fig. IV-21. Chromaticity coordinates after adding a filter 475 nm.

After adding the filter, the light becomes more warm. It can be noticed basing not only

on the CCT and coordinates but also on the spectrum of the light. CRI stays at the similar level. The parameters of the light based on mixture of the phosphor can be qualify as a source of warm white light. However, we still have a blue peak in our spectrum.

As a comparison, the filter of 475 nm was used. On Fig. IV-22 the spectrum is presented. The spectrum shows only the emitted light by BAM (cut in half by filter) at 450 nm and by YAG. The CIE chromaticity coordinates are presented on Fig. IV-23.

The chromaticity coordinates obtained after adding a filter 475 nm indicate the yellowish color of the light, far from the 0.3; 0.3 point, of white light coordinates. This small experiment shows that the small amount of blue light is necessary in spectrum.

In next study, instead of mixture of phosphor, two samples of phosphor were used. The approach was the same – the measurements were performed in the same conditions, with and without the filter.

On Fig. IV-24 we present the spectrum of combination: BAM 20% with YAG 10% and BAM 10% with YAG 10%. The materials with these concentrations were chosen due to their high optical efficiency compering to others. As before, adding a filter result in increasing of emitted light and cutting off the violet light. The peak of violet-blue in case of

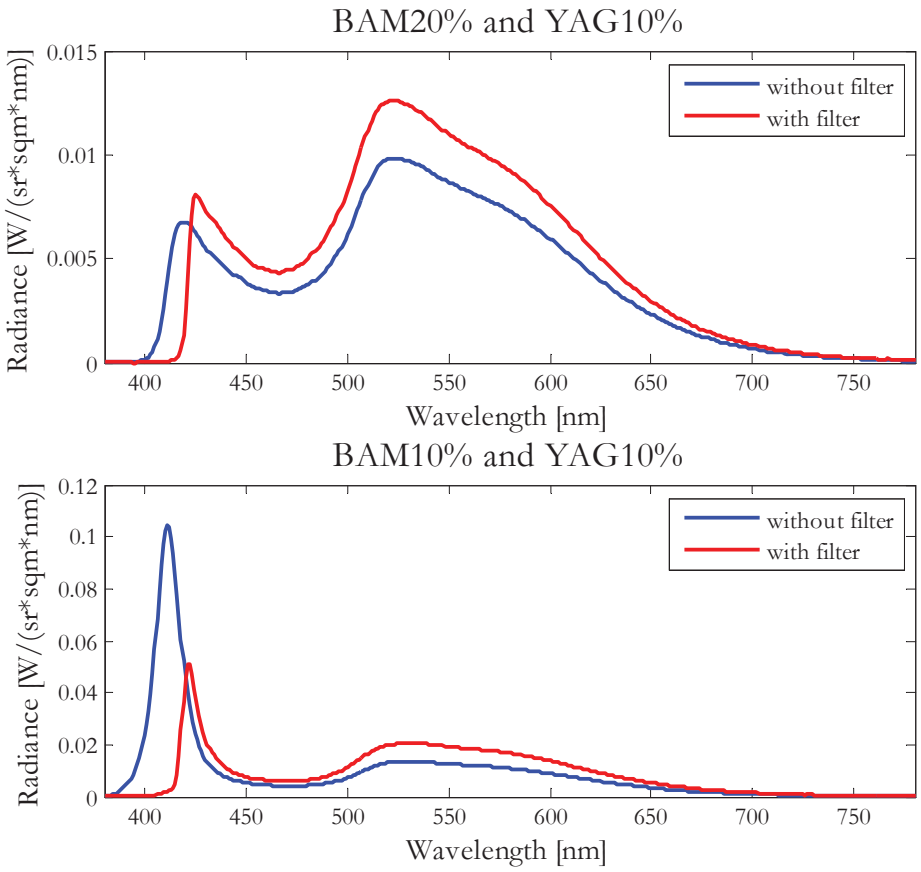

Fig. IV-23. With and without filter - two phosphor in different silicon plate.

conversion with BAM10% is still visibly high. Nevertheless, the parameters of the light are quite close to the "daylight". In contrary, the spectrum of light converted by BAM 20% seems to be interesting due to cutting of the violet light, leaving the part of blue and may be close to the spectrum of incandescent lamp. However, the CRI is lower, and the light is warmer.

Spectro-radiometer Specbos, used in this study, measured all necessaire light parameters like CCT, CRI and CTE chromaticity coordinates, which are presented in Table IV-5 and IV-6.

Table IV-5. Parameters of the light without filter.

Without filter	B20% Y10%	B 10% Y10%
CRI	69	74
CCT [K]	5700	6957
CIE chromaticity	0.33; 0.41	0.28; 0.33

Table IV-6. Parameters of the light with filter.

With filter	B20% Y10%	B 10% Y10%
CRI	70	74
CCT [K]	5679	6861
CIE chromaticity	0.33; 0.43	0.3; 0.37

YAG doped with cerium is a material that where the band emission is at 550 nm. To

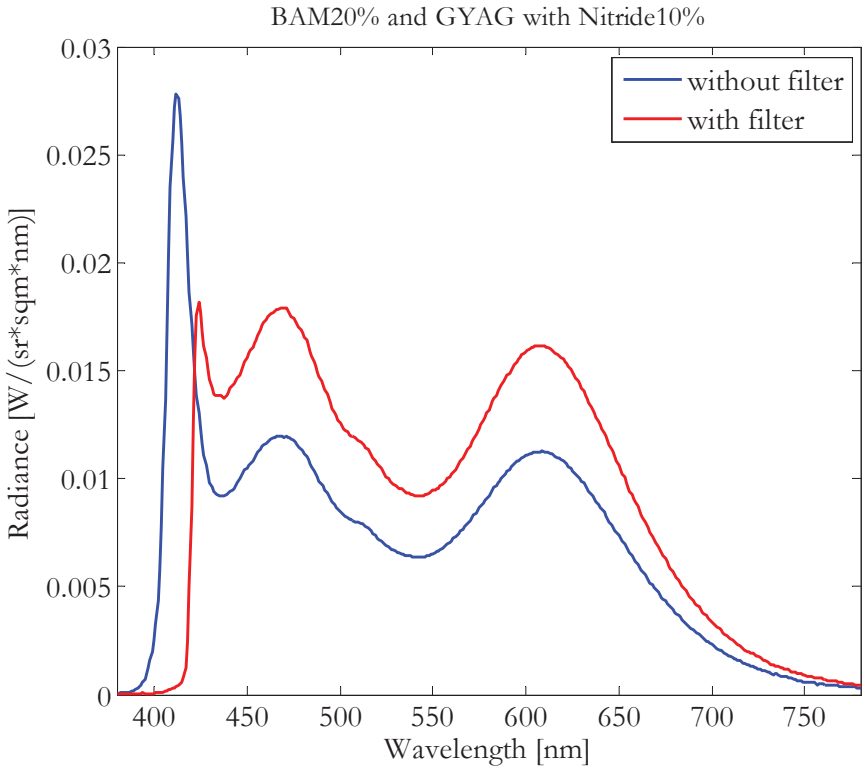

Fig. IV-24. With and without filter - BAM 20% and GYAG with Nitride 5%.

obtain better CRI, the wider spectrum is needed. Nitride, doped with europium used in a mix with GYAG, doped with cerium, should offer wider spectrum.

We used GYAG with nitride 5% and BAM of 20%. We repeated the measurements for a system with and a without filter. The results are presented on Fig. IV-25.

Table IV-7. Parameters of the light.

	Without filter	With filter
CRI	85	85
CCT [K]	5659	5402
CIE chromaticity	0.33; 0.28	0.33; 0.3

CIE chromaticity coordinates after adding a filter are exactly corresponding to the white light. The CRI was improved, compering to the system with YAG, due to red phosphor in a mix with GYAG. The CCT is corresponding to the warm white light.

4.5 Number of particles

The optical power changes with the number of particles. However, the calculations of optical power depend on size of the sample. [5] We decided to calculate the particles number on the dependency of optical power for two types of system.

The first system was based on two separated phosphor sample – YAG:Ce^{3+} and BAM:Eu^{2+}, 1mm of thickness each and diameter of 15mm. The number of particles of this

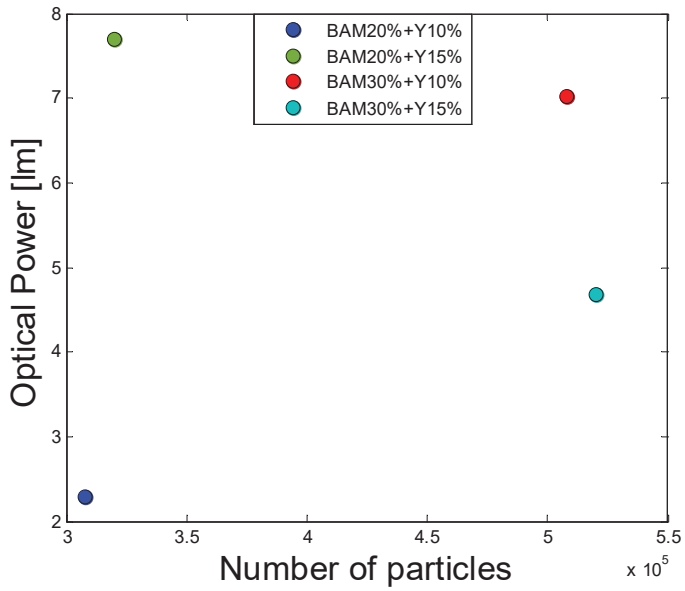

Fig. IV-25. Dependency of the optical power on number of particles for two separated plates of phosphor.

system is basically a sum of particles in two phosphor plates. The optical power was

measured by exacting the phosphors by a laser diode of 405 nm, with a constant current I=120mA, which was an input of integrating sphere. As before, all the measurements were done by spectro-radiometer Specbos, which was applied as an output of the sphere.

From the results on Fig. IV-26 we can clearly noticed that we can obtain the optimal optical power by combining two samples which, excited separately, gives the maximum power.

Another possibility of obtaining white light by a laser diode 405nm is to use phosphors mixed in one silicon resin. To verify if the dependency of optical power on number of particles for YAG:Ce^{3+} and BAM:Eu^{2+} is exactly the same for two types of system (mix of phosphors in one silicone and two separate phosphor plates), the measurement on mixed plates were performed.

Equation offered by Yang et al. [5] assumed that concentration of phosphor is strictly connected with the concentration. It may distinguish the number of particles of different phosphors in one sample, however it is calculated by simple percentage multiplication by total number of particles. Regarding this calculations, the number of particles for the same general concentration of phosphors in silicon resin is the same. And so, the number of particles for the mix of phosphors concentrated in 10% in silicon is 14483. The mix of 20% of general concentration contains 28720 particles of phosphor.

For these values, the optical power was measured. On Fig. IV-27 the results are

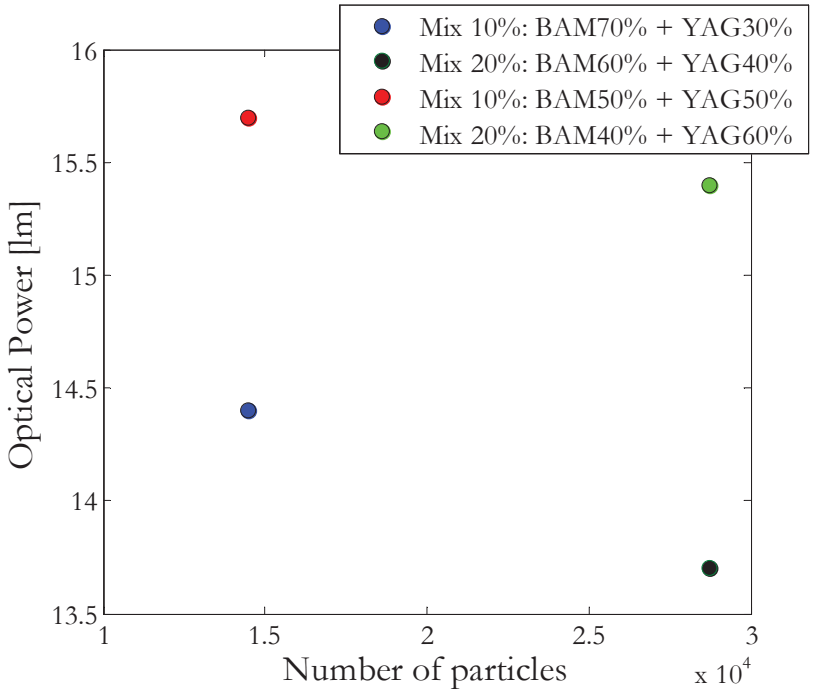

Fig. IV-26. Dependency of optical power on number of particles for mixture of two phosphors.

presented.

The highest optical power was obtained by using the sample of general concentration of 10% and mix BAM and YAG with a ratio 5/5. Samples having more particles obtained lower results in power. The explanation of this phenomenon has been described widely in Chapter II

5 Saturation effects on phosphor materials

Lasers generated white light has recently been introduced for high beams by the top-line cars producers, such as BMW and Audi [115] [116], where the strong directionality of light generated from a small spot is of high importance. However, the saturation of the downconversion in the phosphors may limit the available white light from small spots. In some investigations [117] [118] were carried out on thermal quenching of different types of phosphor materials.

In this part, we investigated the saturation effect in silicon phosphor illuminated with an intense near-UV light in a calibrated integrating sphere. Using different incident laser radiant intensities, the saturation effect was investigated. This part of study was performed in collaboration with Technical University of Denmark in Copenhagen.

Firstly, the output characteristics of LD was measured. In this study we used the 500 mW n-UV laser diode. For different values of current, the power and the beam size was measured.

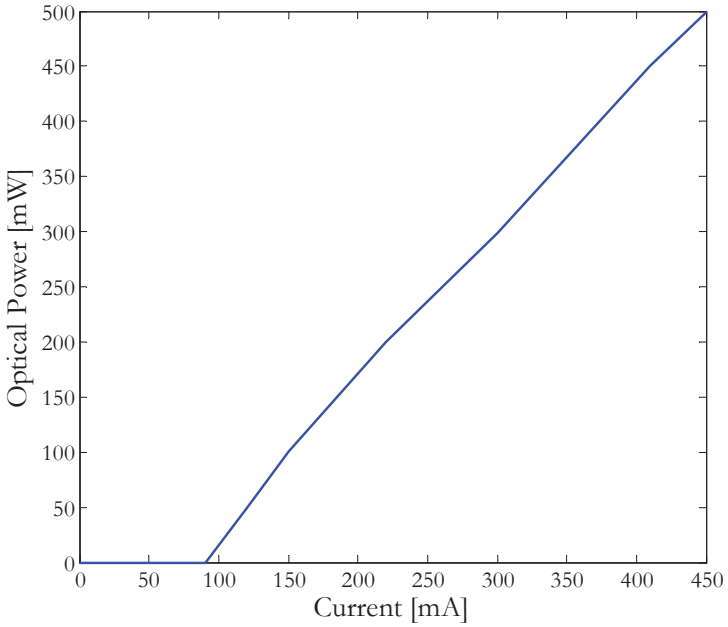

Fig. IV-27. Output characteristics of a laser diode.

The beam propagation parameter was measured at different current level by a laser profiler from Photon Inc, BeamScan. The configuration of the setup for investigating a saturation effect is presented on Fig. IV-29.

The laser light emitted from a laser diode (405nm) was collimated in one axis using an aspherical lens, L1. A cylindrical telescope consisting two cylindrical lenses, L2 and L3, was used in order to make the LD beam circular in the focus. Following the telescope, the laser beam was focused by focusing lens L4. Initially, the laser diode was characterized with respect to the output power and beam properties in order to be able to precisely estimate the radiant intensity. A laser distance-meter was used to ensure precise measurement on the focus position. [119] The distance-meter was set under the beam scanner, to modify the distance from the laser diode.

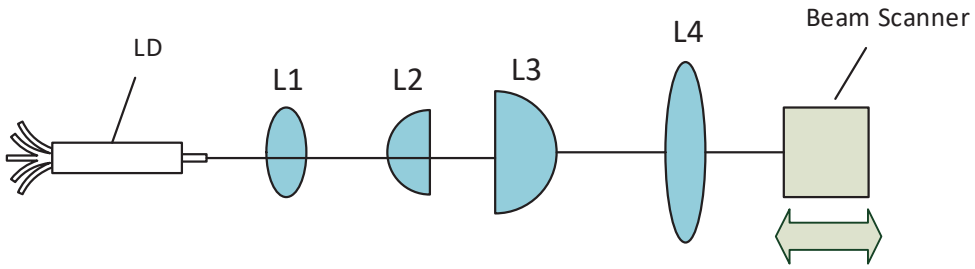

Fig. IV-28. Experimental setup for measuring the beam size.

On Fig. IV-30 we present the size of the spot (area) in a function of distance of the laser on distance-meter. Results in general show that the lower current we have, and the

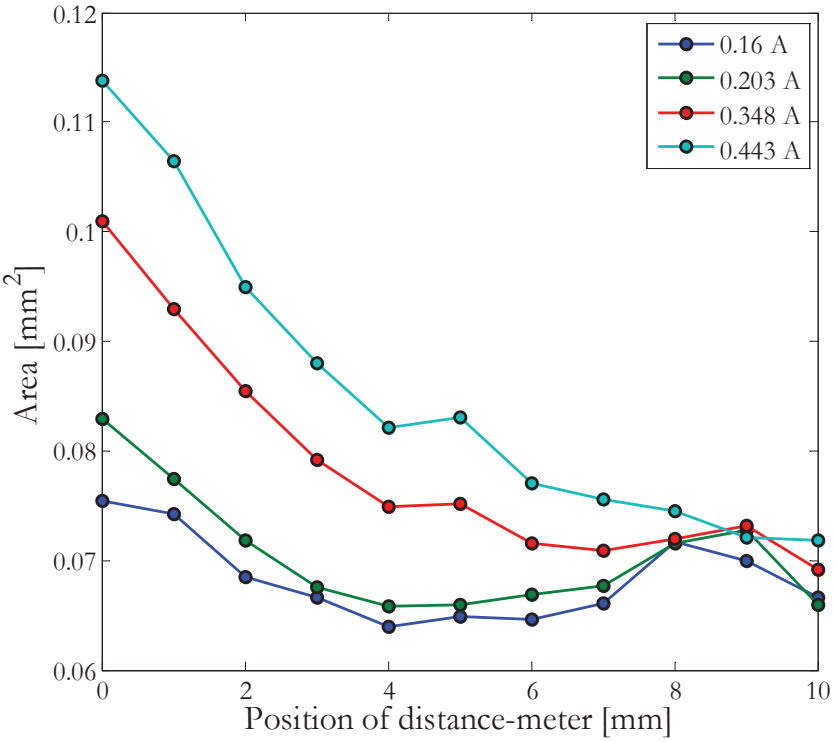

Fig. IV-29. Relation between size of beam and the position of LD.

closer we are, the smaller size of spot we have. However, the cases under 0.29 A does not seem to confirm this tendency, probably due to very weak optical power for these currents.

On Fig. IV-31 we present the relation between the intensity of a laser diode and the position. There is no surprise that intensity increases with the decreasing a distance of the laser from scanner.

Saturation effect on phosphor plate can have source in different phenomenon. The first one is not dense enough phosphor package. The photons, generated by a laser does not collate with phosphor particles all the time, which may lead to variations in CCT and CIE chromaticity coordinates. This is due to energy of photon which is higher than the energy of phosphor. To avoid this phenomenon, the energy of photon should be smaller than the energy of phosphor (Relation Planck – Einstein)

When the size of the spot is very small, this phenomenon can be even more noticeable. Another cause can be temperature quenching [118][117] of phosphor plate, which may lead to the same result as low concentration of phosphor. Another issue causing saturation can be beam, which is dispersed, not focused (difference between laser and LED).

The first experiment we performed for the biggest size of spot (0.15-0.09 mm^2 depending on the current). For the different values of current, we measured the spectrum of a white light obtained by converting the light from a laser, by two phosphor plate: BAM

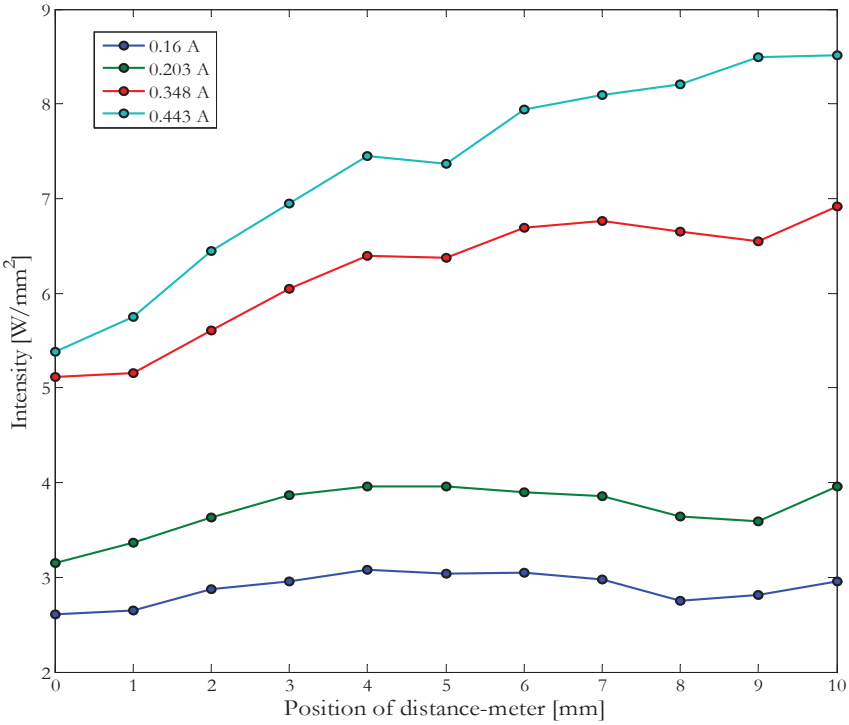

Fig. IV-30. Relation between position of beam scanner and intensity.

doped with Europium in concentration of 20% and YAG doped with Cerium in concentration of 10%. The spectrum was measured by spectro-radiometer Specbos. All the

measurements were performed in the integrating sphere with the diameter of 25 cm. All the graphs on Fig. IV-32

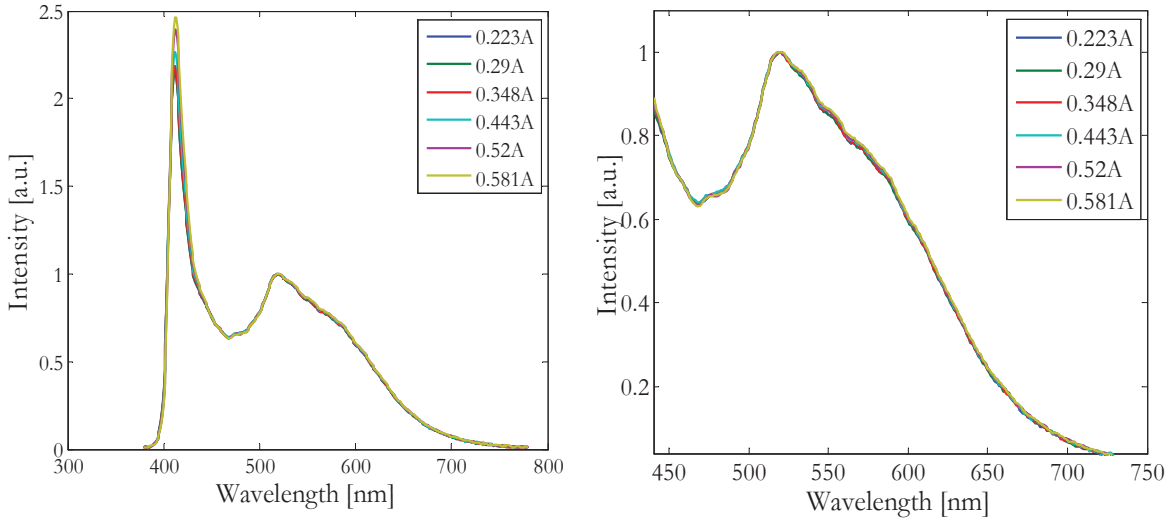

Fig. IV-31. Spectra for different currents for the biggest size beam normalized to peak of emission**.**

were normalized to peak of converted light.

From the results we can see, that the shapes of the graphs didn't change, while the level of current was changing. We can see from the peak at 405 nm, that the level of the peak changes, due to changing of the current.

Subsequently, we decided to repeat the measurement, when the spot size of a laser beam is the smallest (0.07mm^2). These measurements were performed in the same conditions as the one before, with the same two phosphor plates.

On Fig. IV-33 the results of obtained spectrum are presented. We can notice similar

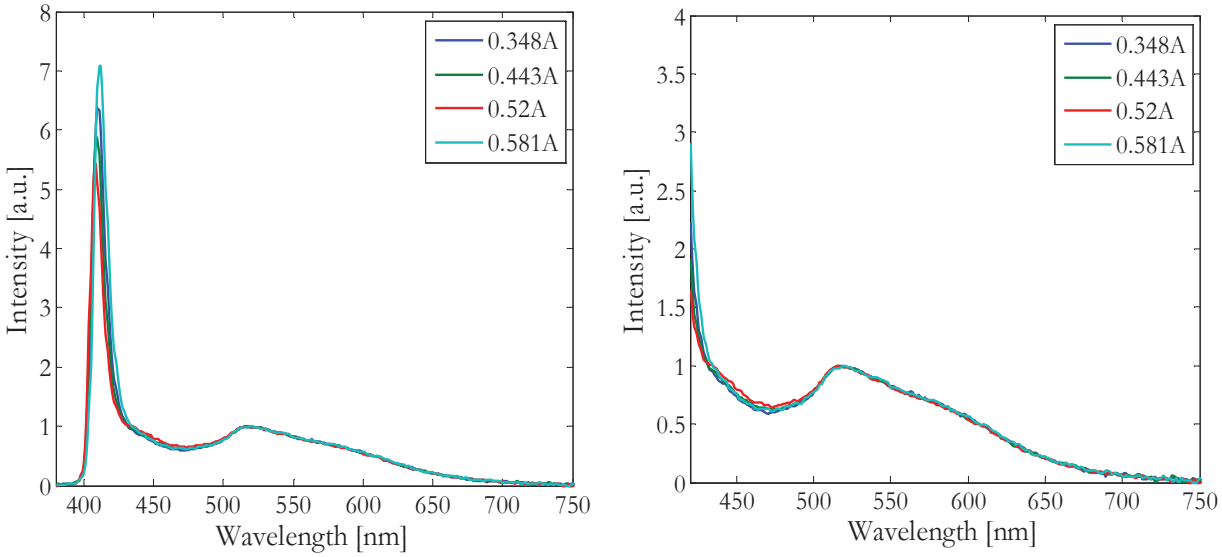

Fig. IV-32. Spectra for different currents for the smallest size of beam normalized to peak of emission.

effect, as for the bigger size of the laser beam spot. When the current is changing, the parameters of the light like CIE chromaticity coordinates or CCT stay at the same level.

Table IV-8. CIE and CCT for different current in condition of small spot size**.**

Current [A]	0.348	0.443	0.52	0.581
CIE coordinates	0.27; 0.31	0.27; 0.31	0.27; 0.31	0.27; 0.30
CCT [K]	9370	9370	9441	9442

This coherent results lead us to the conclusion that we do not find saturation effect in these conditions. This fact can be explained by very dense phosphor concentration in silicon resin.

6 Conclusions

In this chapter the white light obtained by n-UV laser diode 405 nm mixed with blue and yellow phosphor is presented.

Firstly, the basic characteristics of a laser diode was taken. Also the influence of the temperature was verified. The results show that between 30°C and 45°C the intensity of the diode drops 33%, however, no big shift in wavelength was observed.

As a second paragraph of this chapter, the possible blue phosphors were introduced. The phosphor, that has been chosen for further studies was Bam doped with Eu^{2+}. Compering to the other phosphors, as the only one was having high emission, after excitation by 405 nm.

Subsequently, the parameters of BAM from two distributors were investigated. It revealed, that BAM:Eu^{2+} from Sigma Aldrich has higher intensity than the powder from Philips. Due to this property, BAM based on powder from Sigma Aldrich were used for other studies.

Irradiation of the material confirmed the theory, that BAM is a material thermally less stable than for example YAG. However, after 48 hours of intensive irradiation by a laser diode we did not notice the shift into green.

Optical power dependency on the number of particles let us found the concentration that would have the highest luminous efficiency. The optimal concentration for BAM revealed to be 20%.

After finding the concentration of BAM, that allows us to obtain the highest optical power, we coupled it with another yellow phosphor to obtain white light. Firstly, we used two phosphor plate of 1 mm thickness. The results were satisfying, however, the CRI was not very high at reached 75. Changing YAG, by GYAG mixed with nitride, allowed us to obtain a white light with a CRI of 85. Nevertheless, using two separated phosphor plates, causes additional thermal and optical losses. We mixed then BAM and YAG in one silicon

resin, obtaining one phosphor plate of thickness of 1 mm. Unfortunately, due to all conversion of blue light emitted by BAM, converted by YAG, the maximum CRI obtained was 66.

Due to bad influence of blue and violet light on our eyes, we decided to use a filter that will cut wavelengths smaller than 425 nm. (we decided to leave a little bit of blue light, due to improvement of CRI) First results revealed that the filter actually caused decreasing of violet peak coming from a laser diode, but also causes increasing of emission of the light. Also, the filter of 475 nm was introduced, to prove the importance of blue light in the spectrum. We obtained good result with a mixture of BAM and YAG in a ratio 7:3, nevertheless, the best results from the point of view of light parameters were obtained by using a BAM and GYAG in separate plates. However, the intensity of that system is two times smaller, then the system where the mixture of phosphors was used.

We looked also for the system, that has better optical power. The dependency of the optical power on number of particles revealed that the highest optical power can be obtained for a mix of BAM and YAG 50%/50% in concentration of 10% in silicon resin.

In this chapter we also studied the saturation effect on phosphor materials. We verified if for very small size of the beam, the parameters of the light are constant, while changing the forward current. Studies showed, that in case of using two phosphor plates of high concentration, there is no saturation effect. This effect usually appears when there is not a lot of particles in the resin (silicon, ceramic, glass) or if there is a temperature quenching phenomenon in the material.

Conclusions and Perspectives

The purpose of this thesis was to investigate a source of white light based on a laser diode and suitable phosphor. At first, all the parameters that may define a light source were presented in order to be able to characterize it. To position somewhere the source based on a laser, all previous sources were briefly described.

Source based on laser diode shows superiority over other sources due to its intensity, life duration and small size. It also gives a possibility to work in reflection mode. Certainly, it is characterized also by its linear characteristics of voltage-current, which gives a solution to the efficiency droop of LEDs.

The first approach, to obtain white light, was based on blue laser diode 445nm, 1.6 W from OSRAM and a yellow and yellow-red phosphors. We used the phosphors in silicon and on glass. In silicon resin we incorporated YAG:Ce^{3+} and mix of GYAG:Ce^{3+} and Nitride:Eu^{3+}.

Spectra of YAG:Ce^{3+} emission, after excitation of 445 nm of blue laser diode, had a peak at 550 nm. Cerium, responsible for emission had a ground state at $4f^1$. Excited by photon, electron goes to orbital 5d. The energy of the electron is always influenced by the host material – YAG in this case.

Spectra of GYAG:Ce^{3+} mixed with Nitride:Eu^{3+} showed two emission band: one of 625 nm, which belongs to emission of europium, and another one at 528 nm, which corresponds to emission of cerium, influenced by another host material – GYAG.

Phosphor in glass, got from Intematix company, was used due to better thermal stability of glass, than the silicon. However, the exact composition of the material was unknown. The experiment, using a monochromator, was performed to determine the elements that are responsible for emission. Studies revealed that the powder should contain YAG doped with Cerium:Ce^{3+} and Nitride:Eu^{3+}.

The measurements of white light parameters after coupling a blue laser diode and phosphors were taken in integrating sphere. The characterization of a laser diode showed the linearity of current – power characteristics. The results with YAG revealed obtaining light of yellowish color. The CRI was good for low value of the concentration of phosphor in the silicon resin. Nevertheless, the luminous efficiency was the highest for the concentration of 15% - 48 lm/W. Mix of GYAG and Nitride seems to give better results for CRI – the value was about 86. However, the Correlated Color Temperature was very low and light had a color similar to the color given by a candle. The highest luminous efficiency obtained with this material was 38 lm/W.

More promising results for luminous efficiency were obtained by using a phosphor in glass. The value was 97 lm/W. In spite of using two emitting elements: cerium and europium, the maximum CRI was 78.

The silicon materials were able to work in reflection mode. By using reflection, we wanted to reduce the blue light. Unfortunately, studies showed, that our material working in reflection mode converts less light, so the emission of the converted light is lower, and the residuals of the blue light coming from laser are higher.

The studies on dependency of particles number on optical power and on CCT were performed. The results revealed, that, indeed, optical power emitted by a source increases, until it reaches maximum, then it starts to decrease. If there are not enough particles all the light is seldom to be scattered by more other particles. It causes easy escape for the light from the plate, such that the output flux increases When the number of the particles is higher than the optimal one, the phosphor particles are more like too dense in the resins. In this case all the light becomes difficult to escape out of the phosphor plate such that the output flux decreases. The investigation on dependency of number of particles on CCT and CIE chromaticity coordinates showed, that we are not able to define this reliance as a truth for all the materials. For YAG material when the particles were too dense, the CCT almost saturated – and we did not observe variation of coordinates. However, there was no saturation of CCT observed in case of GYAG mixed with Nitride. We think that the CCT is not the appropriate metric in cases out of the range 3000-6000K.

Second approach of obtaining white light was using a n-UV laser diode 405 nm, 500 mW and coupling it with blue and yellow phosphor. For this purpose we chose BAM:Eu^{2+} and we coupled it with before prepared YAG and GYAG. Two ways of generating a white light were verified. Firstly, we used two samples: blue and yellow phosphor, separately. The violet light passed by blue phosphor, causing blue emission, which was absorbed by yellow phosphor and emitted in yellow region of spectrum. Not all the violet and blue light was converted, so at the output, the white light was obtained. With combination of YAG and BAM in separate plates we obtained maximum CRI around 75. Using BAM with GYAG gave CRI of 85. Due to yellow emission, combination with YAG give warm, yellow light, while with GYAG, the color goes more into orange-red.

To avoid the additional losses coming from transmission through the silicon, the powders of YAG and BAM were mixed into one resin. The coordinates were closer to the white light, nevertheless, the CRI was lower than in case of separate plates and it was around 65.

As far as it is known, the blue and violet light is harmful for our eyes. We tried to decrease the peak coming from laser, by using a long pass filter 425 nm. The mixture of BAM and YAG was not very effected by filter and no big changes in white light parameters were observed. However, while coupling BAM and GYAG with filter of 425 nm, the parameters stayed promising with CRI of 85 and CCT of 5402, while the peak of the violet light significantly decreased.

Small size of a laser diode is its big advantage. The usage of small spot size may however cause the saturation effect on phosphor materials. In our approach with using two phosphor plates of BAM and YAG, excited by n-UV laser diode, we did not observe this problem. Lack of saturation effect may be explained by high concentration of the materials and good light scattering.

Studies concerning wider variation of different types of phosphors and its concentration in different resin (silicon, glass, ceramic) may be needed to establish more precise results.

The goal of this thesis was not only to propose source of light with good parameters, but also reliable one. A number of aging processes were performed to reveal the weak points of the system.

Semiconductor is a very important part of proposed light system. Its thermal aging is commonly known problem. Nevertheless, in these studies, untypical approach was proposed. By using FEM software, the simulation of temperature distribution in different layer of semiconductor with and without additional heat sink was performed. Our studies revealed that, the temperature that may instantly reach the value of 190°C. Also, we showed, that the thermal resistance of the diode may increase even three times, when there is no radiator. To fulfill these studies, we verified how the temperature of the diode can influence on the emission of light after conversion by a phosphor. We noticed, that intensity of the diode is lower for 55°C than for 30°C, which lead to lower intensity of a converted light. Moreover, when the diode heats, its wavelength moves to the higher values. By checking the absorption and emission of different materials we show that variation in wavelength can lead to variation in light parameters – especially dangerous case is when we start to convert less blue light, what can cause damages to our eyes.

Another interesting aspect is decrease of optical power which leads to decrease of intensity. Decrease of intensity cause decrease of light conversion. Nevertheless, after 200h of working under stressing current the optical power decreases only about 3%. We also found out that with a time, the threshold current increased about 10%. We compered our results with aging of a blue Light Emitting Diode. We found similar behavior, however, LED's optical power decreased more.

Subsequently, we performed different aging process on materials. First type of aging was a laser irradiation. The silicon sample was left for 90 minutes, directly in front of laser diode, which was working under maximum optical power. Studies revealed that YAG is very strong phosphor, however nitride is more covalent and has lower electronegativity. Shape of emission did not change, which led us to conclusion that there are no structural changings in phosphor.

However, the emission after irradiation dropped. Infrared analysis proved destruction of the bond CH_2=CH_2 in silicon and creation new one – CH_3. Additionally, the optical properties can be modified by the oxidation, thermal extension or thermal quenching. In our case, after aging silicon sample, without phosphor inside, on heating plate (200°C), we saw darkening phenomenon.

Due to darkening issues of silicon we tried phosphor in glass which supposed to be more ridged and have higher thermal conductivity. As before with phosphor in silicon, this time we irradiate with a laser diode, powered with the highest current possible, a sample of phosphor in glass. Regarding properties of glass, we decided to leave a phosphor under radiation for longer than time – 120 hours. Results revealed no aging process, no changing in spectrum or in light parameters. Moreover, the temperature distribution, examined by

infrared camera shows, that glass can better evacuate the heat that the silicon. Also, the temperature on the glass finally saturates, while on the silicon constantly increases.

Aging under artificial sun (xenon lamp), which emits UV light proved that without heating a samples in silicon into very high temperature (>100°C) we are not able to decrease the conversion of a phosphor. Similar conclusion was made after aging by blue LEDs. The variations of the emission are the influence of small variation of light emitted by a diode.

Further studies for aging process for longer time may be needed. We could predict, that after more than 800h of aging under artificial sun we may be able to see some decreasing in conversion efficiency due to changing in the structure of silicon.

To improve the luminous efficiency different resin of incorporation of the materials should be prepared. Glass, as a resin, gave very optimistic results, not only from efficiency point of view, but cost of production and transparency. Mixing glass with BAM:Eu^{2+} and GYAG:Ce^{3+} and nitride:Eu^{3+} may give very interesting results, not only for the efficiency, but also for CRI and color temperature.

The shape of the particles is also not indifferent to light scattering and dispersing. Due to more spherical shape of particles of phosphor in a resin, the results would be more predictable and the conversion would have higher efficiency.

References

[1] S. Nakamura, S. Pearton, and G. Fasol, *The Blue Laser Diode: The Complete Story*. Springer & Business Media, 2013.

[2] E. Pavitra, G. S. R. Raju, J. Y. Park, L. Wang, B. K. Moon, and J. S. Yu, "Novel rare-earth-free yellow Ca5Zn3.92In0.08(V0.99Ta0.01O4)6 phosphors for dazzling white light-emitting diodes," *Sci. Rep.*, vol. 5, no. 1, Sep. 2015.

[3] C. J. Humphreys, "Solid-State Lighting," *MRS Bull.*, vol. 33, no. 4, pp. 459–470, Apr. 2008.

[4] "The Promise and Challenge of Solid-State Lighting: Physics Today: Vol 54, No 12." [Online]. Available: https://physicstoday.scitation.org/doi/10.1063/1.1445547. [Accessed: 08-Mar-2018].

[5] T.-H. Yang, C.-C. Chen, C.-Y. Chen, Y.-Y. Chang, and C.-C. Sun, "Essential Factor for Determining Optical Output of Phosphor-Converted LEDs," *Photonics J. IEEE*, vol. 6, pp. 1–9, Apr. 2014.

[6] A. Czesnakowska, G. Ledru, B. Glorieux, and G. Zissis, "Effect of different phosphor properties for white light generation using a blue laser diode.," *Proceedings of the 15th International Symposium on the Science and Technology of Lighting*, Kyoto, Japan, 2016.

[7] A. Czesnakowska, G. Ledru, B. Glorieux, and G. Zissis, "YAG and greenYAG+nitride properties for white-light generation using a blue laser diode," *J Photon Energy*, vol. 8, no. 2, p. 026001, 2018.

[8] "History of research on light," *Photon terrace*. [Online]. Available: http://photonterrace.net/en/photon/history/. [Accessed: 11-Dec-2017].

[9] *The Physics of Invisibility - A Story of Light and Deception | Martin Beech | Springer*. .

[10] "Isaac Newton | Biography, Facts, Discoveries, Laws, & Inventions," *Encyclopedia Britannica*. [Online]. Available: https://www.britannica.com/biography/Isaac-Newton. [Accessed: 11-Dec-2017].

[11] "Albert Einstein | Biography & Facts," *Encyclopedia Britannica*. [Online]. Available: https://www.britannica.com/biography/Albert-Einstein. [Accessed: 11-Dec-2017].

[12] *Light and Light Sources - High-Intensity Discharge Lamps | Peter G. Flesch | Springer*. .

[13] W. S. Stiles, "The Directional Sensitivity of the Retina and the Spectral Sensitivities of the Rods and Cones," *Proc. R. Soc. Lond. B Biol. Sci.*, vol. 127, no. 846, pp. 64–105, 1939.

[14] R. G. Foster and Professor of Circadian Neuroscience, and Head, Nuffield Laboratory of Ophthalmology, University of Oxford, "The 'Third' Photoreceptor System of the Eye – Photosensitive Retinal Ganglion Cells," *Eur. Ophthalmic Rev.*, vol. 02, no. 01, p. 84, 2009.

[15] S. Pappas, L. S. C. | April 29, and 2010 03:28pm ET, "How Do We See Color?," *Live Science*. [Online]. Available: https://www.livescience.com/32559-why-do-we-see-in-color.html. [Accessed: 13-Dec-2017].

[16] "EBSCOhost | 32174740 | The Degree of Color Metamerism and Its Specification." [Online]. Available: http://web.b.ebscohost.com/abstract?site=ehost&scope=site&jrnl=0040490X&AN=32174740&h=ocoun%2brf%2bu1DgU2akGEcgOvnROFYepfEVaLify7tv70z71FnSgcBGrV%2fETCZxkHheBwD9fQdL288frGVt1jfRw%3d%3d&crl=c&resultLocal=ErrCrlNoResults&resultNs=Ehost&crlhashurl=login.aspx%3fdirect%3dtrue%26profile

%3dehost%26scope%3dsite%26authtype%3dcrawler%26jrnl%3d0040490X%26AN%3d32174740. [Accessed: 13-Dec-2017].
[17] J. Schanda, *Colorimetry: Understanding the CIE System*. John Wiley & Sons, 2007.
[18] *Traité d'éclairage 2e édition - William Sanial*. .
[19] O. Svelto and D. C. Hanna, *Principles of Lasers*. Springer US, 1976.
[20] "Field Guide to Illumination | (2007) | Arecchi | Publications | Spie." [Online]. Available: https://spie.org/Publications/Book/764682. [Accessed: 09-Jan-2018].
[21] F. W. Billmeyer, "Optical Radiation Measurements. Volume 1: Radiometry, by Franc Grum and Richard J. Becherer. Academic, New York, 1979, 335 pp. Price: $34.00," *Color Res. Appl.*, vol. 6, no. 3, pp. 184–184, Sep. 1981.
[22] B. Valeur and M. N. Berberan-Santos, "A Brief History of Fluorescence and Phosphorescence before the Emergence of Quantum Theory," *J. Chem. Educ.*, vol. 88, no. 6, pp. 731–738, Jun. 2011.
[23] S. Muthu, F. J. P. Schuurmans, and M. Pashley, "Red, Green, and Blue LEDs for White Light Illumination," *IEEE J. Sel. Top. Quantum Electron.*, vol. 8, no. 2, pp. 333–338, 2002.
[24] "IRC : Indice de Rendu des Couleurs," *Guide de l'éclairage*. [Online]. Available: http://leclairage.fr/irc/. [Accessed: 13-Mar-2018].
[25] "Color temperature," *Wikipedia*. 18-Feb-2018.
[26] E. F. Schubert and J. K. Kim, "Solid-State Light Sources Getting Smart," *Science*, vol. 308, no. 5726, pp. 1274–1278, May 2005.
[27] V. K. Khanna, *Fundamentals of Solid-State Lighting: LEDs, OLEDs, and Their Applications in Illumination and Displays*. CRC Press, 2014.
[28] "History of the Incandescent Light." [Online]. Available: http://www.edisontechcenter.org/incandescent.html. [Accessed: 10-Feb-2018].
[29] "Halogen light bulbs | Philips Lighting," *Philips*. [Online]. Available: https://www.philips.com.hk/en/c-m-li/halogen-light-bulbs. [Accessed: 12-Feb-2018].
[30] "The Low Pressure Sodium Lamp." [Online]. Available: http://www.lamptech.co.uk/Documents/SO%20Introduction.htm. [Accessed: 13-Feb-2018].
[31] "The Sodium Lamp - How it works and history." [Online]. Available: http://www.edisontechcenter.org/SodiumLamps.html. [Accessed: 01-Mar-2018].
[32] "The Fluorescent Lamp." [Online]. Available: http://www.lamptech.co.uk/Documents/FL%20Introduction.htm. [Accessed: 05-Mar-2018].
[33] "Solar Power for Ordinary People," *Solar Power for Ordinary People*. [Online]. Available: https://livingonsolarpower.wordpress.com/. [Accessed: 08-Mar-2018].
[34] S. Pimputkar, J. S. Speck, S. P. DenBaars, and S. Nakamura, "Prospects for LED lighting," *Nature Photonics*, 01-Apr-2009. [Online]. Available: https://www.nature.com/articles/nphoton.2009.32. [Accessed: 12-Mar-2018].
[35] "Osram Opto unveils R&D results from GaN LEDs grown on silicon - LEDs." [Online]. Available: http://www.ledsmagazine.com/articles/2012/01/osram-opto-unveils-r-d-results-from-gan-leds-grown-on-silicon.html. [Accessed: 12-Mar-2018].
[36] H.-Y. Ryu and D.-H. Kim, "High brightness phosphor-conversion White light source using InGaN Blue Laser Diode," *J. Opt. Soc. Korea*, vol. 14, no. 4, pp. 415–419, 2010.
[37] K. A. Denault, M. Cantore, S. Nakamura, S. P. DenBaars, and R. Seshadri, "Efficient and stable laser-driven white lighting," *AIP Adv.*, vol. 3, no. 7, p. 072107, Jul. 2013.

[38] A. Misra, P. Kumar, M. N. Kamalasanan, and S. Chandra, "White organic LEDs and their recent advancements," *Semicond. Sci. Technol.*, vol. 21, no. 7, pp. R35–R47, Jul. 2006.

[39] G. M. Farinola and R. Ragni, "Electroluminescent materials for white organic light emitting diodes." [Online]. Available: http://pubs.rsc.org/en/content/articlepdf/2011/CS/C0CS00204F. [Accessed: 12-Mar-2018].

[40] F. Yan *et al.*, "Efficient three-color white organic light-emitting diodes with a spaced multilayer emitting structure," *Appl. Phys. Lett.*, vol. 106, no. 2, p. 023302, Jan. 2015.

[41] X. Liu, J. Zhang, J. Yu, and G. Cao, "Comparison study between lasers and light-emitting diode for achieving higher efficiency," *Light. Reaserch Technol.*, 2015.

[42] N. Bohr, "I. *On the constitution of atoms and molecules*," *Lond. Edinb. Dublin Philos. Mag. J. Sci.*, vol. 26, no. 151, pp. 1–25, Jul. 1913.

[43] "The quantum mechanical model of the atom," *Khan Academy*. [Online]. Available: https://www.khanacademy.org/science/physics/quantum-physics/quantum-numbers-and-orbitals/a/the-quantum-mechanical-model-of-the-atom. [Accessed: 03-May-2018].

[44] "1.2: Atomic Structure - Orbitals," *Chemistry LibreTexts*, 03-May-2015. [Online]. Available: https://chem.libretexts.org/Textbook_Maps/Organic_Chemistry_Textbook_Maps/Map%3A_Organic_Chemistry_(McMurry)/Chapter_01%3A_Structure_and_Bonding/1.02%3A_Atomic_Structure%3A_Orbitals. [Accessed: 03-May-2018].

[45] S. Ye, F. Xiao, Y. X. Pan, Y. Y. Ma, and Q. Y. Zhang, "Phosphors in phosphor-converted white light-emitting diodes: Recent advances in materials, techniques and properties," *Mater. Sci. Eng. R Rep.*, vol. 71, no. 1, pp. 1–34, Dec. 2010.

[46] M. Shang *et al.*, "Blue Emitting Ca8La2(PO4)6O2:Ce3+/Eu2+ Phosphors with High Color Purity and Brightness for White LED: Soft-Chemical Synthesis, Luminescence, and Energy Transfer Properties," *J. Phys. Chem. C*, vol. 116, no. 18, pp. 10222–10231, May 2012.

[47] C. Devadoss, P. Bharathi, and J. S. Moore, "Energy Transfer in Dendritic Macromolecules: Molecular Size Effects and the Role of an Energy Gradient," *J. Am. Chem. Soc.*, vol. 118, no. 40, pp. 9635–9644, Jan. 1996.

[48] C. Fouassier, "Luminescent materials," *Curr. Opin. Solid State Mater. Sci.*, vol. 2, no. 2, pp. 231–235, Apr. 1997.

[49] J. L. Wu, G. Gundiah, and A. K. Cheetham, "Structure–property correlations in Ce-doped garnet phosphors for use in solid state lighting," *Chem. Phys. Lett.*, vol. 441, no. 4, pp. 250–254, Jun. 2007.

[50] "Structural and optical properties of YAG:Ce3+ phosphors by sol–gel combustion method - ScienceDirect." [Online]. Available: https://www.sciencedirect.com/science/article/pii/S0022024805000965. [Accessed: 29-Mar-2018].

[51] N. P. Bedrijven, "Philips J ourn al of Research," p. 331.

[52] A. A. Setlur, W. J. Heward, M. E. Hannah, and U. Happek, "Incorporation of Si4+–N3− into Ce3+ -Doped Garnets for Warm White LED Phosphors," *Chem. Mater.*, vol. 20, no. 19, pp. 6277–6283, Oct. 2008.

[53] "Crystal Field Theory," *Chemistry LibreTexts*, 02-Oct-2013. [Online]. Available: https://chem.libretexts.org/Core/Inorganic_Chemistry/Crystal_Field_Theory/Crystal_Field_Theory. [Accessed: 30-Mar-2018].

[54] R.-J. Xie and N. Hirosaki, "Silicon-based oxynitride and nitride phosphors for white LEDs—A review," *Sci. Technol. Adv. Mater.*, vol. 8, no. 7, pp. 588–600, Oct. 2007.

[55] K. Han, S. H. Lee, Y. G. Choi, W. B. Im, and W. J. Chung, "Improved color rendering index and thermal stability of white LEDs with phosphor-in-glass using the SiO2-B2O3-ZnO-Na2O glass system," *J. Non-Cryst. Solids*, vol. 445–446, pp. 77–80, Aug. 2016.

[56] S. C. Allen and A. J. Steckl, "A nearly ideal phosphor-converted white light-emitting diode," *Appl. Phys. Lett.*, vol. 92, no. 14, p. 143309, Apr. 2008.

[57] H. Lin *et al.*, "Phosphor-in-Glass for High-Powered Remote-Type White AC-LED," *ACS Appl. Mater. Interfaces*, vol. 6, no. 23, pp. 21264–21269, Dec. 2014.

[58] Zhang Rui, Lin Hang, Yu Yunlong, Chen Daqin, Xu Ju, and Wang Yuansheng, "A new-generation color converter for high-power white LED: transparent Ce3+:YAG phosphor-in-glass," *Laser Photonics Rev.*, vol. 8, no. 1, pp. 158–164, Jan. 2014.

[59] V. Dubey, J. Kaur, and S. Agrawal, "Effect of europium doping levels on photoluminescence and thermoluminescence of strontium yttrium oxide phosphor," *Mater. Sci. Semicond. Process.*, vol. 31, pp. 27–37, Mar. 2015.

[60] I. P. Sahu, D. P. Bisen, N. Brahme, and R. K. Tamrakar, "Photoluminescence properties of europium doped di-strontium magnesium di-silicate phosphor by solid state reaction method," *J. Radiat. Res. Appl. Sci.*, vol. 8, no. 1, pp. 104–109, Jan. 2015.

[61] P. P. Lohe, S. K. Omanwar, N. S. Bajaj, and P. D. Belsare, "Study of optical properties of cerium ion doped barium aluminate phosphor," *AIP Conf. Proc.*, vol. 1728, no. 1, p. 020519, May 2016.

[62] S. Uysal Satilmis *et al.*, "Luminescence characterization of cerium doped yttrium gadolinium aluminate phosphors," *Opt. Mater.*, vol. 34, no. 11, pp. 1921–1925, Sep. 2012.

[63] S. Tanabe, S. Fujita, S. Yoshihara, A. Sakamoto, and S. Yamamoto, "YAG glass-ceramic phosphor for white LED (II): luminescence characteristics," in *Fifth International Conference on Solid State Lighting*, 2005, vol. 5941, p. 594112.

[64] Algvere Peep V., Marshall John, and Seregard Stefan, "Age-related maculopathy and the impact of blue light hazard," *Acta Ophthalmol. Scand.*, vol. 84, no. 1, pp. 4–15, Jan. 2006.

[65] M. L. Daley, R. C. Watzke, and M. C. Riddle, "Early Loss of Blue-Sensitive Color Vision in Patients With Type I Diabetes," *Diabetes Care*, vol. 10, no. 6, pp. 777–781, Nov. 1987.

[66] "LASER COMPONENTS Germany." [Online]. Available: https://www.lasercomponents.com/de-en/. [Accessed: 29-Mar-2018].

[67] "BMW Laserlight Technology: How It Works and Benefits | BMW of Freeport." [Online]. Available: https://www.bmwoffreeport.com/blogs/827/how-bmw-lasterlight-work-and-what-are-benefits/. [Accessed: 29-Mar-2018].

[68] A. Czesnakowska, G. Ledru, B. Glorieux, and G. Zissis, "YAG and greenYAG+nitride properties for white-light generation using a blue laser diode," *Proceedings of the SPIE Photonics WEST*, San Fransisco, 2018.

[69] Z. Liu, S. Liu, K. Wang, and X. Luo, "Measurement and numerical studies of optical properties of YAG:Ce phosphor for white light-emitting diode packaging," *Appl. Opt.*, vol. 49, no. 2, pp. 247–257, Jan. 2010.

[70] D. A. Steigerwald *et al.*, "Illumination with solid state lighting technology," *IEEE J. Sel. Top. Quantum Electron.*, vol. 8, no. 2, pp. 310–320, Apr. 2002.

[71] R. C. Jordan, J. Bauer, and H. Oppermann, "Optimized heat transfer and homogeneous color converting for ultra high brightness LED package," in *Photonics in the Automobile II*, 2006, vol. 6198, p. 61980B.
[72] M. Arik, S. Weaver, C. Becker, M. Hsing, and A. Srivastava, "Effects of Localized Heat Generations Due to the Color Conversion in Phosphor Particles and Layers of High Brightness Light Emitting Diodes," pp. 611–619, Jan. 2003.
[73] P. Wen *et al.*, "Identification of degradation mechanisms of blue InGaN/GaN laser diodes," *J. Phys. Appl. Phys.*, vol. 48, Oct. 2015.
[74] G. Hatakoshi, M. Onomura, M. Yamamoto, S. Nunoue, K. Itaya, and M. Ishikawa, "Thermal Analysis for GaN Laser Diodes," *Jpn. J. Appl. Phys.*, vol. 38, no. 5R, p. 2764, May 1999.
[75] M. Meneghini *et al.*, "Degradation of InGaN-based laser diodes analyzed by means of electrical and optical measurements," *Appl. Phys. Lett.*, vol. 97, no. 26, p. 263501, Dec. 2010.
[76] A. Uddin, A. C. Wei, and T. G. Andersson, "Study of degradation mechanism of blue light emitting diodes," *Thin Solid Films*, vol. 483, no. 1–2, pp. 378–381, Jul. 2005.
[77] Hatakoshi Gen-ichi, Onomura Masaaki, and Ishikawa Masayuki, "Optical, electrical and thermal analysis for GaN semiconductor lasers," *Int. J. Numer. Model. Electron. Netw. Devices Fields*, vol. 14, no. 4, pp. 303–323, Apr. 2001.
[78] F. Mei-Xin *et al.*, "Thermal analysis of GaN laser diodes in a package structure," *Chin. Phys. B*, vol. 21, no. 8, p. 084209, 2012.
[79] "Laser Diodes • Application Notes • OSRAM Opto Semiconductors | Opto Semiconductors." [Online]. Available: https://www.osram.com/os/applications/application-notes/application_notes_lasers.jsp. [Accessed: 06-Apr-2018].
[80] A. Czesnakowska, G. Ledru, B. Glorieux, and G. Zissis, "Thermal Analysis of Blue Laser Diode for Solid State Lighting Application," *Opt. Photonics J.*, vol. 8, pp. 40–49, 2018.
[81] K. Maemura, N. Takeda, and R. Nagai, "Circadian rhythms in the CNS and peripheral clock disorders: role of the biological clock in cardiovascular diseases," *J. Pharmacol. Sci.*, vol. 103, no. 2, pp. 134–138, Feb. 2007.
[82] T. Ebisawa, "Circadian rhythms in the CNS and peripheral clock disorders: human sleep disorders and clock genes," *J. Pharmacol. Sci.*, vol. 103, no. 2, pp. 150–154, Feb. 2007.
[83] T. Kudo, K. Horikawa, and S. Shibata, "Circadian rhythms in the CNS and peripheral clock disorders: the circadian clock and hyperlipidemia," *J. Pharmacol. Sci.*, vol. 103, no. 2, pp. 139–143, Feb. 2007.
[84] M. Meneghini *et al.*, "Degradation of InGaN/GaN laser diodes investigated by micro-cathodoluminescence and micro-photoluminescence," *Appl. Phys. Lett.*, vol. 103, no. 23, p. 233506, Dec. 2013.
[85] M.-H. Chang, D. Das, P. V. Varde, and M. Pecht, "Light emitting diodes reliability review," *Microelectron. Reliab.*, vol. 52, no. 5, pp. 762–782, May 2012.
[86] Y.-Y. Chang *et al.*, "Influence of ZrO2 particles on the optical properties of pc-LEDs," *Opt. Mater.*, vol. 55, pp. 55–61, May 2016.
[87] C. E. Schäffer and C. Klixbüll Jørgensen, "The nephelauxetic series of ligands corresponding to increasing tendency of partly covalent bonding," *J. Inorg. Nucl. Chem.*, vol. 8, pp. 143–148, Jan. 1958.

[88] D. Cai, A. Neyer, R. Kuckuk, and H. M. Heise, "Raman, mid-infrared, near-infrared and ultraviolet-visible spectroscopy of PDMS silicone rubber for characterization of polymer optical waveguide materials," *J. Mol. Struct.*, vol. 976, pp. 274–281, Jul. 2010.
[89] J. Qin *et al.*, "Temperature-Dependent Luminescence Characteristic of SrSi2O2N2:Eu2+ Phosphor and Its Thermal Quenching Behavior," *J. Mater. Sci. Technol.*, vol. 30, no. 3, pp. 290–294, Mar. 2014.
[90] S. Poncé, Y. Jia, M. Giantomassi, M. Mikami, and X. Gonze, "Understanding Thermal Quenching of Photoluminescence in Oxynitride Phosphors from First Principles," *J. Phys. Chem. C*, vol. 120, no. 7, pp. 4040–4047, Feb. 2016.
[91] A. Torikai and H. Hasegawa, "Accelerated photodegradation of poly(vinyl chloride)," *Polym. Degrad. Stab.*, vol. 63, no. 3, pp. 441–445, Mar. 1999.
[92] N. Narendran, Y. Gu, J. P. Freyssinier, H. Yu, and L. Deng, "Solid-state lighting: failure analysis of white LEDs," *J. Cryst. Growth*, vol. 268, no. 3, pp. 449–456, Aug. 2004.
[93] J. L. Down, "The Yellowing of Epoxy Resin Adhesives: Report on High-Intensity Light Aging," *Stud. Conserv.*, vol. 31, no. 4, pp. 159–170, 1986.
[94] J. Zhong, D. Chen, Y. Zhou, Z. Wan, M. Ding, and Z. Ji, "Stable and chromaticity-tunable phosphor-in-glass inorganic color converter for high-power warm white light-emitting diode," *J. Eur. Ceram. Soc.*, vol. 36, no. 7, pp. 1705–1713, Jun. 2016.
[95] S. Fujita, S. Yoshihara, A. Sakamoto, S. Yamamoto, and S. Tanabe, "YAG glass-ceramic phosphor for white LED (I): background and development," in *Fifth International Conference on Solid State Lighting*, 2005, vol. 5941, p. 594111.
[96] B.-J. Shih *et al.*, "Study of temperature distributions in pc-WLEDs with different phosphor packages," *Opt. Express*, vol. 23, no. 26, p. 33861, Dec. 2015.
[97] X. Luo, J. Fan, M. Zhang, C. Qian, X. Fan, and G. Zhang, "Degradation mechanism analysis for phosphor/silicone composites aged under high temperature and high humidity condition," in *2017 18th International Conference on Electronic Packaging Technology (ICEPT)*, 2017, pp. 1331–1336.
[98] J. S. Lee, S. Unithrattil, S. Kim, I. J. Lee, H. Lee, and W. B. Im, "Robust moisture and thermally stable phosphor glass plate for highly unstable sulfide phosphors in high-power white light-emitting diodes," *Opt. Lett.*, vol. 38, no. 17, pp. 3298–3300, Sep. 2013.
[99] "Color Rendering Index for White Light Sources." OSRAM.
[100] Y. Narukawa, I. Niki, K. Izuno, M. Yamada, Y. Murazaki, and T. Mukai, "Phosphor-Conversion White Light Emitting Diode Using InGaN Near-Ultraviolet Chip," *Jpn. J. Appl. Phys.*, vol. 41, no. 4A, p. L371, Apr. 2002.
[101] Y. Xu *et al.*, "Phosphor-conversion white light using InGaN ultraviolet laser diode," *Appl. Phys. Lett.*, vol. 92, no. 2, p. 021129, Jan. 2008.
[102] H. Daicho *et al.*, "A novel phosphor for glareless white light-emitting diodes," *Nat. Commun.*, vol. 3, p. 1132, Oct. 2012.
[103] H. Guo *et al.*, "Structure and luminescence properties of a novel yellow super long-lasting phosphate phosphor $Ca_6BaP_4O_{17}:Eu^{2+},Ho^{3+}$," *J. Mater. Chem. C*, vol. 3, no. 22, pp. 5844–5850, 2015.
[104] "Method of manufacturing a phosphor screen for a CRT," 22-Dec-1995.
[105] Maki J. N., Lorre J. J., Smith P. H., Brandt R. D., and Steinwand D. J., "The color of Mars: Spectrophotometric measurements at the Pathfinder landing site," *J. Geophys. Res. Planets*, vol. 104, no. E4, pp. 8781–8794, Apr. 1999.
[106] S. GALAJEV, "Degradation processes in BaMgAl10O17:Eu2+ and BaMgAl14O23:Eu2+," p. 72.

[107] L. Ye, X. Peng, S. Zhang, Y. Wang, and W. Chang, "Photoluminescence properties of Ca-doped BaMgAl10O17:Eu2+,Mn2+ blue phosphor using BaF2 and CaF2 as co-flux," *J. Rare Earths*, vol. 32, no. 12, pp. 1109–1113, Dec. 2014.

[108] "High Thermal Stability and Photoluminescence of Si–N-Codoped BaMgAl10O17:Eu2+ Phosphors - Wang - 2010 - Journal of the American Ceramic Society - Wiley Online Library." [Online]. Available: https://onlinelibrary.wiley.com/doi/full/10.1111/j.1551-2916.2009.03557.x. [Accessed: 30-Apr-2018].

[109] E. Zych, W. Goetz, N. Harrit, and H. Spanggaard, "Spectroscopic properties of sintered BaMgAl10O17:Eu2+ (BAM) translucent pellets," *J. Alloys Compd.*, vol. 380, pp. 113–117.

[110] S. Zhang, "Vacuum-ultraviolet/visible conversion phosphors for plasma display panels," *IEEE Trans. Plasma Sci.*, vol. 34, no. 2, pp. 294–304, Apr. 2006.

[111] C. Cozzan *et al.*, "Monolithic translucent BaMgAl10O17:Eu2+ phosphors for laser-driven solid state lighting," *AIP Adv.*, vol. 6, no. 10, p. 105005, Oct. 2016.

[112] J. R. Sparrow, K. Nakanishi, and C. A. Parish, "The Lipofuscin Fluorophore A2E Mediates Blue Light–Induced Damage to Retinal Pigmented Epithelial Cells," *Invest. Ophthalmol. Vis. Sci.*, vol. 41, no. 7, pp. 1981–1989, Jun. 2000.

[113] B. F. Godley, F. A. Shamsi, F.-Q. Liang, S. G. Jarrett, S. Davies, and M. Boulton, "Blue Light Induces Mitochondrial DNA Damage and Free Radical Production in Epithelial Cells," *J. Biol. Chem.*, vol. 280, no. 22, pp. 21061–21066, Mar. 2005.

[114] C. Grimm, A. Wenzel, T. P. Williams, P. O. Rol, F. Hafezi, and C. E. Remé, "Rhodopsin-Mediated Blue-Light Damage to the Rat Retina: Effect of Photoreversal of Bleaching," *Invest. Ophthalmol. Vis. Sci.*, vol. 42, no. 2, pp. 497–505, Feb. 2001.

[115] L. Ulrich, "Whiter brights with lasers," *IEEE Spectr.*, vol. 50, no. 11, pp. 36–56, Nov. 2013.

[116] L. Ulrich, "Audi Pixelated Laser Headlights Light the Road and Paint It Too," *IEEE Spectrum: Technology, Engineering, and Science News*, 05-Jun-2015. [Online]. Available: https://spectrum.ieee.org/cars-that-think/transportation/advanced-cars/audi-lights-the-road-with-pixelated-laser-headlights-. [Accessed: 22-May-2018].

[117] I. H. Cho, G. Anoop, D. W. Suh, S. J. Lee, and J. S. Yoo, "On the stability and reliability of $Sr_{1-x}Ba_xSi_2O_2N_2:Eu^{2+}$ phosphors for white LED applications," *Opt. Mater. Express*, vol. 2, no. 9, pp. 1292–1305, Sep. 2012.

[118] Y. H. Song, E. K. Ji, B. W. Jeong, M. K. Jung, E. Y. Kim, and D. H. Yoon, "High power laser-driven ceramic phosphor plate for outstanding efficient white light conversion in application of automotive lighting," *Sci. Rep.*, vol. 6, p. 31206, Aug. 2016.

[119] A. Krasnoshchoka, A. Thorseth, C. Dam-Hansen, D. D. Corell, P. M. Petersen, and O. B. Jensen, "Investigation of Saturation Effects in Ceramic Phosphors for Laser Lighting," *Mater. Basel Switz.*, vol. 10, no. 12, Dec. 2017.

Publications and communications

[1] A. Czesnakowska, G. Ledru, B. Glorieux and G. Zissis **« Thermal Analysis of Blue Laser Diode for Solid State Lighting Application** » Optics and Photonics Journal, 8, 40-49 (2018).

[2] A. Czesnakowska, G. Ledru, B. Glorieux and G. Zissis « **Effect of different phosphor properties for white light generation using laser diode and remote phosphor** » 15th International Symposium on the Science and Technology of Lighting, 22-27 May 2016, Kyoto, Japan

[3] A. Czesnakowska, G. Ledru, B. Glorieux, and G. Zissis « **YAG and greenYAG + nitride properties for white-light generation using a blue laser diode** » SPIE Photonics West, 27 January – 1st February 2018, San Francisco, USA

[4] A. Czesnakowska, G. Ledru, B. Glorieux, and G. Zissis « **Phosphor-converted white light using near-ultraviolet laser diode**» 16th International Symposium on the Science and Technology of Lighting, 17-22 June 2018, Sheffield, England

[5] A. Czesnakowska, G. Ledru, B. Glorieux, and G. Zissis « **YAG and greenYAG + nitride properties for white-light generation using a blue laser diode** » J. Photon. Energy 8(2), 026001 (2018)

[6] A. Czesnakowska, G. Ledru, B. Glorieux, and G. Zissis « **Production de lumière blanche à l'aide de diode laser** » Optique 2018, Toulouse, France